THE UNIVERSITY OF CHICAGO

# THE ROLE OF CYTOKINE RECEPTOR-JAK AFFINITY AND JAK-JAK GEOMETRY IN LIMITED TYPE III INTERFERON RESPONSE

A DISSERTATION SUBMITTED TO

THE FACULTY OF THE DIVISION OF THE PHYSICAL SCIENCES

IN CANDIDACY FOR THE DEGREE OF

DOCTOR OF PHILOSOPHY

DEPARTMENT OF CHEMISTRY

BY

THEINT NANDAR AUNG

CHICAGO, ILLINOIS

AUGUST 2022

‘We dance round in a ring and suppose,

But the Secret sits in the middle and knows.’

-Robert Frost

## TABLE OF CONTENTS

**LIST OF FIGURES**

## LIST OF TABLES

**ACKNOWLEDGEMENTS**

As I write this acknowledgements section – the last to be completed, it dawns on me that this +100-page ledger holds an account of everything and nothing of my past five years in the PhD program. True, this document spells out every last detail of every gainful experiment I conducted but between its lines, it says nothing of the relentless smacks upside my head, so frequent that they felt like one five-year long whack. Or the selective amnesia that I feigned to be afflicted with, just to keep propelling myself onward when time felt static with nothing but setbacks that graduated its axis. On occasion, time seemed to me a warped construct; just as distinctly as I felt the long drag of time working at the bench, sentenced to the stagnating march of trial-and-error, thumping in my heart was the clock ticking down mercilessly on my time in the program.

Albeit less talked about, but nonetheless can be equally, if not even more, stressful than research work was the human element of it. In all its isolation and general sense of dread, being in graduate school is somewhat akin to an extremely long flight on a budget airline. After all, you coexist with strangers in a pressurized bubble, perpetually rocked by turbulences that threaten to drop you from a great height. Pressure also wrings out the best, and the worst from its unsuspecting victims. Working for years in close quarters with others where the repercussions of one's actions are so acutely felt by many, has taught me the importance of two qualities – empathy and self-awareness. The former encourages forgiveness by separating a wrong from its source, and the latter, mindfulness of my own actions on the most trying days. In retrospect, I am grateful to all those individuals without whom, I suspect, my personal growth would likely have progressed at a rather glacial pace.

Thankfully, I have also been blessed with some great mentors and colleagues along the way. I am profoundly indebted to my thesis advisor, Prof. Juan Mendoza, *pro forma* advisor, Prof. Andrei Tokmakoff, the members of the thesis committee, Prof. Chuan He and Prof. Tony Kossiakoff, and the director of academic programs, Dr. Vera Dragisich, for their generosity with guidance, wisdom, kindness, and time. I would also like to thank my friends and labmates who, in my moments of crises, propped up my collapsed mentality with their grace and strength. To my closest friends and confidantes – my two sisters, thank you for putting things in perspective and me in my place whenever I am in the middle of yet another existential crisis.

Last but not least, I would not be where I am now without my parents. They have not simply given me a life but all the freedom I need to make it my own. They have not simply bestowed on me their unconditional love but trusted that I merit it completely. They have not simply watched on as I navigate through life but stood by me through every high and low, every thick and thin. I owe my parents all the resolve and strength I needed to see this work through. To my Mom and Dad, thank you. I have come as far as I have in life, walking on your tireless legs; I have seen as much as I have of the world, climbing atop your selfless shoulders. I would not be without you. Thank you.

**ABSTRACT**

Type I and III interferons (IFNs) constitute the host system's first line of defense against viral infections. Although the two families form distinct heterodimeric receptor complexes, the ligand-inducible signals are believed to be propagated through an identical Janus kinase (JAK)-mediated intracellular signaling pathway. Consequently, type I and III IFNs activate a largely overlapping set of interferon stimulated genes (ISGs), eliciting similar biological responses. Despite the apparent overlap in the signaling pathway and functions, the two families of IFN exhibit a pattern of spatiotemporal division of labor that serves to provide a protective state of immunity whilst minimizing collateral damage due to unabated inflammation. Type III IFNs are attractive alternatives to type I IFNs as therapeutics because of their tissue specificity and lower systemic toxicity. However, type III IFNs are significantly less potent than type I IFNs in their physiological activities. Previous studies have described the stability of extracellular receptor-ligand complex and receptor expression levels as factors contributing to the potency gap between type I and III IFNs. Here, we probe the intracellular receptor-JAK (Janus kinase) interactions to further account for the differences between type I vs III IFN signaling. Two facets of the receptor-JAK axis are examined –1) the affinity of the receptor- JAK interactions, and 2) the relative geometry of the proximal JAKs within a signaling complex. To interrogate the effects of the former, we engineered high-affinity cytokine receptors toward their associated JAKs and assayed the changes in downstream signaling. Our results indicate that while the native IFN-αR1-TYK2 affinity is low, the affinity is relatively higher than that of the IL-10Rβ-TYK2 interaction. We show that the signaling potency of type III IFNs can be significantly improved by improving the affinity between the IL-10Rβ receptor and TYK2 whereas the type I IFN signaling is unchanged when the affinity of IFN-αR1 toward TYK2 is enhanced. In order to

evaluate the role of receptor geometry in IFN signaling, we induced IFNλ non-responsive cell lines to express either the wild-type or mutant IFN-λR1 receptors with a specified number of alanines inserted into the transmembrane domain. Such alanine insertion mutagenesis approach enables direct assaying of downstream signaling and biological activities of type III IFNs as a function of JAK- JAK geometry within a complex. We have identified three biophysical properties of the IFNλ signaling complex that limit its signaling potency – 1) the affinity of the extracellular receptor complex, 2) lL-10Rβ/TYK2 affinity, and 3) the relative JAK1/TYK2 geometry. Based on our cell-based assays, we report near equivalent functional activities between type I and III IFNs by simultaneously optimizing the affinity of the extracellular receptor complex and JAK- JAK geometry. We believe that our findings will not only guide future efforts in understanding IFN biology and serve as a model system of cytokine signaling but also provide novel strategies for successful applications of type III IFNs in clinics.

## Chapter 1: Introduction

### 1.01 Overview: Cytokines orchestrate vast networks of biological processes

Cytokines are soluble extracellular proteins or glycoproteins (<40kDa) that are secreted by virtually every nucleated cell[1]. They can act on the same cell where they are produced in an autocrine fashion, on nearby cells in a paracrine fashion, or distant cells in an endocrine fashion[2]. As crucial mediators and mobilizers of both innate and adaptive arms of the immune system, cytokines influence a broad range of physiological processes including host inflammatory responses to injurious stimuli, regulation of cellular proliferation, differentiation and cell death, and restoration of homeostasis post molecular perturbation via control of repair and remodeling processes[3,4]. Currently, over 130 known cytokines are classified into superfamilies that include interleukins, chemokines, colony-stimulating factors (CSF), interferons, and the transforming growth factors (TGF) and tumor necrosis factor (TNF)[5]. It should be noted that such classification does not necessarily connote common genes or functional similarity. Here, cytokines are classified based on common structural motifs and sequence homology[6].

The remarkable range of cytokine functions can be attributed to the highly pleiotropic nature of many cytokines. The same cytokines produced by different cell populations can induce different biological responses in cells that they act on, depending on the types and availability of complementary receptors engaged as well as other co-factors or cytokines already present in the extracellular space[2,7,8]. Such hallmark ability of cytokines to retain multiple biological properties also leads to many shared and redundant or non-redundant synergistic functions among cytokines. Although parallels can be drawn between cytokines and hormones in terms of their cellular productions and endocrinal actions, cytokines are far more potent than hormones on a

molar basis. The smallest amounts of proteins, often on picomolar scales, can trigger signaling cascades that lead to significant biological responses[9].

**1.02 Cytokines signal through two major families of receptors**

Cytokines are classified according to the type of receptors that they engage. Cytokine receptors are grouped into two major families based on common structural features: class I and class II cytokine receptors[10]. Class I receptors represent the largest among receptor families with 34 receptor chains encoded in the human genome[11-14]. These type I single-pass membrane proteins have conserved intracellular and extracellular features. The extracellular domain features a cytokine receptor homology region (CHR), which is comprised of two type III fibronectin (FnIII) domains at near right angles to one another. The junction formed by the FnIII pair within the CHR provides a signature recognition module for the four α-helical bundle structures of class I cytokines that they engage[15]. Class I receptors are further structurally distinguished by their conserved cysteine sequence within the first FnIII domain and Trp-Ser-Xaa-Trp-Ser (WSXWS) motif in the second FnIII domain[15,16]. These motifs are crucial for the tertiary structure of the receptors but are not involved in ligand interactions[17].

There are three principal shared signaling receptors – gp130, $\beta_c$, $\gamma_c$ –which, along with a cytokine-specific receptor chain, form hetero-oligomeric complexes with ligands[10]. Cytokines that form signal-transducing subunits with gp130 include IL-6, IL-10, IL-27, LIF, ciliary neurotrophic factor (CNTF), oncostatin M (OSM), cardiotrophin 1 (CT-1), NNT-1/BSF3[18,19]. Conversely, cytokines such as IL-3, IL-5 and GM-CSF recruit $\beta_c$ , and interleukins including IL-2, IL-4, IL-7, IL-9, IL-15 and IL-21 interact with $\gamma_c$ receptor[7,20-23]. On their own, the shared receptors exhibit no appreciable affinity to the cytokines. To initiate signaling, the ligand first binds with high affinity to its cognate receptor (the alpha chain)[23]. The dimeric subunit then

recruits a shared receptor to form a signaling complex with variable stoichiometry and organization[10].

In parallel to the class I receptors, class II cytokine receptors are grouped on the basis of the structure of their ectodomain, which consists of a single CHR (with the exception of IFN-αR1 which has two) but lacks the characteristic Trp-Ser-Xaa-Trp-Ser motif of class I receptors[15,24]. The receptor assembly and stoichiometry are more consistent within class II receptors. All receptors form heterodimers and each heterodimer associates with a cytokine molecule to form a signaling complex. Currently, there are 12 known members of the class II family, ten of which are type I transmembrane proteins that form heterodimeric complexes with class II cytokines. These receptors are either long or short-chained, which is indicative of the length of their cytoplasmic tails and two receptors of different lengths usually constitute a heterodimeric complex[25]. Unlike class I receptors, class II receptors are more restrictive with their binding substrates. Only IL-10 family cytokines (IL-10, IL-19, IL-20, IL-22, IL-24, IL-26) and interferons are recognized by class II receptors[26]. These cytokines share a common structural theme based on six α-helices despite a low sequence homology (15-25%)[25]. In cases of IL-10 and IFN-γ which are natural homodimers, the complete signaling complexes comprise a pair of heterodimeric receptors[27-29].

**1.03 Three Interferon families modulate the immune response**

Interferons (IFNs) are the oldest known cytokines that were originally identified for their ability to make cells resistant to viral infections[30]. Further studies have since shed light on their many other important functions in modulating innate and adaptive immune responses[31]. Interferons are classified into three types based on their sequence homology, genetic loci, cells of origin, shared receptor usage and biological functions[32,33]. Type II IFN family consists of only

one member, IFN-γ, which is functionally and structurally distinct from all other interferons. IFN-γ is a homodimer restrictively expressed by specific immune cell subtypes such as activated lymphocytes (CD4 T helper cells, CD 8 cytotoxic T cells, NK cells)[34]. In a canonical signaling pathway, each polypeptide subunit recruits two receptors – ligand-binding IFN-γR1 chain and signal-transducing IFN-γR2 chain, forming a signaling competent hexameric complex[35]. Type II IFN signaling is pivotal to host immune response against viral infections as well as cancerous tumors (Figure 1).

Type I IFN family encompasses 13 functional IFN-α subtypes along with IFN-β, IFN-ε, IFN-κ, and IFN-ω[36]. Remarkably, although all type I IFNs signal through a common pair of receptors – the low-affinity IFN-αR1 and high-affinity IFN-αR2, differences in promoter sequences and biochemistries of ligand-receptor interactions give each type I IFN a distinct set of functional activities[37,38]. Type III IFNs, on the other hand, have four subtypes – IFN-λ1 (IL-29), IFN-λ2 (IL-28A), IFN-λ3 (IL-28B), and IFN-λ4[39,40]. Existing in many human populations as a pseudogene, IFN-λ4 was a late addition to the IFN-λ family[41]. Despite the common genetic loci and receptor usage, IFN-λ4 is functionally distinct and shares <29% amino acid identity with the other subtypes. As a member of a family of proteins known for their antiviral properties, IFN-λ4 is paradoxically linked to impaired clearance of hepatitis C virus (HCV), the mechanisms of which are still unclear[41]. All type III IFNs signal by forming a ternary complex with the high-affinity IFN-λR1 and low-affinity IL-10Rβ receptors[39,42]. Together, both type I and III IFNs constitute the vertebrate first-line defense against infectious stimuli.

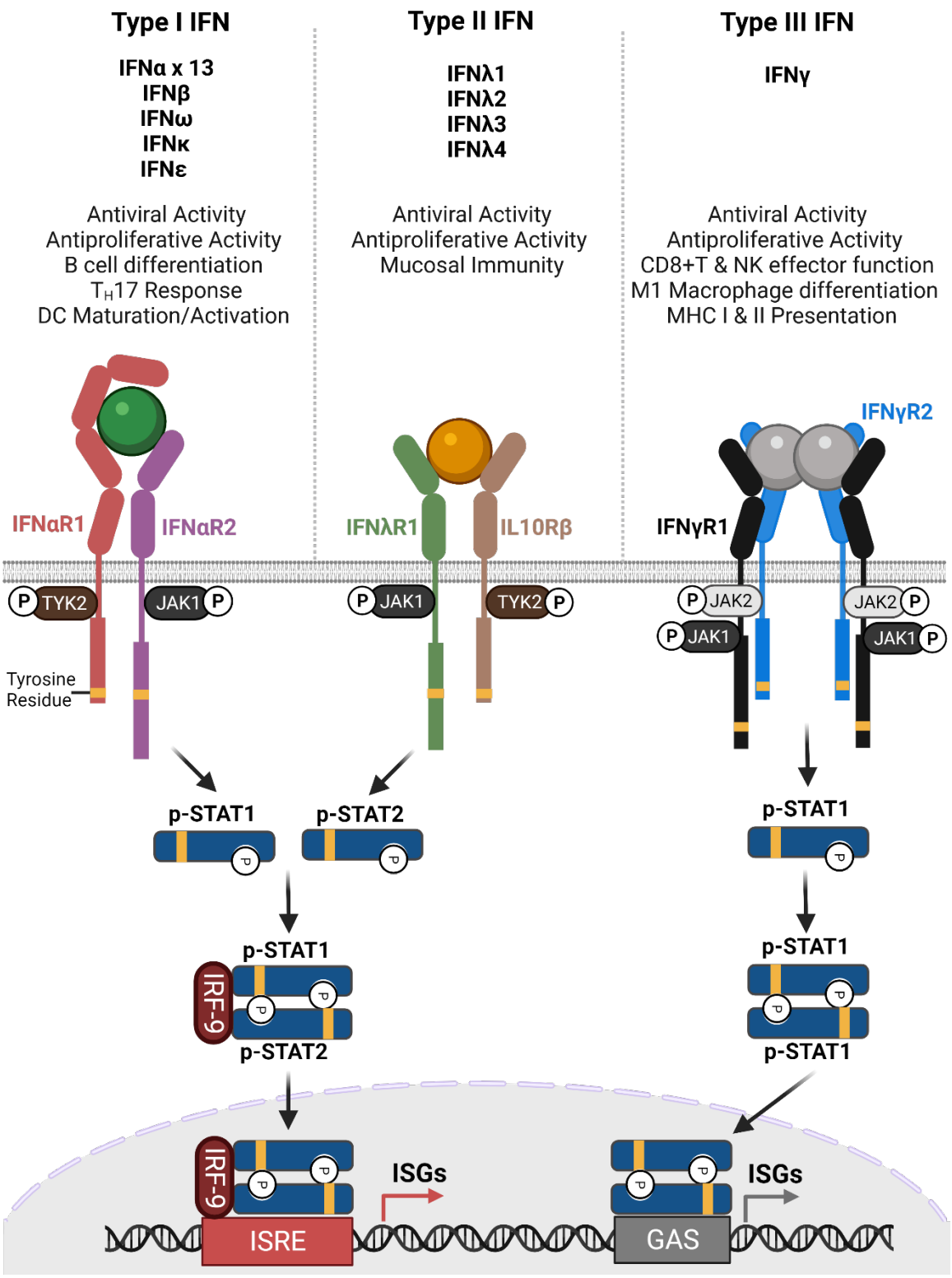


**Figure 1: A schematic diagram depicts three families of Interferons (IFNs), associated biological functions and intracellular signaling pathways.** JAK, Janus Kinase. STAT, Signal

**Figure 1, Continued**

Transducer and Activator of Transcription. IRF-9, Interferon-Regulatory Factor 9. ISRE, Interferon-Sensitive Response Element. GAS, Gamma Interferon Activation Site. ISG, Interferon Stimulated Genes.

### 1.04: Type I and III Interferons respond to viral stimuli through similar pathogen sensing pathways

Although type I and III IFNs are genetically distinct and signal through different receptors, they are activated by similar pathogen sensing pathways[43]. In the absence of noxious stimulus, IFN gene expression levels are near silent due to a lack of transcription factors and repressive mechanisms constitutively in place[44]. However, in the event of a viral or non-viral pathogenic infection, both type I and III IFNs are induced by the cellular sensing of pathogen-associated molecular patterns (PAMPs) via either cytosolic or endosomal pattern-recognition receptors (PRRs). There are four classes of microbial sensors – endosomal Toll-like receptors (TLRs), cytoplasmic RIG-I like receptors (RLRs), nucleotide binding oligomerization domain (NOD)-like receptors and a family of nuclear DNA sensors including cGAS, DAI, AIM2, IFI16, pol III, DDX41[45,46]. The type of IFN produced can be affected by the cellular location of PAMPs engaged. For instance, it has been shown that endosomal TLR4 signaling induces type I IFN expression while similar engagement at the plasma membrane leads to the production of type III IFNs[47,48].

PRR activation by the pathogens subsequently upregulates the mRNA levels of specific IRFs, which belong to a family of nine transcription factors termed interferon regulatory factors (IRF-1 through 9)[49,50]. In the canonical model, it is understood that IRF-3 is first to be activated post PRR activation, leading to the induction of IFN-β. Downstream signaling of IFN-β then stimulates the first transcriptional wave of interferon stimulated genes (ISGs), which include the

IFN-inducible transcriptional factor IRF-7[51]. In a positive feedback fashion, the activation of IRF-7 leads to further induction of multiple IFN-α subtypes, leading to a signaling cascade. Notably, in certain cell types, IRF-5 and IRF-7 have been shown to be involved in the initial induction of type I IFNs. Similarly, type III IFNs are also induced by IRF-3 and/or IRF-7[52]. IFN-λ1 has also been shown to be induced by IRF-1[53]. The distinct IRF induction profiles of specific IFN types and/or subtypes are speculated to affect the kinetics and magnitude of inflammatory responses to viral infection *in vivo*[54].

**1.05: Type I vs III Interferon signaling exhibits overlapping but distinct features**

While type I and III IFNs induce an overlapping transcriptional profile of antiviral, anti-proliferative and immunomodulatory genes, there are significant differences between type I and III IFN signaling responses. Firstly, there appears to be a spatial division of labor between type I and III IFNs by virtue of their receptor tissue distributions and abundance[55]. Type III IFN receptors are expressed primarily on non-hematologic cells especially of epithelial origins, which are concentrated at anatomic barrier sites such as respiratory, gastrointestinal, and reproductive tracts[56-58]. Conversely, type I IFN receptors are universally expressed on all somatic cells[59]. While type I IFNs respond efficiently to innumerable viruses such as West Nile Virus (WNV), Herpes Simplex Virus (HSV), Dengue fever (DENV) and vesicular stomatitis virus (VSV), type III IFNs play a more prominent role in protecting and reacting against enteric viruses such as norovirus, reovirus and rotavirus owing to the high level of IFN-λR1 receptor expression on epithelial cells[60-62]. From a therapeutic standpoint, the restrictive expression of type III IFN receptors on specific cell types is a desirable feature since IFN-λs are expected to recapitulate a core set of beneficial attributes of IFN signaling without the systemic adverse side effects associated with type I IFNs.

Secondly, there are temporal differences in the induction of pro-inflammatory genes between type I and III IFNs[63]. Following a microbial challenge, type I IFNs induce a swift but transient transcriptional response of inflammatory ISGs, that peaks at ~8h post PRR detection and resolves afterwards. The negative self-regulation of type I signaling occurs via the degradation of signal-transducing IFN-αR1 receptors in a multifactorial ligand-specific manner. In a classical model, ligand binding phosphorylates the IFN-αR1 receptor at Ser535, which is necessary to recruit E3 ubiquitin ligase. The subsequent ubiquitination triggers the degradation of the receptor via lysosomal receptor proteolysis, curtailing the magnitude and duration of type I IFN signaling[64]. In addition, rapid induction of negative regulatory ISGs such as ISG15, USP18, Tyro3, Axl and Mer (TAM) receptors also plays a role in the downregulation of type I signaling[63]. On the contrary, type III IFNs mount a delayed transcriptional response that peaks at ~24h and is sustained up to 72h post-infection. From an evolutionary standpoint, such a non-overlapping temporal pattern of responses exhibited by type I and III IFNs may be tightly regulated to confer the host with a prolonged state of protection while minimizing the collateral damage to tissues due to redundant and unabated inflammation.

Thirdly, type III IFNs are considered to be generally less potent inducers of ISGs than type I IFNs. There is a core repertoire of ~90 antiviral ISGs stimulated by type I IFNs, only a subset of which is shown to be induced by type III IFNs[65-68]. Although higher concentrations of IFN-λ can expand the number of ISGs to match that induced by type I IFNs, the fold-induction level of ISGs is unaffected by increased dosage and remains lower than that seen in type I IFNs[69]. Furthermore, it should be noted that while such observation holds true for antiviral ISGs such as MX1, viperin, IFITM, IFIT and OAS family members, target cell types also influence the differential ISG induction between type I and III IFNs. For instance, IFN-λ1 induces a subset

of ISGs such as CXCL10, CXCL11, IFIT2, IFI30, and TDRD7 to a higher extent than IFN-β in human vaginal epithelial cells[70]. At first glance, Type III IFNs may seem redundant since they induce a smaller subset of ISGs compared to type I IFNs; however, a holistic examination of the spatiotemporally dependent signaling potency of type I and III IFNs provides a clue as to why type III IFN system is optimally primed to protect at anatomical barriers. Given the constant exposure to immunological insults from commensal and pathogenic microbes, the barriers require a careful balance of protective and pathological inflammatory responses. Unlike type I IFNs, type III IFNs are able to meet the challenge since type III IFN signaling is intrinsically lower in magnitude, less inflammatory, and concentrated at the epithelial sites due to the localized abundance of IFN-λ receptors than type I IFNs.

**1.06: Interferons drive gene expression through the JAK/STAT signaling pathway**

The intrinsic discrepancy between type I and III IFN signaling strength is of particular interest because the intracellular signaling machinery employed by the two systems is near identical. Unlike receptor tyrosine kinases (RTKs) including insulin, epidermal growth factor receptors (EGFR) and human epidermal growth factor receptors 2 (HER2), type I and II cytokine receptors lack intrinsic tyrosine kinase domains in the cytoplasmic regions of their polypeptide chains[71]. As a result, cytokine receptors recruit other families of protein kinases to propagate the signal to the cytoplasmic components of the cascade. Known signaling pathways activated by cytokines include MAP kinase, PI3-K, CaMKII, NF-κB, and JAK/STAT, the last of which is a crucial communication node for more than 40 cytokines and growth factors including the interferon family (Figure 2)[72,73].

There are four Janus tyrosine kinase (JAK) proteins –JAK1, JAK2, JAK3 and TYK2. All JAK proteins share seven JAK homology (JH) regions that include N-terminal FERM (JH5, 6,

and 7) and SH2 domains (JH3, JH4), that are responsible for JAK/receptor interaction, and C-terminal kinase (JH1) and catalytically inactive pseudokinase domains (JH2)[10]. In the canonical model, cytoplasmic tails of cytokine receptors are constitutively associated with a specific member of JAK protein via membrane-proximal binding sites, forming a complex that is functionally equivalent to RTKs[74-77]. Ligand binding event oligomerizes the receptors, bringing the receptor-JAK complexes into close proximity and allowing the JAKs to transphosphorylate each other at the double-tyrosine sequence within the activating loops of the kinase domain. Activated JAKs in turn phosphorylate specific tyrosine/serine residues on the cytoplasmic regions of the associated cytokine receptor, creating docking sites for the SH2 domains of signal transducers and activators of transcription (STAT) proteins[78,79].

The STAT family of proteins is composed of seven members – STAT1, STAT2, STAT3, STAT4, STAT5a, STAT5b, STAT6, that transmit signals from cytokine receptors to the nucleus[80]. Based on the current understanding, inactivated or latent STATs mainly reside in cytosol in their monomeric forms prior to cytokine stimulation[81]. During the stimulation, specific STATs are recruited to the docking sites on the receptors, where they are phosphorylated and then released to allow formation of homo-or heterodimeric STAT complexes[82,83]. These complexes then subsequently translocate to the nucleus and bind to target sequences in the genome to initiate gene transcription[73]. The JAK/STAT pathway has three major classes of negative regulators – suppressors of cytokine signaling (SOCS), protein inhibitors of activated STATs (PIAS) and protein tyrosine phosphatases (PTPs)[84-88]. These regulatory processes conspire to keep the signaling in check by promoting proteasomal degradation of JAK/receptor complexes, downregulating surface receptor density, mediating JAK/receptor dissociation and/or active transport of STATs out of the nucleus[89].

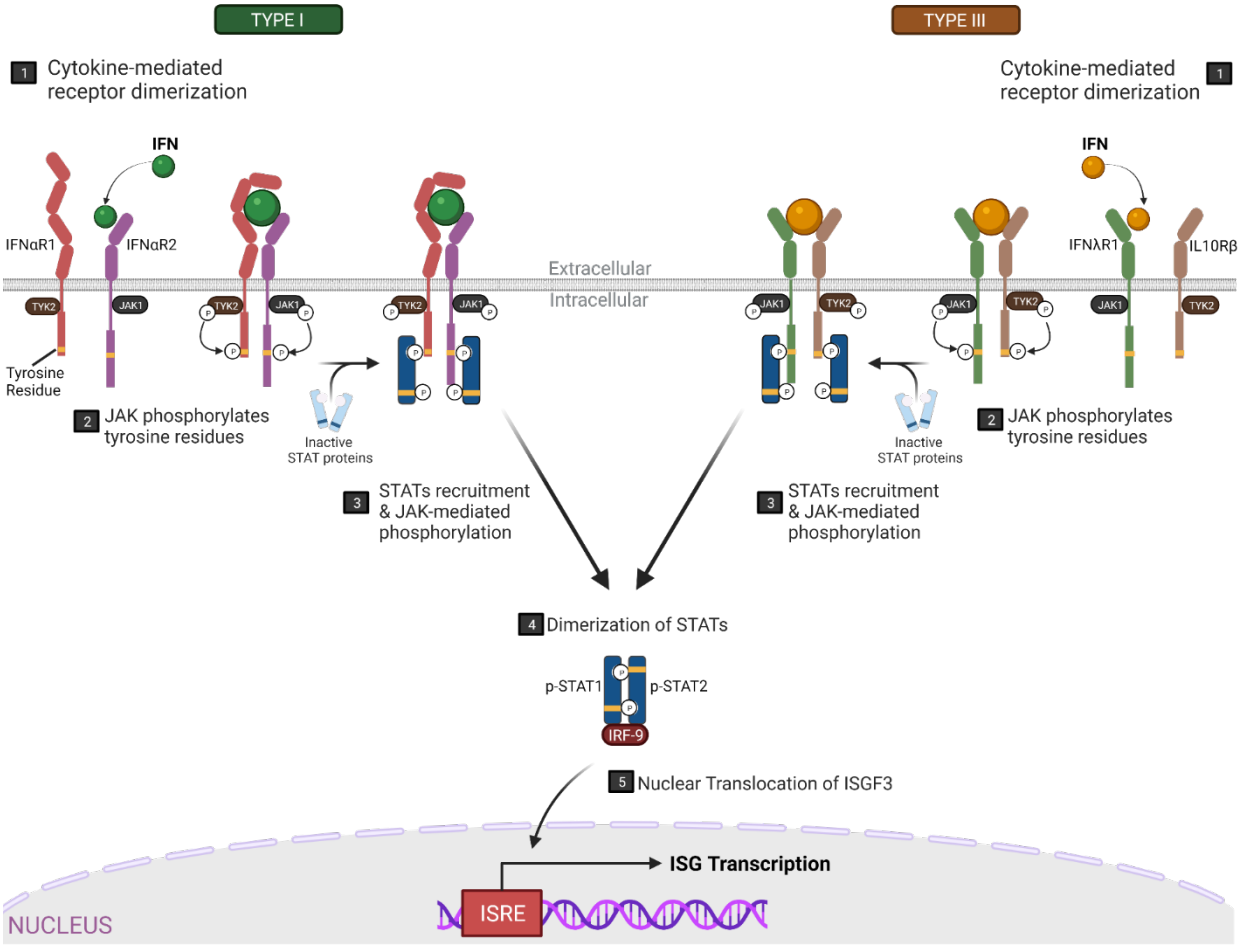


**Figure 2: A schematic diagram shows how the ligand-induced dimerization of Type I and III IFN receptors initiates signaling through the JAK-STAT intracellular pathway.** JAK, Janus Kinase. STAT, Signal Transducer and Activator of Transcription. IRF-9, Interferon-Regulatory Factor 9. ISGF3, Interferon Stimulated Gene Factor 3. ISRE, Interferon-Sensitive Response Element. ISG, Interferon Stimulated Genes.

Since there exists a limited number of JAK/STAT combinations for >40 cytokine receptors, a certain level of receptor promiscuity is expected. However, different classes of receptors have been shown to preferentially signal through one JAK or a specific JAK pairing (Figure 3) [90]. For instance, receptors required for hemopoietic development and proliferation (e.g. EPO, Leptin, GM-CSF) use JAK2 exclusively whereas class I cytokine receptors with shared $\gamma_c$ receptor (e.g. IL-2, IL-4, IL-7, IL-9, IL-15 and IL-21) utilize the JAK1/JAK3 pairing[91]. For type II IFN, IFN-γ receptors signal via JAK1/JAK2 pair, activating predominately STAT1

homodimers although STAT3 and 5 homodimers and STAT1/3 heterodimers can also be formed[32,92]. Although variations exist based on the type of target cells and viral stimulus, canonically, type I and III IFN receptors both utilize JAK1/TYK2 kinases to form the STAT1/STAT2/IRF-9 signaling complex, known collectively as ISGF3 complex (Interferon Stimulated Gene Factor 3), which is an integral transcriptional regulator of antiviral genes[93].

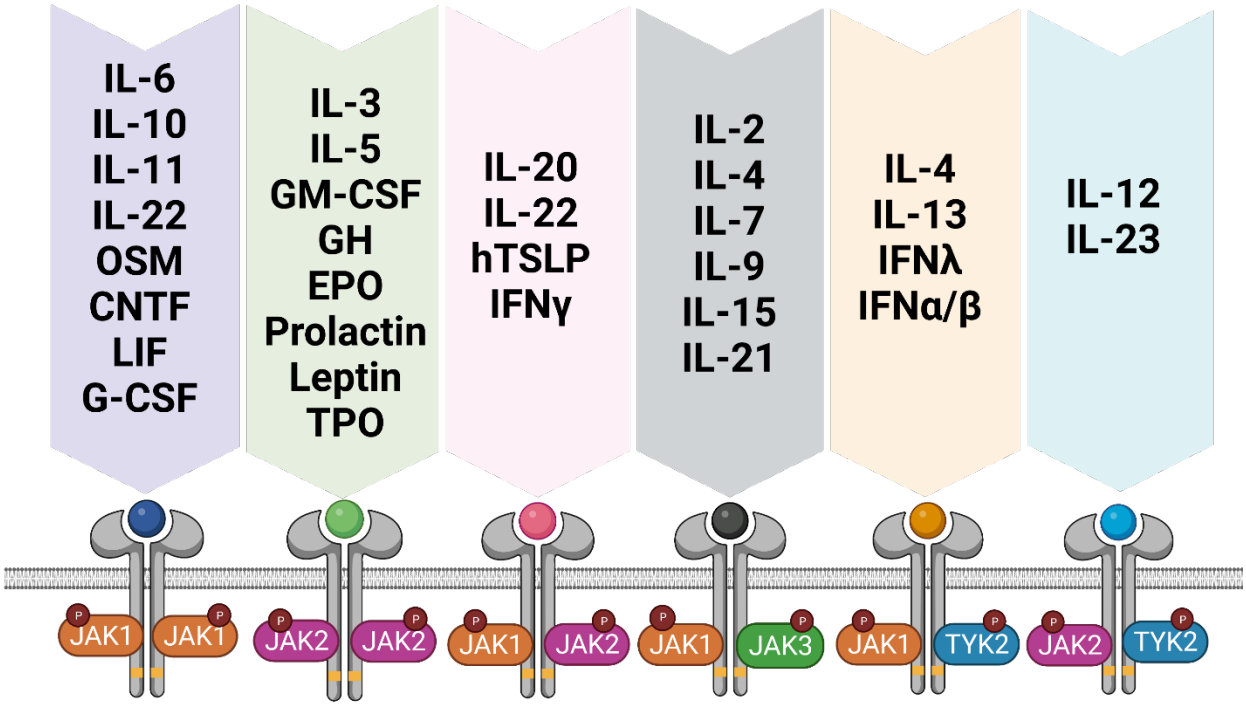


**Figure 3: Cytokine receptors show preferential signaling through a specific JAK or JAK pairing.** IL, Interleukin. OSM, Oncostatin M. CNTF, Neurotrophic Factor. LIF, Leukemia Inhibitory Factor. G-CSF, Granulocyte Colony-Stimulating Factor. GM-CSF, Granulocyte Macrophage Colony-Stimulating Factor. GH, Growth Hormone. EPO, Erythropoietin. TPO, Thrombopoietin. hTSLP, Thymic Stromal Lymphopoietin.

**1.07: Preferential cytokine receptor-JAK pairings raise fundamental questions**

The obligate relationship that exists between cytokine receptors and the JAK family proteins raises several important questions. Firstly, the driving factor behind this restrictive relationship is unanswered. If the JAK proteins solely serve to activate the receptors via phosphorylation of the cytoplasmic tyrosine residues, then any JAK with a kinase domain should

suffice for cytokine receptor signaling[94]. In other words, if chimeric receptors are engineered with swapped intracellular domains that bind a non-cognate JAK, such altered receptor/JAK axis should not affect downstream gene expression profiles, affirming that the functions provided by JAKs are generic and hence, the choice of JAKs is inconsequential. The reverse can also hold true. The non-canonical pathway forced by swapping of cytoplasmic domains can lead to modifications or deletions in specific functions of a given cytokine[73]. In that case, it would implicate that each member of JAK family holds specific structural and functional cues that have direct consequences on the outcomes of the cytokine signaling.

Secondly, it remains unclear how a small family of JAKs is able to cross-react with a large number of receptors while retaining sufficient specificity to prevent errant signaling. As of this writing, there are only a few reported structures (PDBID: 5LO4, 5IXD) featuring partial intracellular polypeptide chains of cytokine receptors in complex with N-terminal FERM and SH2 domains of JAKs[74,95]. It is also unknown if or how the intracellular domain of receptors reorients with respect to the associated JAKs before, during, and after ligand stimulation. Ultimately, carefully preserved snapshots of native full-length cytokine receptors in complex with JAK structures pose a major structural frontier in our attempt to gain a better understanding of receptor-JAK relationships.

Thirdly, there appears to be significant distinctions in the gene expression profiles generated by receptors that employ seemingly identical JAK/STAT combinations. For instance, both IL-10 and IL-6 activate the JAK1/STAT3 pathway in stimulated macrophages[96,97]. Despite the identical intracellular signal propagation pathway, the downstream outputs of signaling from these receptors are distinct with few overlapped genes. The core set of IL-10 activated genes is

anti-inflammatory in nature whereas that of IL-6 is markedly pro-inflammatory, which suggests that there may be other unexplored factors governing the machinations of the receptor/JAK axis.

### 1.08: Receptor-JAK interactions may account for the differences between type I and III Interferons

The notion that distinctions exist for receptors utilizing an identical JAK/STAT pathway, while raising several fundamental questions, also opens up new venues in interrogating the mechanisms behind differential signaling strengths of type I and III IFNs. As mentioned previously, the intracellular signaling machinery used by type I and III IFNs is identical. However, given that the extracellular complexes formed by type I and III IFNs have distinctly different biochemistries, the first instinct toward decoding the differences between type I and III signaling would be to probe the interactions of cytokines with the receptor ectodomains[33]. It is well-characterized that the type I IFNs form more stable, higher-affinity complexes with their receptors compared to type III IFNs. Although different type I IFNs display varying degrees of receptor binding affinity ($K_d$ values ranging from 0.5- 5μM for IFN-αR1 and 0.4- 5nM for IFN-αR2), IFN-ω (as a benchmark of activity for type I IFNs) binds IFN-αR1 with 0.4μM affinity and IFN-αR2 with 2nM affinity[98,99]. On the other hand, IFN-λ3, which induces the most potent antiviral response within the type III family with an EC50 value ~60 fold over that of IFN-λ2, binds IL-10Rβ with indeterminably low affinity (>μM) and IFN-λR1 with 0.85μM affinity[42,100-102]. While the stability of the extracellular ligand-receptor complexes is a contributing factor to the downstream signaling outputs, it has been shown that engineered IFN-λ ligands with higher receptor affinities exhibit limited effects on bridging the potency gap between type I and III IFNs[100]. In a previous study, a high affinity variant of IFN-λ3 (termed H11) was engineered to increase the overall stability of the IFN-λ ternary complex by 150-fold compared to the wild-

type. While H11 was able to improve the antiviral activity in Huh 7.5 cells infected with hepatitis C virus (HCV) by 12-fold compared to IFN-λ3, it remained 10-fold weaker than IFN-ω [100].

In Hap1 cells, H11 showed a 100-fold improvement in the EC50 (half maximal effective concentration) for downstream phospho-STAT1 signaling, effectively matching the type I IFN-ω in terms of sensitivity. However, the maximum signaling potency ($E_{max}$) remained unaffected by the increased complex stability. Both H11 and wild-type IFN-λ3 displayed $E_{max}$ values ~30% of that afforded by IFN-ω. A comparative study of anti-proliferative activities in Huh7.5 cells showed little activity by type III IFNs regardless of binding affinity. However, when the same cells are transduced to overexpress IFN-λR1, robust anti-proliferative activity was observed with H11 significantly outperforming the wild-type[100]. The studies indicate that the stability of the extracellular ligand-receptor complexes, while a contributing factor to the magnitude and/or sensitivity of IFN responses, does not fully account for the differences. Although receptor abundance also seems to be a limiting factor for certain IFN activities, we speculate that there may be other characteristics inherent to receptor/JAK interactions that can further shed light on the differential functional capabilities of type I and III IFNs.

**1.09: Interrogation of receptor-JAK interaction takes a two-pronged approach**

In the absence of reported structures of any full-length cytokine receptor-JAK protein complexes, the all-important details delineating the similarities and differences between type I and type III IFN receptor- JAK interactions are not well understood and have yet to be explored. There are two central aspects to the receptor-JAK association that may be pertinent to the differential signaling outputs of type I vs III IFNs – 1) the affinity of the interaction, and 2) the geometrical alignment of the proximal JAKs during the cytokine stimulation. A previous study using the IFN-αR1/IL-12 receptor system has shown that different receptor chains compete for

the same JAK protein, which exists in a limited amount[103]. Cells overexpressing IL-12 receptors showed a markedly reduced transcriptional response to stimulation with IFN-α due to TYK2 kinase being competed off of IFN-αR1 receptor intracellular domain. We therefore hypothesize that the affinity of receptor-JAK interaction can influence IFN signaling output in two distinct ways (Figure 4). Firstly, if type I IFN receptors bind with higher affinity to their respective JAKs compared to the type III receptors (IFN-λR1, IFN-αR2 to JAK1 and IFN-αR1, IL-10Rβ to TYK2), it is possible that at any given time, there are fewer 'active' type III IFN receptors than type I IFN receptors available for signaling within a cell. Secondly, the affinity of the interaction defines the overall stability of the receptor-JAK complex, and it remains to be seen if the downstream signaling potency is a function of complex stability. In order to address these questions experimentally, we propose to engineer type I and III IFN receptors with higher affinities for JAKs in an effort to compare the functional outcomes of IFN signaling between the native and engineered receptors.

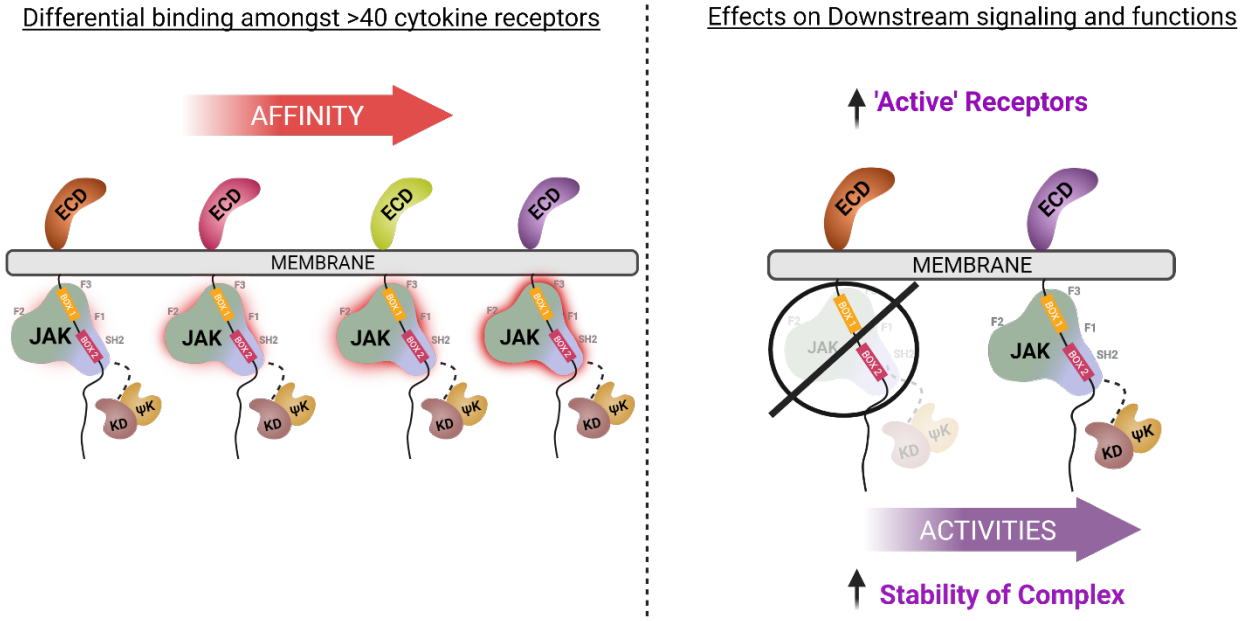


**Figure 4: A schematic diagram depicts a potential affinity gradient among cytokine receptors that utilize the same JAK for signaling (left) and how it may affect the strength of downstream signaling and functions (right).**

A similar line of questioning follows regarding the spatial arrangement of the JAKs when the receptors orient themselves upon cytokine binding (Figure 5). It is unknown whether an optimal geometrical alignment exists for the juxtaposed JAKs within the same heterodimeric IFN signaling complex that favors efficient transphosphorylation. Some key factors to consider include the register and proximity of the JAKs as well as the vertical distance of the JAKs from the cell membrane. The challenge is to determine if the type I IFN receptors are heterodimerized in such a way that their associated JAKs are better positioned to transmit signals downstream than type III IFN counterparts. In that case, it needs to be addressed whether the type III IFN signaling can be made more potent by fine-tuning the geometry of their intracellular signaling complex. Taken together, we hypothesize that the two-pronged approach to interrogating the receptor-JAK interaction holds the key to a more complex understanding of the differences in the signaling maneuvers between type I and III IFNs. We are optimistic that the insights from our study can not only expound upon current understanding of IFN signaling but also usher in new strategies for the clinical utilizations of type III IFNs in the future.

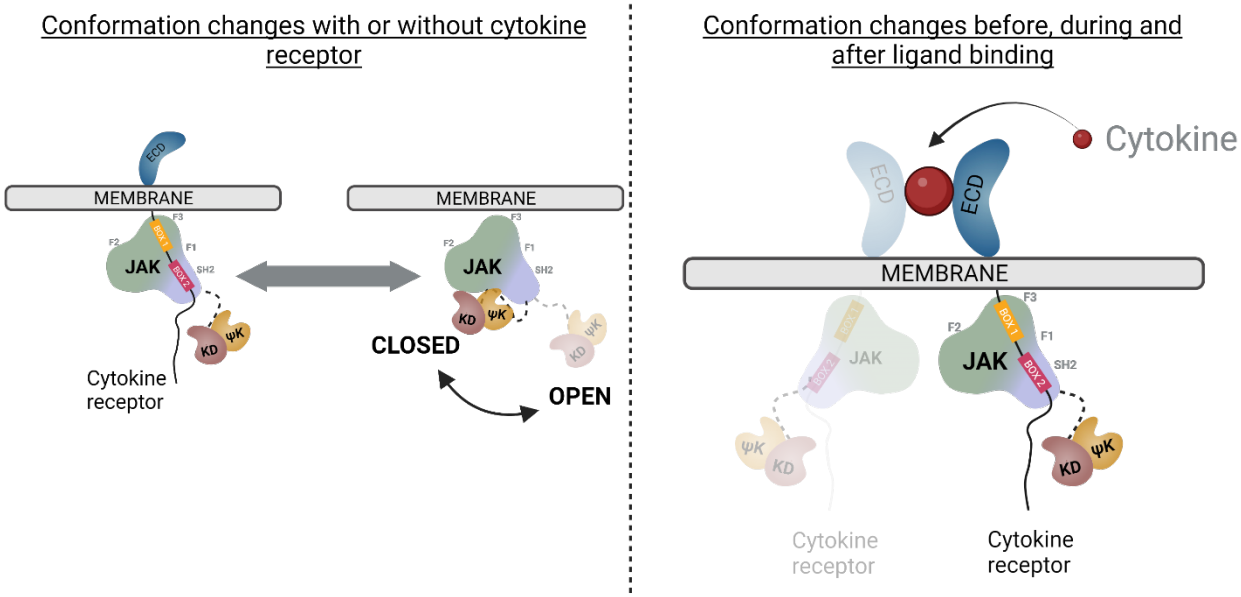


**Figure 5: A schematic diagram shows the overall conformation changes of the N and C-terminal domains of JAK when the protein is in free form vs in bound state to a cytokine**

**Figure 5, continued**

**receptor (left). The conformation of JAK may also change in response to a ligand-binding event (right).**

## Chapter 2: Materials and Methods

### 2.01 Cell lines and cell culture

Authentication of cell lines used in this study is guaranteed by the sources. SF9 cells in Sf-900™ II SFM (Gibco), Hi5 cells in Express Five™ Medium (Gibco) and HEK 293 cells in FreeStyle™ 293 Expression Medium (Gibco) were purchased from Thermo Fisher and maintained in their respective recommended media. Sf-900™ II SFM and Express Five media were supplemented with 50µg/mL gentamicin and FreeStyle™ 293 Expression medium, with 10U/mL of penicillin/streptomycin. Lenti-X 293T cells were a gift from Dr. Jun Huang of the University of Chicago and cultured in DMEM +10% fetal bovine serum. Original validation of Hap1 cells was by whole-genome sequencing and EBY100 yeast cells by genotyping and sequencing. All cell lines were checked for mycoplasma contamination prior to usage.

### 2.02 Site-saturation mutagenesis

Site-saturation mutagenesis (SSM) libraries were constructed from synthetic DNA from Twist Bioscience. For each amino acid within the targeted polypeptide chain, forward and reverse primers were designed such that PCR amplification would result in a 5′ PCR product with a degenerate NNK codon and a 3′ PCR product with a 20-nt overlap region, respectively. Amplification of ‘left’ and ‘right’ products by FF and FR primers yielded a series of template products each consisting of a degenerate NNK codon at a different residue position. For each intracellular chain, these products were pooled at equal molar ratios to create the SSM library. SSM library ‘inserts’ along with linearized pETcon3 vectors were introduced into conditioned Saccharomyces cerevisiae strain EBY100 cells by electroporation. For the complete list of primers used in the construction of SSM libraries, please refer to Table 1, 2 and 3.

### 2.03 Yeast surface display of interferon receptor intracellular domains

IFN-αR1 and Il-10Rβ receptor intracellular domains (ICDs) were displayed on yeast as previously described[104]. A Myc-tag and 3C rhinovirus protease tag were at the N and C-terminus of the displayed ICDs respectively. Staining and selection were performed via streptavidin-Alexa 647 labeled biotinylated FERM SH2 domains of JAK1 and TYK2 proteins. Separation of receptor-yeast cell population was achieved by paramagnetic anti-Alexa 647 microbeads or Streptavidin microbeads (Miltenyi). Expression on the yeast surface was determined by staining with Myc-tag mouse antibody conjugated to Alexa 647(Cell Signaling Technology). Enrichment of target yeast population was monitored by their fluorescence signal using flow cytometry (BD Accuri).

### 2.04 Protein expression and purification

IFN-ω and IFN-λ3 were expressed and purified using a baculovirus expression system, as described previously[38]. Briefly, Hi5 express insect cells were infected with a pre-titered amount of baculovirus and cultured at 28°C for 72h before being harvested for proteins. The high-affinity IFN-λ3 variant, H11, was expressed similarly in HEK 293 cells. All proteins contained C-terminal hexa-histidine tags and were isolated by Ni-NTA affinity chromatography and further purified by size exclusion chromatography on a Superdex 200 column (GE Healthcare, UK), equilibrated in 10 mM HEPES (pH 7.4) and 150 mM NaCl. Proteins were stored in buffer with 10% added glycerol as a cryoprotectant.

The FERM-SH2 domains of human JAK1 and TYK2 (residues 35-559 and 23-566 respectively) were cloned into the expression vector pAcGP67 modified to contain an N-terminal Sumo-tag followed by a 3C rhinovirus protease cut-site and a C-terminal Avi-Tag (LNDIFEAQKIEWHE). The baculovirus expression and purification in SF9 cells were as

previously described[74,76]. Briefly, Sf9 cells were infected with a pre-titered amount of virus and cultured at 28°C for 72h. The cells were then pelleted by centrifugation and resuspended in ice-cold lysis buffer containing 50mM TRIS/HCl at pH 8.5, 500mM NaCl, 5mM imidazole, 1mM TCEP, 0.25mM PMSF, EDTA-free protease inhibitor cocktail tablets (Roche) and 10% glycerol prior to dounce homogenization. Lysate was then incubated with 0.15% CHAPS (ThermoFisher) for 1h at 4°C with gentle rotation. Following detergent solubilization, the lysate was then clarified by ultracentrifugation at 75,000g for 1hr at 4°C. The supernatant was further cleared by filtration with 0.45μm filter and left to bulk bind with Ni-NTA resin overnight at 4°C with gentle stirring. The resin was collected in a polyprep column and washed with copious volumes of lysis buffer supplemented with 0.1% CHAPS and 30mM imidazole. The proteins were finally eluted in the buffer with 250mM imidazole. The concentrated protein was then purified on the Superdex 200 column equilibrated in 20mM TRIS/HCl at pH 8.8, 300mM NaCl, 1mM TCEP and 10% glycerol. The purified proteins were then enzymatically biotinylated using purified BirA enzyme before column-purification and storage. Biotinylation was confirmed by a strep-shift SDS-PAGE assay and visualized with Criterion stain free imager (Bio-Rad).

**2.05 Generation of CRISPR/Cas9 knock-out cell lines**

sgRNA sequences were designed using CHOPCHOP online CRISPR sgRNA design tool (https://chopchop.cbu.uib.no/)[105]. For each sgRNA design, top and bottom strands of oligos were custom ordered from Sigma-Aldrich. The vector for cloning sgRNA to coexpress with Cas9 enzyme (pSpCas9n(BB)-2A-Puro) was purchased from Addgene (PX462). The plasmid construction, cell transfection, validation and establishment of knock-out cell lines were performed according to the procedure outlined here[106]. The sequence-verified plasmids were used to transfect Hap1 cells cultured in DMEM supplemented with 10% FBS. Following

antibiotic selection and clonal expansion of transfected cells, individual clones were screened for loss of type I or III IFN induced cell signaling. Clones displaying loss of function were then Sanger sequenced to detect indels. Validated knock-out cell lines were stored at -80°C in 10% DMSO supplemented media for future use. Please refer to Table 4 for details regarding sgRNA sequences and primers used to create these cell lines.

**2.06 Generation of lentivirus transduced mutant cell lines**

For the generation of lentiviral pseudoparticles, Lenti-X 293T cells were plated in 6-well plates at a density of 0.6 x $10^6$ cell/mL overnight. Next day, the cells were co-transfected with a plasmid encoding a cytokine receptor of interest, packaging and envelope plasmids at a fixed ratio of 0.75/0.5/0.26µg per well respectively. For each transfection, 4.5uL Fugene HD transfection reagent (Promega) was combined with 1.5µg total DNA in 100µL of Opti-MEM (GIBCO). Cells were incubated with the transfection media for 3 days with added fresh media on day 2 before the supernatants were collected, passed through a 0.45µm filter and stored at -80°C in 10% FBS supplemented media. 1mL of lentivirus containing supernatant was used to transduce 1 x $10^6$ target cells with fresh media being added to transduced cells every 2-3 days. On day 5, stable expression of target receptors was determined by staining against their N-terminal Flag-tag with mouse anti-Flag conjugated to Alexa 488 (Abcam).

**2.07 *In vitro* pSTAT1 signaling assay**

Cells were plated overnight in a 96-well format at a density of 10,000 cells/well and treated with serial dilutions of IFN-ω, wild-type IFN-λ3 or its high-affinity variant (H11) for 15 min at 37°C. The medium was removed, and cells were detached with Trypsin (Gibco) for 5 min at 37°C. Cells were transferred to a deep-well 96-well block containing an equal volume of 4% (w/v) paraformaldehyde (PFA) solution and incubated for 15 min at room temperature. Fixed

cells were then washed three times with phosphate-buffered saline containing 0.5% (w/v) BSA (PBSA), resuspended in 100% methanol for 1h on ice. Cells were next stained with Alexa 488 conjugated pSTAT1 antibody (Cell Signaling Technology). The half-maximal response concentration ($EC_{50}$) and $E_{max}$ of signaling was determined by fitting the data to a sigmoidal dose–response curve (GraphPad Prism v.9).

### 2.08 *In vitro* antiviral assay

Recombinant VSV harboring a green fluorescent protein (GFP) transgene (VSV-GFP) was a gift from Horvath lab, Northwestern University. HEK 293 cells were seeded at a density of 12,500 cells/well in a 96 well format and after 48h, the cells were then treated with serial dilutions of IFN-ω, wild-type IFN-λ3 or its high-affinity variant (H11). Cell medium containing IFN treatment was removed after 24h and VSV-GFP virus diluted in serum-free media was added to the cells at 80,000 PFU/well. At 18h post-VSV-GFP infection, the cytopathic effects (CPE) were measured via a fluorescence plate reader[107].

### 2.09 *In vitro* anti-proliferative assay

Cells were plated overnight in a 96-well format at a density of 10,000 cells/well. On the following day, the media was replaced with fresh media containing serial dilutions of IFN-ω, wild-type IFN-λ3 or its high-affinity variant (H11). Four days post IFN-treatment, cell density was measured using CellTiter-Glo (Promega) according to the manufacturer's protocol.

### 2.10 Quantification of gene induction by RT-qPCR

For measuring gene induction, 600,000 cells were plated in a 6-well format overnight and treated with 100nM each of IFN-ω, wild-type IFN-λ3 or IFN-λ3 H11 for 6 or 24h on the following day. RNA was extracted with the Monarch Total RNA miniprep kit T2010 (NEB), 1ug of which was converted to cDNA by a RT-PCR reaction using the High Capacity RNA-to-cDNA

kit (Applied Biosystems). ISG induction relative to the untreated controls in wild-type cells was measured by qPCR assay (PowerSYBR Green PCR Master Mix, Applied Biosystems) on a QuantStudio 3 instrument (Thermo Fisher Scientific) following manufacturer's instructions. Transcription quantification was normalized to 18S internal controls. Primers were purchased from Sigma-Aldrich. Please refer to Table 5 for a complete list of primers used.

### 2.11 RNA sequencing and Transcriptome Analysis

Whole human transcriptome sequencing over 20,000 genes was performed on the Ion GeneStudio S5 Plus System using the Ion Ampliseq™ Transcriptome Gene Expression Kit (Thermo Fisher). Transcriptome libraries were barcoded, templated and sequenced using either Ion 550™ Kit-Chef and Ion 550 Chip Kit as one 16-plex library pool or Ion 540™ Kit-Chef and Ion 540 Chip Kit as one 8-plex library pool (Thermo Fisher). Two independent sequencing analyses were performed on a panel of eight samples. The RNA samples included in each panel are extracted from the following categories – untreated WT IFN-λR1 cells, untreated IFN-λR1 3A cells, IFNω treated WT IFN-λR1 cells, IFNω treated IFN-λR1 3A cells, IFN-λ3 treated WT IFN-λR1 cells, IFN-λ3 treated IFN-λR1 3A cells, H11 treated WT IFN-λR1 cells and H11 treated IFN-λR1 3A cells. Gene mapping and analysis was performed using Ion Torrent Suite™ v.5.10.0 (Thermo Fisher). All data analysis was generated in MATLAB v.R2018b (MathWorks).

### 2.12 Statistical Analyses

The results were presented as means ± standard deviation (STD). The statistical significance of differences between the groups was determined by two-way ANOVA analysis with subsequent correction for multiple comparisons using Tukey test. All statistical analyses were performed using GraphPad 9.0.2. Differences were considered statistically significant at

****$p < 0.0001$, ***$p < 0.001$, **$p < 0.01$ and * $p < 0.05$. The statistical analysis of experiments with biological replicates is detailed in figures' legends.

## Chapter 3: Results

### 3.01 Intracellular fragments of cytokine receptors displayed on yeast surface bind recombinant JAKs

As described previously, the heterodimeric signaling complexes formed by class II cytokine receptors invariably consist of two receptors with different cytoplasmic chain-lengths[25]. The receptors with short intracellular domains (<100 residues) such as IFN-γR2, IL10-Rβ and IFN-αR1 typically bind to either JAK2 or TYK2. Conversely, those with long intracellular domains (>200 residues) such as IFN-γR1, IFN-λR1 and IFN-αR2 interact exclusively with JAK1. Mutagenesis studies first identified that certain regions on these unstructured cytoplasmic domains are critical for JAK association and kinase activation[108]. The first region termed Box 1 is a membrane-proximal proline rich motif located approximately 10 residues from the C-terminus of the transmembrane region of the receptor. Sequence alignment analysis of six long-chain class II receptors indicates that the Pro-Xaa-Xaa-Leu-Xaa-Phe (PXXLXF) motif found within Box 1 is highly conserved, indicating the importance of Box 1 in JAK1 recruitment and subsequent activation[109-112]. The second region, Box 2, locates 10-40 residues downstream to Box 1 and is rich in hydrophobic residues[113-115]. Mutations or relocation of these two segments further from the membrane have been shown to disrupt JAK binding and signaling[116]. However, due to a low sequence homology among receptor intracellular sequences, a consensus theory of the molecular logic behind receptor-JAK interactions remains elusive[95].

The molecular basis of IFN-αR1/TYK2 interaction was one of the first to be characterized[117,118]. While a peptide sequence within the cytoplasmic domain of IFN-αR1 (residues 479-511) was identified to be crucial for TYK2 binding, structural information of the

interaction did not become available until more than two decades later when a crystal structure was obtained for the partial intracellular domain (ICD) of IFN-αR1 (residues 465-512) in complex with the FERM-SH2 domain of TYK2 (residues 23-583)[76,114,119]. The box 2 motif –a segment of four hydrophobic residues generally followed by one to two negatively charged residues –is shown to be weakly conserved in multiple cytokines and JAKs across orthologs from multiple species[76,108]. The study indicated that a classical proline-rich box 1 motif was not necessary for the receptor/TYK2 association[76].

On the contrary, the structural and mutagenesis studies of IFN-λR1/JAK1 showed that a classical box 1 and a putative box 2 regions were both required for high-affinity JAK1 binding[74]. The effective dissociation constant between JAK1 FERM-SH2 (residues 35-559) and the partial ICD of IFN-λR1 (residues 250-299) was determined to be 70.5 ± 0.2 nM. Deletion of box 1 region of the ICD (residues 250-270) completely abolished binding to JAK1 while deletion of box 2 (residues 270-299) significantly reduced the binding affinity to 1.23 ± 0.01 μM. This indicates that box 1 serves as the primary binding site for JAK1 whereas box 2 contributes to the complex stability via hydrophobic interactions[74].

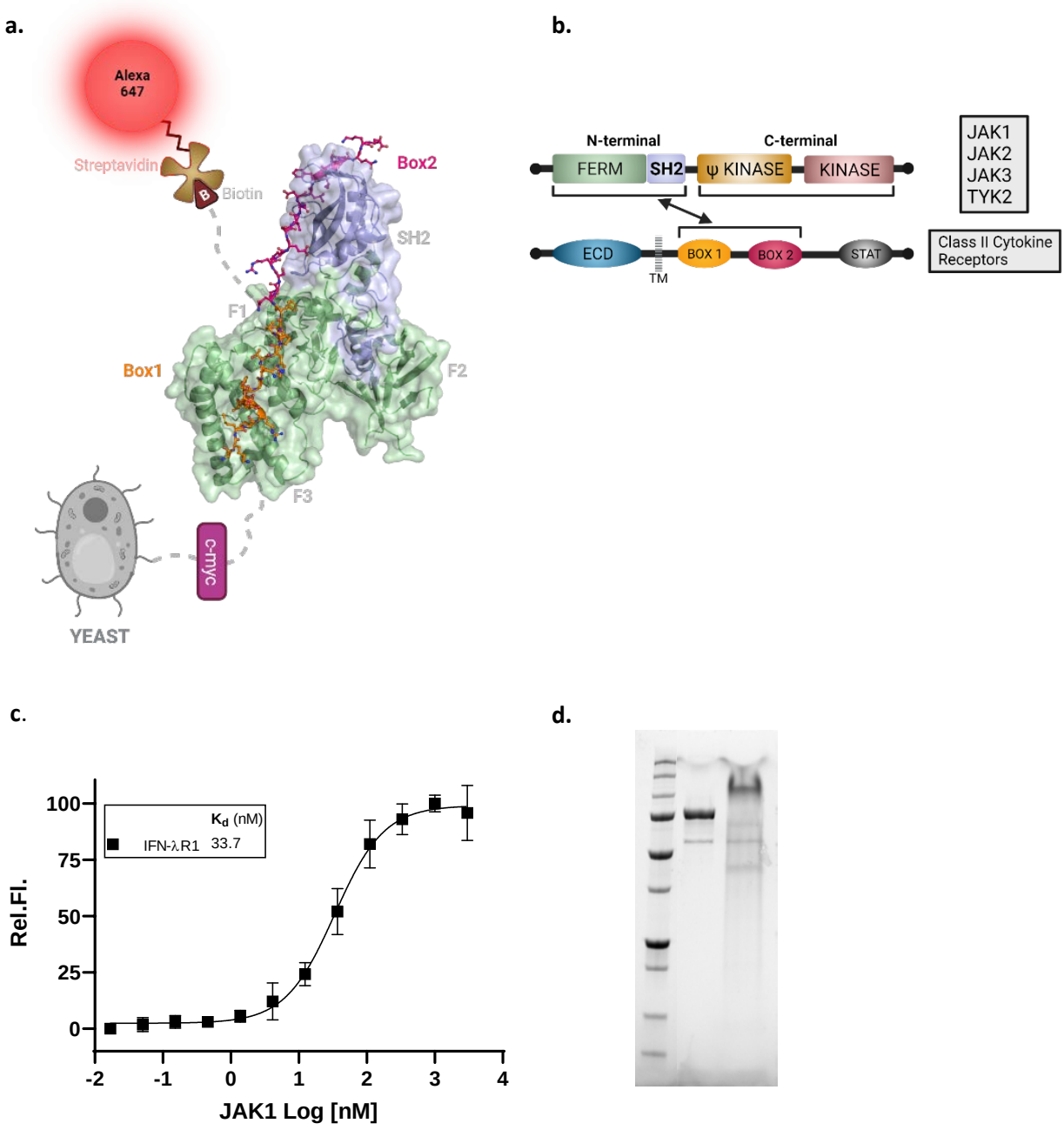


**Figure 6: The intracellular domain of IFN-λR1 is displayed on yeast surface for determination of receptor binding affinity to JAK1. a**, Schematic representation of yeast display and binding assay with biotinylated JAK1 FERM-SH2 (PDB: 5L04) stained with Alexa 647-streptavidin conjugate. **b**, Schematic diagram of class II cytokine receptors and JAKs showing the domains involved in the binding interface. JAK pseudokinase and kinase domains are noted ϕ–KD and KD respectively. **c**, Relative quantification of fluorescence staining in yeast cells incubated with varying concentrations of JAK1 by flow cytometry. $K_d$ values were determined by fitting to a non-linear sigmoidal dose-response model. Error bars represent ± SEM (n=3). **d**, Representative SDS-PAGE gel-shift assay showing complete biotinylation of JAK1.

**Figure 6, continued**

The lanes indicate purified and N-terminal biotinylated JAK1 by itself (left) and with streptavidin (SA) (right).

These prior studies gave us a basis for determining potential box 1 and box 2 regions for all four type I and III IFN receptors of interest for our studies –IFN-λR1, IL10-Rβ, IFN-αR1 and IFN-αR2. We used directed evolution with yeast surface display to engineer high-affinity receptors. First, we determined the validity of the approach by confirming that the cytoplasmic domains of receptors displayed on the cell surface are capable of binding their respective JAK proteins. As a benchmark of functional activity, we displayed the partial ICD of IFN-λR1 (residues 250-299) on yeast and determined the 'on yeast' dissociation constant of the ICD/JAK1 interaction (Figure 6a). It should be noted that JAK1 FERM-SH2 subdomain utilized in our study is Sumo-tagged at the N-terminus to enhance expression and solubility. Since our $K_d$ value of 33.7 ± 1.6 nM was similar to the reported value (70.5 ± 0.2 nM) determined by surface plasmon resonance, it indicated that yeast display can be reliably utilized as a means for evaluating receptor ICD/JAK interactions and more importantly, engineering cytokine receptors via directed evolution (Figure 6c).

**3.02 ICDs of IFN-λR1 and IFN-αR2 bind JAK1 FERM-SH2 with similar affinity**

Previous studies have shown that in type I IFN signaling complexes, IFN-αR2 functions analogously to IFN-λR1 in terms of its intracellular tethering of JAK1[120]. While sequence homology analysis shows that the box 1 motif (PXXLXF) is conserved in the ICD of IFN-αR2, there is minimal interaction between the box 1 domain (residues 268-292) and JAK1. Mutations within this region have little effects on the activation of JAK1. Instead, the speculative 'box 2' region localized to a site 10-30 residues C-terminal to Box 1 (residues 300-346) is responsible

for the majority of the binding interaction. Although the box 1 domain is minimally involved in the recruitment of JAK1, it is possible that the segment is still necessary for full kinase activation. This stands in contrast to the structural and mutagenesis studies conducted on IFN-λR1/JAK1 system, where the box 1 is indispensable to JAK1 binding with the box 2 in a complex-stabilizing role[74].

So far, there is no reported data on the binding affinity between the ICD of IFN-αR2 and JAK1. In order to evaluate whether the interchanged roles of the box 1 and box 2 domains within the cytoplasmic domain of IFN-αR2 have a significant effect on the binding interaction with JAK1, we sought to determine the dissociation constant of the interaction using yeast display. When displayed on yeast, the combined box 1 and box 2 region of IFN-αR2 cytoplasmic tail (residues 265-375) bound to the FERM-SH2 domains of JAK1 with an affinity of 61.07 ± 0.9 nM (Figure 7). Firstly, this result indicates that JAK1 binds with comparable affinities to both IFN-αR2 and IFN-λR1 regardless of the contradictory molecular details involved in the interactions. Secondly, the low dissociation constants of the interactions (within nM range) suggest that both wild-type IFN-λR1 and IFN-αR2 bind with sufficiently high and near equivalent affinities to JAK1, and hence, it seems improbable that these interactions are limiting factors in downstream signaling. Consequently, we determined that further engineering of these two receptors to augment their respective JAK1 binding affinities would elicit little gain in IFN signaling potency. Thirdly, it follows that the JAK1 binding halves of the receptor complexes are unlikely to contribute to the differences in the strength of type I and III IFN signaling through differential binding affinities.

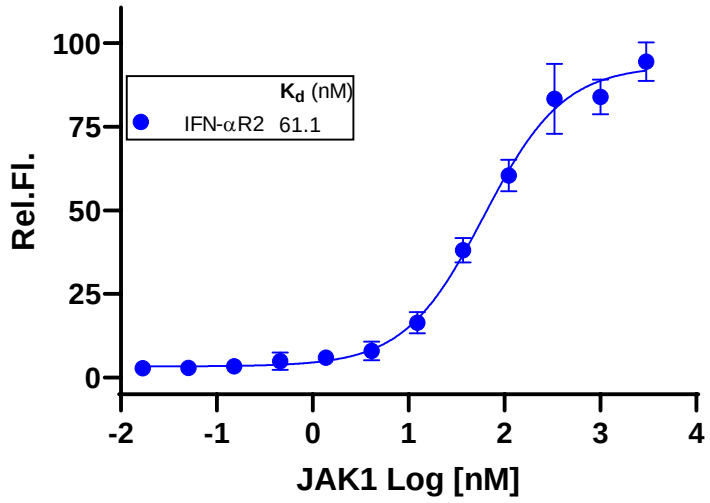


**Figure 7: IFN-αR2 ICD displayed on yeast shows high-affinity binding to JAK1.** Relative quantification of fluorescence staining in yeast cells displaying IFN-αR2 ICD incubated with varying concentrations of JAK1 by flow cytometry. $K_d$ values were determined by fitting to a non-linear sigmoidal dose-response model. Error bars represent ± SEM (n=3).

### 3.03 ICDs of IFN-αR1 and IL-10Rβ bind weakly to TYK2 FERM-SH2

The other two receptors that comprise the heterodimeric complexes of type I and III IFN signaling, IFN-αR1 and IL-10Rβ respectively, are associated with TYK2 kinase in their cytoplasmic domains[117,118,121-123]. In order to directly compare the binding affinities of the receptors to TYK2 FERM-SH2, we displayed the entire intracellular regions of IFN-αR1 and IL-10Rβ (residues 459-557 and 243-325 respectively) on yeast surface and titrated against the recombinant N-terminal Sumo-tagged TYK2 FERM-SH2 domain (residues 23-583). Within the range of concentration titrated, both receptor ICDs displayed weak affinities to TYK2 (>μM estimated dissociation constants) (Figure 8c). Notably, IFN-αR1 ICD showed a comparatively greater affinity toward TYK2 than IL-10Rβ ICD, which showed little appreciable affinity.

Collectively, our results imply that JAK1 kinase is more tightly associated with the cytoplasmic domains of its receptors than TYK2 within both type I and III IFN complexes.

However, it remains unclear whether this feature is universal to all JAK1/TYK2 utilizing heterodimeric receptors. These results also raise the question as to whether such a sizable gap in affinities between these TYK2-associated receptors has direct functional consequences on their respective downstream signaling. We hypothesized that engineering IFN-αR1 and IL-10Rβ receptors with higher affinities for TYK2 would inform us on two fundamental aspects of receptor-JAK interactions. Firstly, a functional comparison between the wild-type and engineered receptors for each IFN family can elucidate whether the improved receptor affinity to TYK2 can enhance the biological activities of their corresponding ligands. Secondly, we can establish the extent to which a gain in signaling potency, if observed, from the use of engineered IL-10Rβ receptor contributes to narrowing the functional gap between type I and III IFNs.

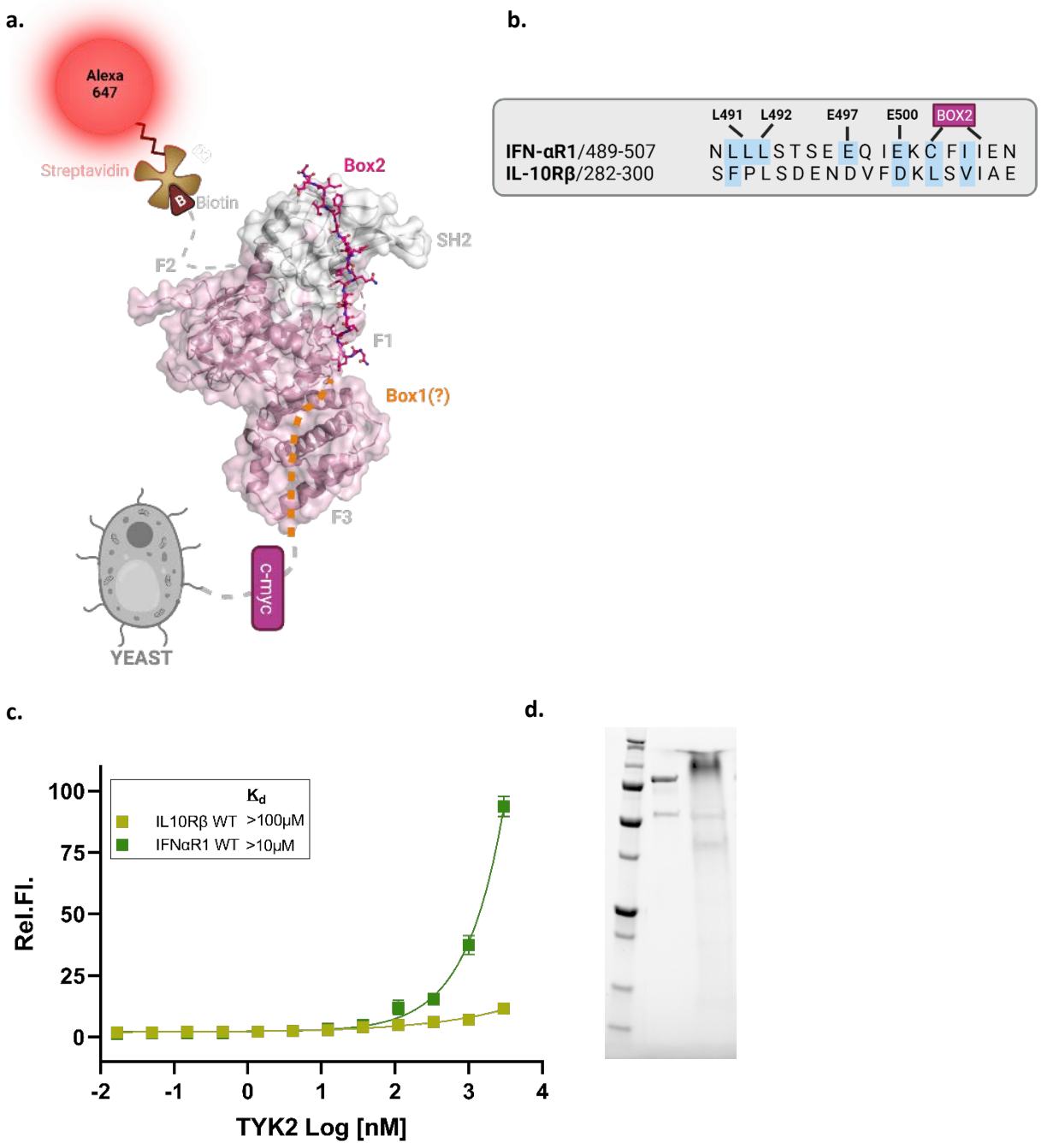


**Figure 8: On-yeast titrations with biotinylated TYK2 show weak binding affinities from ICDs of IFN-αR1 and IL-10Rβ. a**, Schematic representation of 'on-yeast' binding assay with biotinylated TYK2 FERM-SH2 (PDB: 4PO6) stained with Alexa 647-streptavidin conjugate. **b**, Conservation analysis on the putative box 2 sequences of TYK-2 receptor-binding interface with key residues highlighted in blue. **c**, Relative quantification of fluorescence staining in yeast cells displaying either IFN-αR1 or IL-10Rβ ICDs incubated with varying concentrations of TYK2 by flow cytometry. Kd values were estimated by fitting to a non-linear sigmoidal dose-response model. Error bars represent ± SEM (n=3). **d**, Representative SDS-PAGE gel-shift assay showing

**Figure 8, continued**

complete biotinylation of TYK2. The lanes indicate purified and N-terminal biotinylated TYK2 by itself (left) and with streptavidin (SA) (right).

**3.04 IFN-αR1 can be engineered to bind TYK2 with high affinity**

Prior studies have shown that the 33 amino-acid spanning intracellular region (residues 479-511) of IFN-αR1 is the minimally required motif to bind TYK2[114]. Mutational analyses indicate that the surface contacts mediated by IFN-R1α at Leu491, Leu492, Glu497, and Glu500 are essential to maintain the stability of the receptor-TYK2 complex. The structure of TYK2 FERM-SH2 in complex with the partial ICD (residues 465-512) which was obtained much later, has provided a molecular basis for the interaction interface[95]. The di-leucine motif (Leu491 and Leu492) is shown to be required to interact with a hydrophobic groove formed by the second subdomain within the FERM domain whereas the Glu497 and Glu500 form significant anchor points via forming hydrogen bonds and salt bridges with TYK2.

Based on the structural model, the putative box 2 motif (Cys-Xaa-Ile-Ile) is located five residues carboxy-terminal to Glu497 (residues 502-505). These hydrophobic residues are buried in a groove formed within the SH2 domain of TYK2 and are considered to be key for binding TYK2 with high affinity and fidelity[95]. Although IFN-αR1 ICD lacks a classical proline-rich box 1 region, *in vitro* immunoblotting studies indicate that the deletion of the cytoplasmic juxtamembrane region (residues 459-478) reduces receptor binding to TYK2[114]. This finding leads us to hypothesize that the aforementioned region may present a suitable basis for further engineering via affinity maturation. Hence, we selected the 31 amino-acid polypeptide segment C-terminal to the transmembrane domain of the receptor (residues 459-489) and subjected it to site-saturation mutagenesis.

The yeast display library underwent five rounds of selection against N-terminal Sumo-tagged TYK2 FERM-SH2 with increasing stringency in selection criteria to enrich for yeast subpopulations with high binding affinity to TYK2 (Figure 9a and b). After the final round, we conducted a 96-well screen for the highest-affinity variants. Out of the twelve clones selected and sequenced, we identified five clones that had distinct sets of point mutations. The finalized mutant, referred to as IFN-αR1m, had the fewest number (one mutation) of affinity-enhancing substitutions (C463W) and more importantly, exhibited the highest affinity toward TYK2 ($K_d$ of 175.8 ±12.5nM) which represented at least 10-fold improvement in affinity over the wild-type receptor (Figure 9d).

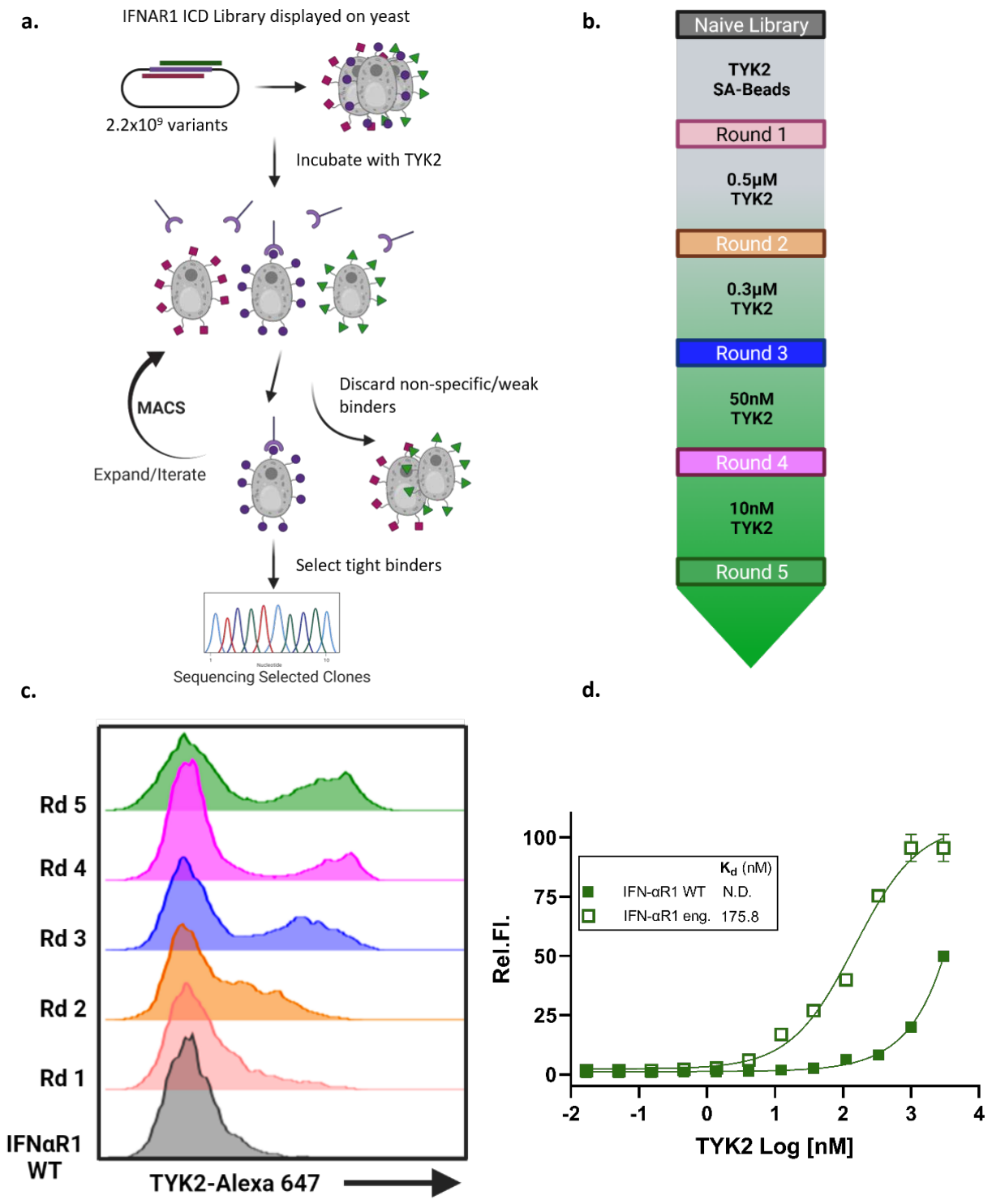


**Figure 9: High-affinity IFN-αR1 receptor is engineered via affinity-maturation approach using yeast display. a**, Schematic representations of yeast-display directed evolution process. **b**, Schematic diagram of conditions used in each round of selection. **c**, Representative histogram assessing staining in cells incubated with monomeric TYK2 at 200nM by flow cytometry of

**Figure 9, continued**

yeast display library after each round of selection. **d**, Relative quantification of fluorescence staining in yeast cells displaying either the wild-type or engineered IFN-αR1 ICDs incubated with varying concentrations of TYK2. $K_d$ values were determined by fitting to a non-linear sigmoidal dose-response model. Error bars represent ± SEM (n=3).

### 3.05 IL-10Rβ requires two libraries of engineering to bind TYK2 with a comparable affinity as engineered IFN-αR1 receptor

In an analogous fashion, we then endeavored to engineer an IL-10Rβ receptor with improved binding affinity toward TYK2. Due to the poor sequence homology between IFN-αR1 and IL-10Rβ ICDs, the cytoplasmic di-leucine sequence and the hydrophobic box 2 motif observed in IFN-αR1 are both absent in the IL-10Rβ sequence[95]. Hence, we selected the 19 amino-acid segment (residues 282-300) which locates 40 residues downstream from the carboxy-terminal of the transmembrane region to serve as an exploratory box 2-containing site. The first generation of variants were obtained by subjecting this region of interest to site-saturation mutagenesis. After four rounds of selection using yeast display, the highest-affinity mutants were selected from a 96-well functional screen and sequenced (Figure 10a and b). Nine individual clones were then displayed on yeast surface and titrated against TYK2. The selected mutant, referred to as RD42, showed improved binding affinity to TYK2 ($K_d$ in ~μM range) and had two amino acid substitutions (F283H, S296E).

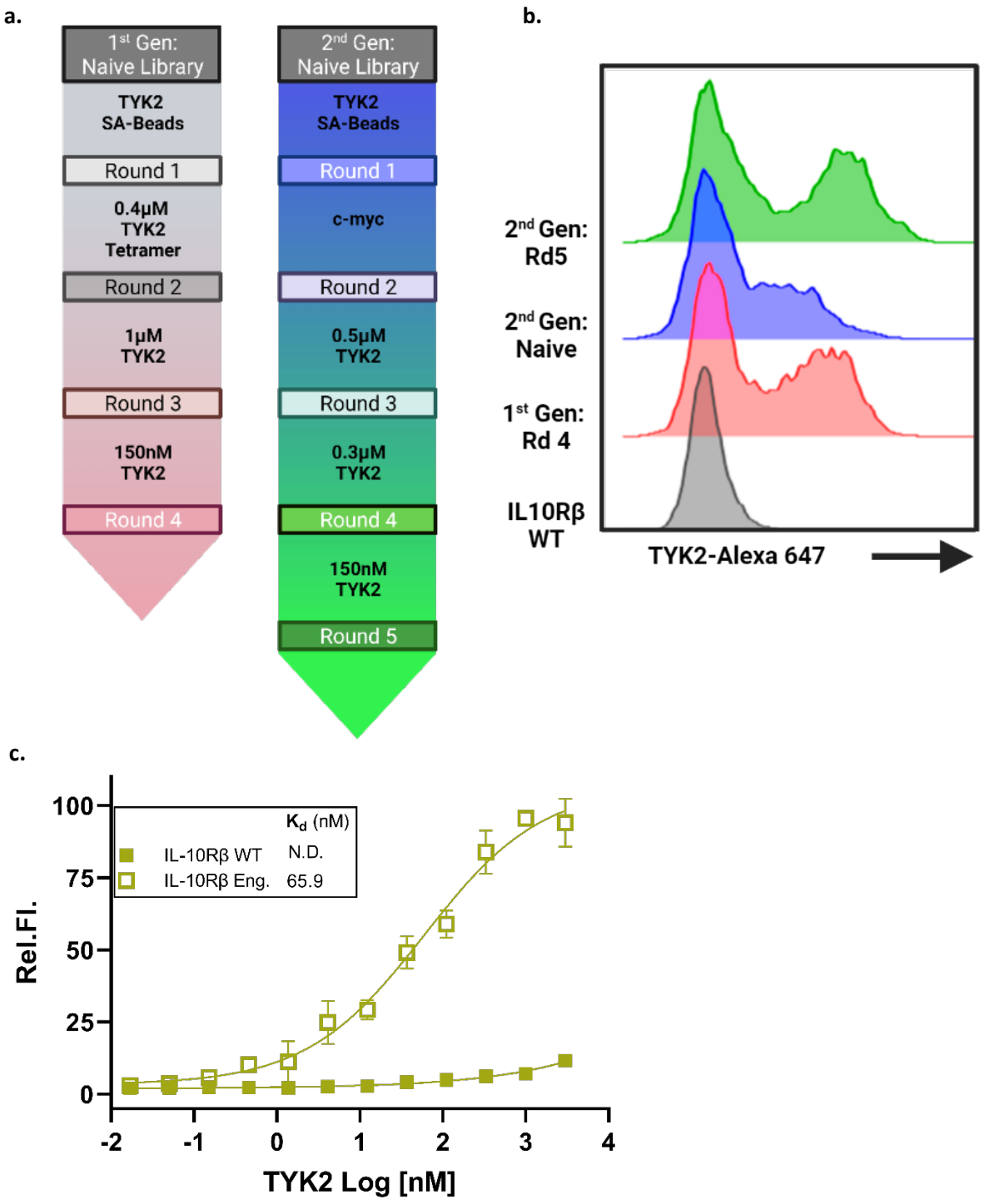


**Figure 10: High-affinity IL-10Rβ receptor is engineered after two generations of yeast-display directed evolution process. a,** Schematic diagram of conditions used in each round of selection for two generations of library. **b**, Representative histogram assessing staining in cells incubated with monomeric TYK2 at 200nM by flow cytometry of yeast display library prior to and at the end of selection process for each generation. **c**, Relative quantification of fluorescence staining in yeast cells displaying either the wild-type or engineered IL-10Rβ ICDs incubated

**Figure 10, continued**

with varying concentrations of TYK2 by flow cytometry. $K_d$ values were estimated by fitting to a non-linear sigmoidal dose-response model. Error bars represent ± SEM (n=3).

In order to match the binding affinities of the engineered IFN-αR1 and IL-10Rβ ICDs to TYK2, we subjected the first-generation mutant for further affinity maturation. This time, we targeted the membrane proximal region of 39 amino acids (residues 243-281), which would represent a de facto box 1-containing region. In an analogous manner to the previous generation, the yeast library underwent five rounds of selection against TYK2 (Figure 10a and b). Afterwards, we sequenced selected clones and conducted 'on-yeast' binding studies against TYK2. The finalized variant, termed IL-10Rβm, added two mutations (W246N, N260W) to the existing ones, bringing the total number of mutations to four. The dissociation constant was determined to be 65.9 ±5.4nM, marking a dramatic improvement in TYK2 binding affinity over the wild type (Figure 10c).

### 3.06 Engineered high-affinity IFN-αR1 receptor fails to improve *in vitro* phospho-STAT1 signaling

With engineered high-affinity receptors for TYK2 in place, we next sought to determine if the enhanced affinity in the receptor-TYK2 axis translated to significant changes in the IFN-inducible biological responses. As a direct downstream target in cytokine-mediated JAK/STAT pathway, we aimed to compare the level of activated STAT1 or phosphorylated STAT1 (pSTAT1) proteins in cells expressing either the wild-type or engineered IFN-αR1 receptors[124]. Despite being present in low copies (100-5000 molecules/cell), IFN-αR1 is expressed by nearly all nucleated cells, necessitating the use of a receptor knock-out cell line to accurately access any changes in signaling mediated by the engineered IFN-αR1 receptor *in vitro*[125]. We therefore

created a CRISPR-Cas9-mediated IFN-αR1 gene knock-out (KO) Hap1 cell line for the *in vitro* signaling assay. In order to best mimic natural receptor expression in cells, the lentiviral vectors were constructed with native IFN-αR1 signaling peptide. We then transduced the KO cells with lentiviruses that induce stable expression of either the wild-type or engineered IFN-αR1 receptor (Figure 11a and b). These modified cell lines were next stimulated with either type I IFN, IFN-ω, or type III IFN, IFN-λ3 with the latter serving as a functional control. All data points were normalized with respect to receptor expression in order to eliminate any interference from differences in receptor expression levels.

We determined that the $EC_{50}$ values of pSTAT1 signaling induced by IFN-ω were identical between cells expressing either the wild-type or high-affinity IFN-αR1 receptor, which were ~3 logs greater than the values recorded for IFN-λ3 (Figure 11c). In addition, the strength of IFN signaling as measured by the $E_{max}$ value was also observed to be unchanged with respect to the improved affinity of IFN-αR1 to TYK2. Stimulation with IFN-ω resulted in the same potency maxima in both cell lines – roughly 3-fold over those achieved with IFN-λ3, which is consistent with previous literature[39,100,126]. For type I IFNs, our results indicate that neither the sensitivity nor strength of signaling can be tuned by improving the affinity with which the receptor ICD binds TYK2.

We speculate that the observed lack of improvement may indicate two likely causes. Firstly, there is evidence that various distinct receptors compete for their shared JAK proteins out of a limited cytosolic stock[103]. From our 'on yeast' binding study against TYK2, we have determined that IFN-αR1 ICD already binds with much higher affinity to TYK2 than IL-10Rβ ICD. It therefore reasons that IFN-αR1 receptor with its inherent advantage in recruiting TYK2 over other competing receptors such as IL-10Rβ, can gain little from an improved affinity to

TYK2. In other words, the limited availability of TYK2 minimally affects the transcriptional outputs of comparatively higher-affinity receptors such as IFN-αR1. The second reason may be due to a speculative functional cap to IFN signaling, which likely involves a carefully curated network of molecular checks and balances. From an evolutionary standpoint, such a limit may exist to check unbridled inflammation in response to potential gain-of-function somatic mutations in the cytokine JAK/STAT pathway. Given the vast disparity in signaling strength between type I and III IFNs however, it is likely that the enhanced affinity of receptor-JAK interaction may play a more tangible role in improving the downstream signaling for type III IFNs.

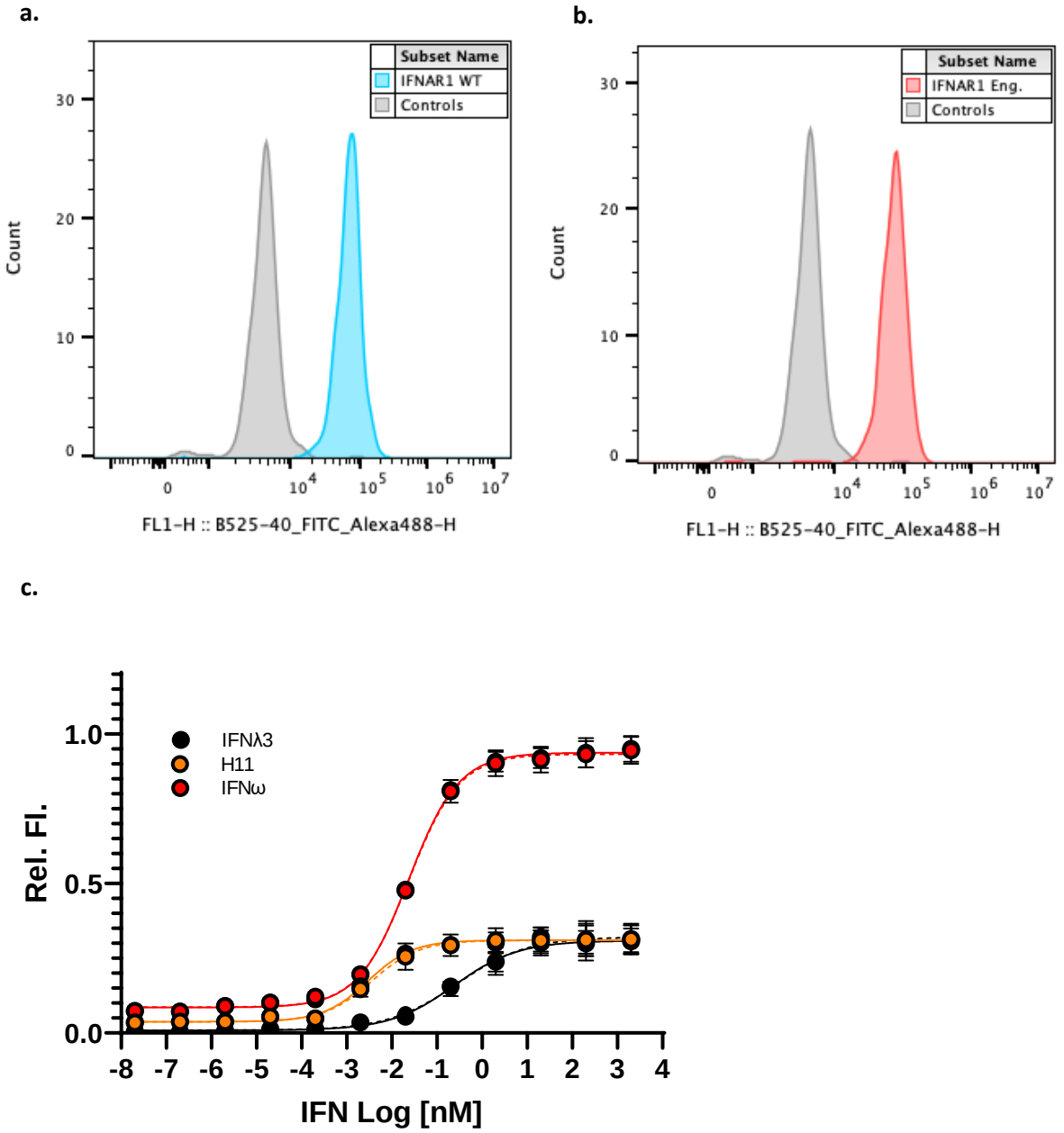


**Figure 11: Type I IFN signaling is immune to the improved affinity of IFN-αR1 to TYK2.** **a**, Histograms depicting the surface levels of the wild-type (blue) or **b**, high-affinity IFN-αR1 receptors (red) relative to non-transduced controls (grey). The IFN-αR1 KO Hap1 cells were transduced to stably express N-terminal Flag-tagged wild-type or mutant IFN-αR1 receptors, which were stained with anti-Flag conjugated to Alexa 488 and analyzed by flow cytometry. **c**, Relative quantification of pSTAT1 staining in cells expressing either the wild-type (dashed line) or engineered IFN-αR1 receptors (solid line) by flow cytometry. Cells were treated with serial

**Figure 11, Continued**

dilutions of IFN-ω (red), IFN-λ3 (black) or H11 (orange) for 15 min. Curves were fit to a first-order logistic model. Error bars represent ± SEM (n=3).

### 3.07 Engineered high-affinity IL-10Rβ receptor improves *in vitro* phospho-STAT1 signaling

In an effort to test our hypothesis, we next conducted the *in vitro* pSTAT1 signaling assay with the engineered IL-10Rβ receptor expressing cell line. Since IL-10Rβ, similar to IFN-αR1, is universally expressed in all somatic cells, we created a IL-10Rβ-KO Hap1 cell line using CRISPR-Cas9[127]. Again, the native signaling peptide was used in constructing the lentiviral vectors used to transduce the KO cells (Figure 12a and b). Cells were then stimulated with IFN-ω, the wild-type IFN-λ3 or its engineered high-affinity variant, H11, which was previously reported[100]. As described in the preceding section, all data points included in our analysis were normalized with respect to receptor expression.

In both cell lines expressing the wild-type or mutant IL-10Rβ, the $EC_{50}$ values of pSTAT1 signaling induced by H11 were ~100-fold over those induced by the wild-type IFN-λ3, which is consistent with previously reported data[100]. While the EC50 values of both type III IFN ligands were only marginally improved in mutant cell line over wild-type, the pSTAT1 $E_{max}$ values, on the contrary, were increased by ~25% in cells signaling through IL-10Rβm receptor. Interestingly, both the $EC_{50}$ and $E_{max}$ values of pSTAT1 signaling by IFN-ω were appreciably diminished in mutant cell line compared to the wild-type (Figure 12c and d). Collectively, it is evident that while the improved affinity of IL-10Rβ toward TYK2 minimally affects the sensitivity of ligand-inducible signaling in type III IFNs, it plays a significant role in determining the strength of downstream signaling.

While this stands in apparent contradiction to our previous findings with the engineered IFN-αR1 receptor, for which we failed to observe any further gain in downstream pSTAT1 signaling, we argue that these results, evaluated collectively, support our earlier hypothesis. First, we can make the case that the engineered IL-10Rβ receptors are able to induce more potent pSTAT1 response by siphoning TYK2 proteins off their competitors. It is supported by an evident decrease in the sensitivity and potency of type I IFN signaling in the mutant IL-10Rβ cell lines. When IL-10Rβ has been 'activated' via acquisition of TYK2, the added stability of the IL-10Rβ-TYK2 complex may also play a role in the downstream signaling. Secondly, we proposed earlier that the kinetics and potency of type I IFN signaling have likely reached a maximum plateau and are therefore intractable to further attempts at improving the system. Indeed, our results show that type III IFN signaling responded positively to the improved affinity between IL-10Rβ and TYK2. It should be noted here that the improvements targeted at the affinity of the receptor-JAK interaction only managed to narrow, not eliminate, the potency gap between type I and III IFNs. This notion indicates a need to explore beyond the affinity side of receptor-JAK interactions if we are to fully account for the differences between type I and III JAK/STAT pathways.

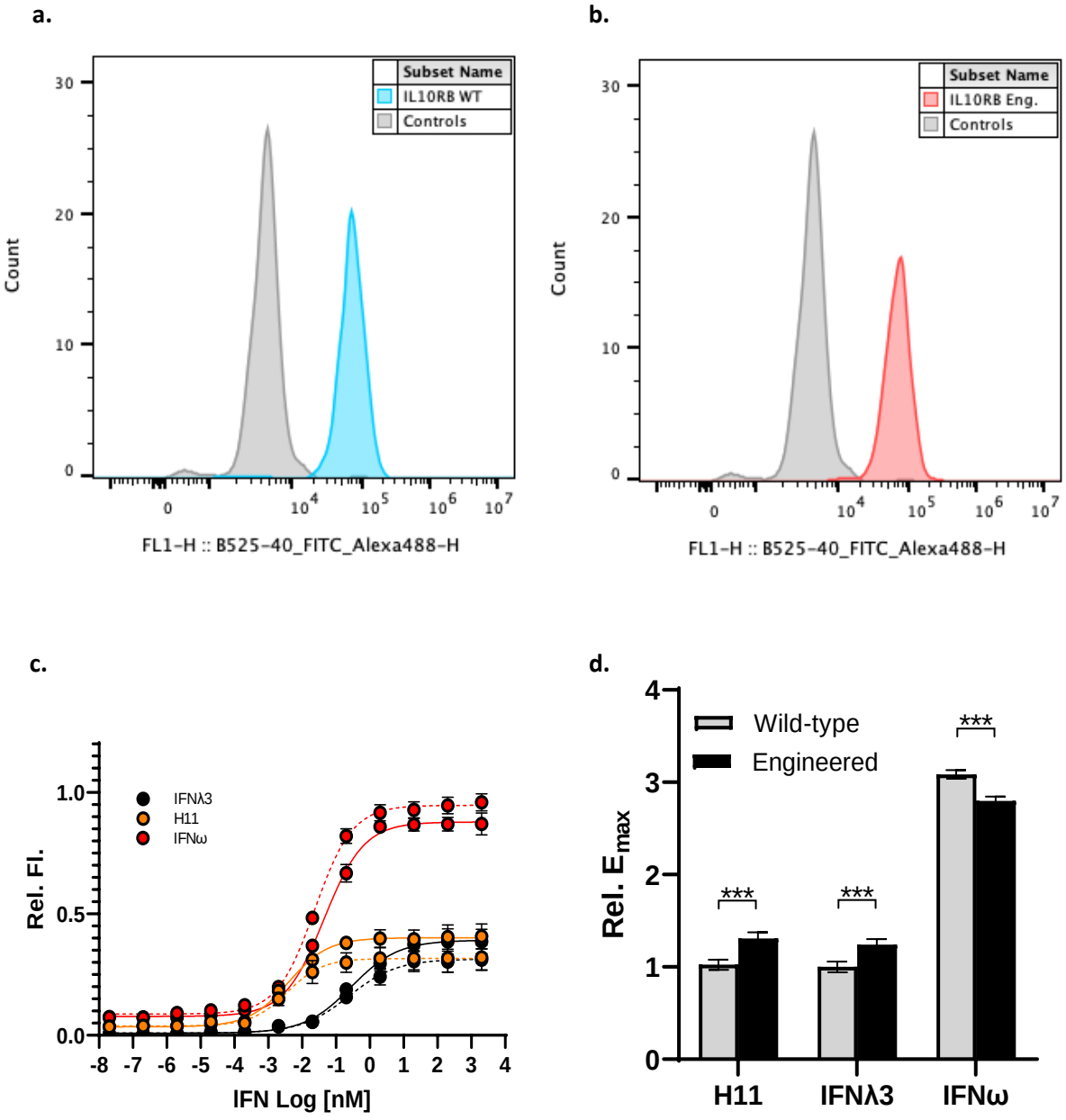


**Figure 12: Cells expressing high-affinity IL-10Rβ receptors induce stronger pSTAT1 responses. a**, Histograms depicting the surface levels of the wild-type (blue) or **b**, high-affinity IL-10Rβ receptors (red) relative to non-transduced controls (grey). The IL-10Rβ KO Hap1 cells were transduced to stably express N-terminal Flag-tagged wild-type or mutant IL-10Rβ receptors, which were stained with anti-Flag conjugated to Alexa 488 and analyzed by flow cytometry. **c**, Relative quantification of pSTAT1 staining in cells expressing either the wild-type (dashed line) or engineered IFN-αR1 receptors (solid line) by flow cytometry. Cells were treated with serial dilutions of IFN-ω (red), IFN-λ3 (black) or H11 (orange) for 15 min. Curves were fit to a first-order logistic model. **d**, Comparison of $E_{max}$ values induced in the wild-type (grey) vs

**Figure 12, continued**

engineered IL-10Rβ (black) expressing cells by 2μM of each indicated IFN. All values are normalized to the wild-type receptor expressing cells treated with IFN-λ3. Error bars represent ± SEM (n=3). *p < 0.05; **p < 0.01; ***p < 0.001; ****p < 0.0001.

### 3.08 Geometry of proximal JAKs within the IFN-λ heterodimeric complex affects biological activities

For the next chapter of our interrogation of receptor-JAK interactions, we turned our focus to the role that the intracellular geometry of heterodimeric complexes plays in IFN signaling. Previous studies have shown that the efficiency of cytokine signaling via the JAK/STAT pathway depends on proper orientation of the participating receptors[128-130]. Upon ligand-induced oligomerization of the receptors, the intracellularly associated JAKs must be brought within a specific proximity in order for reciprocal transphosphorylation to occur. This is best demonstrated in a study using chimeric receptors of interchanged extracellular EpoR (erythropoietin receptor) and intracellular IFN-γR1 domains or vice versa, referred to as EpoR/IFN-γR1 and IFN-γR1/EpoR[131]. Epo (erythropoietin) signals via forming a homodimeric complex of EpoR receptors associated with JAK2[132]. Conversely, IFN-γ is a natural non-covalent homodimer and requires two sets of IFN-γR1 and IFN-γR2 receptors, intracellularly tethered to JAK1 and JAK2 respectively, in order to signal[133,134]. Even in the absence of IFN-γR2 receptor and its associated JAK2, the results show that EpoR/IFN-γR1 receptor is able to signal upon stimulation with Epo via JAK1. From the known Epo/EpoR complex structure, it is inferred that Epo binding brings the intracellular IFN-γR1 domains, and JAK1 proteins by extension, into closer proximity than in a canonical IFN-γ signaling complex in which the JAK1 proteins are separated by more than 27Å. This is consistent with the next finding that IFN-γR1/EpoR fails to

signal for IFN-γ. In this case, the JAK2 kinase domains are simply located too far apart in the cytosol to induce transphosphorylation[131].

However, a close proximity of complex sharing JAKs is not a guarantee of successful JAK autoactivation. The register of complex-sharing JAKs may be another key factor. A previous study has shown that when EpoR receptors are subjected to alanine-insertion mutagenesis in which 1-4 alanine residues are inserted within the juxtamembrane region, the resultant rotations in the register of the receptor intracellular domains cause significant differentiations in *in vitro* Epo downstream signaling[135]. EpoR with one added alanine residue displayed a near complete loss of cell proliferative activity whereas three added alanine residues recovered the activity to match that of the wild type. The findings also suggest that graduated changes in the spatial alignment of cytokine receptor ICDs can be achieved by manipulating the helical structure of transmembrane regions. We hypothesize that we can adapt this approach to IFN-λR1 expressing cells to observe how the register twists of the ICD modulate type III IFN signaling.

We used human embryonic kidney (HEK) 293 cells which are normally non-responsive to type III IFNs due to their very low expression levels of IFN-λR1 but become responsive after they have been transduced to express exogenous IFN-λR1[136,137]. The lentiviral vectors were constructed for the wild-type and mutant IFN-λR1 receptors which have either 1, 2, 3 or 4 alanine residues inserted after V242 within the juxtamembrane region (Figure 13a and b). Then we measured the pSTAT1 signaling in transduced HEK 293 cells treated with IFN-ω, wild-type IFN-λ3 or high-affinity IFN-λ3, H11. As predicted, the $E_{max}$ values of pSTAT1 induced by IFN-ω were largely unaffected in all cell lines (Figure 13c). In cells treated with IFN-λs, maximum displacements in signaling amplitude were recorded for cells expressing 2 or 3 alanine inserted

IFN-λR1 receptors. Cells with 2 alanine inserted IFN-λR1 receptors displayed near obliteration of pSTAT1 signaling whereas cells with 3 alanine inserted IFN-λR1 receptors increased the $E_{max}$ value by ~65% compared to that of the wild-type receptor expressing cells. Some improvements were also observed in cells with 1 or 4 alanine inserted IFN-λR1 receptors, with latter cells outperforming the former. Both wild-type and high-affinity IFNλ3 ligands displayed similar trends in the modulation of signaling strength among differently mutated cell lines. In accordance with existing literature, we found that type III IFNs trailed significantly behind type I IFNs in terms of pSTAT1 signaling potency; our experimental $E_{max}$ of IFN-ω was ~2.67 fold over that of wild-type IFN-λ3 in wild-type IFN-λR1 expressing cells[100]. Notably, the fold difference is reduced to ~1.5 (44% reduction) by having IFN-λ3 signal through the mutant IFN-λR1 with three added alanine residues. It should be noted that while the signaling maxima for both IFN-λ3 or H11 ligands were markedly increased by the change in the receptor orientation, $EC_{50}$ values remained largely unperturbed (Figure 13d and e). These results imply that the geometry of the intracellular receptor-JAK complex determines the strength of the signaling while the stability of the extracellular receptor-ligand complex, the sensitivity.

Based on the results, we can argue that the relative positioning of intracellular JAKs in native heterodimeric complexes of type III IFNs is not optimized toward efficient downstream signaling. We have shown here that we can effectively rotate the register of IFN-λR1 ICD by introducing helical twists in the juxtamembrane region of the receptor. The consequences of the resultant rotations are particularly evident in cells expressing 2 alanine inserted IFN-λR1 receptors. In this cell line, pSTAT1 signaling is virtually lost due to a near 180-degree flip in the orientation of JAK1 with respect to TYK2, which likely poses a physical impossibility for the JAKs to transphosphorylate. In contrast, when the register of IFN-λR1 ICD is offset by a

predicted 327-degree from its native position by the insertion of 3 alanine residues in the transmembrane region, we observed a significant gain in the signaling amplitude. Taken collectively, we reason that for optimal type III IFN signaling, the complex-sharing JAKs must not only be within a defined distance but also that the proximity must be complemented with proper register.

Additionally, it should be noted that in introducing additional alanine residues to optimize the register, we also appended to the vertical distance of the JAK1 binding motif (box 1 and 2 subdomain) from the membrane. The combined box 1 and 2 region in 3 alanine inserted IFN-λR1 receptors is approximately 5Å further away from the membrane than that in native receptors. Although a significant fold improvement in signaling amplitude was still observed for 3 alanine inserted IFN-λR1 receptors, it is unclear whether the increment occurred despite or regardless of the additional vertical distance. To determine this experimentally, an IFN-λ mimetic ligand can be engineered so that it complexes with IFN-λR1 in an orientation that displaces the receptor from that of the canonical complex by the same degree. We postulate that the change in orientation of the extracellular complex can be transmitted to its cytosolic region in a fashion analogous to a previous study conducted on EpoR[129]. A comparative study of the $E_{max}$ values induced by the engineered IFN-λ ligand vs the engineered 3 alanine inserted IFN-λR1 receptor should further elucidate the role of vertical distance in type III IFN signaling.

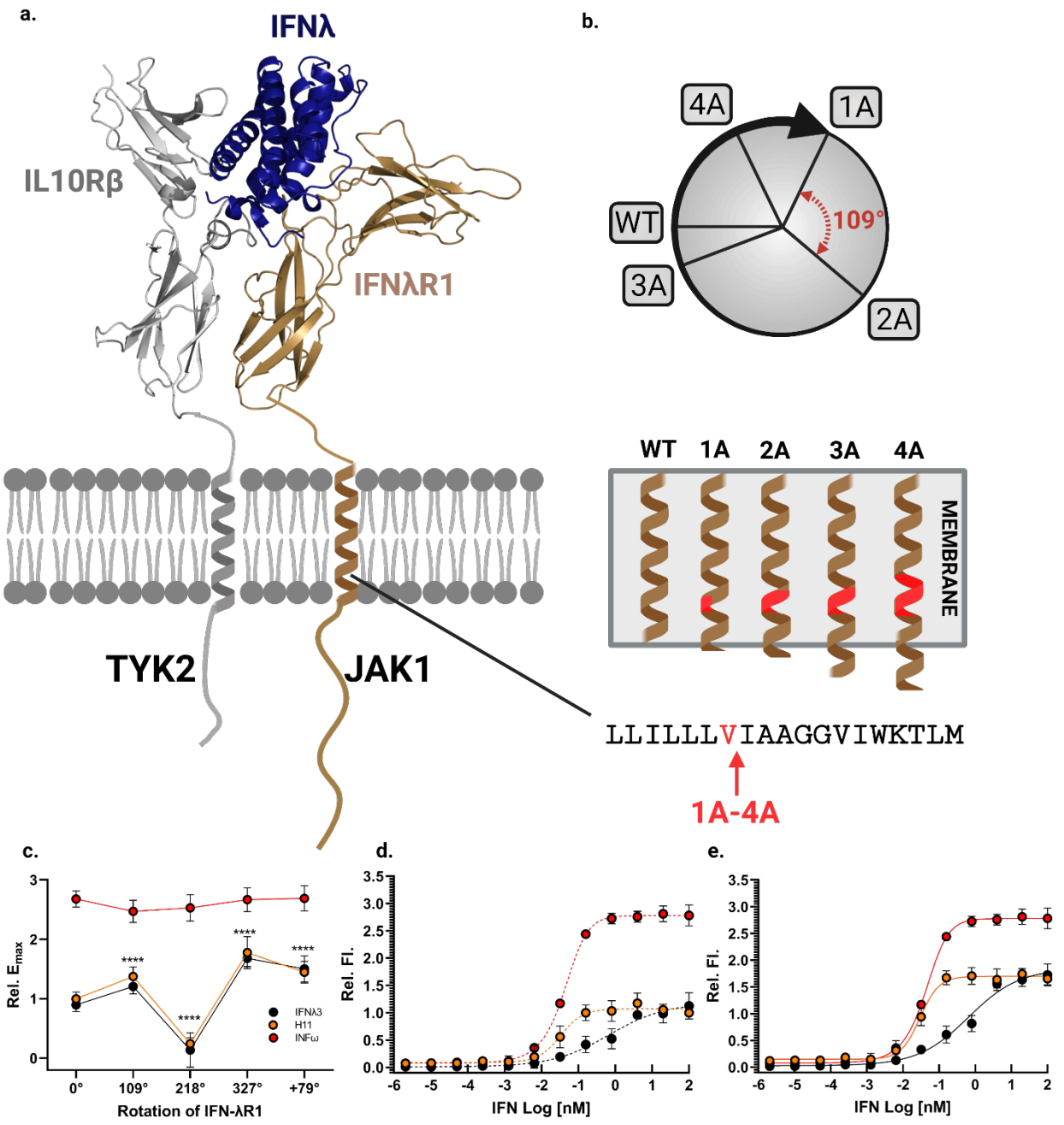


**Figure 13: Modifications in the geometry of IFN-λR1 modulate pSTAT1 responses. a,** Schematic diagram of alanine insertion mutagenesis of the IFN-λR1 transmembrane domain. **b,** α-helical wheel projections of the register rotations introduced by addition of each alanine residue are shown (top) and alanine residues (ranging from 1 to 4) were inserted after V242 (bottom). The direction of rotation is arbitrarily assigned with each residue adding a 109° rotation. **c**, Comparison of $E_{max}$ values induced in the wild-type vs mutant IFN-λR1 expressing cells by 1μM each of IFN-ω (red), IFN-λ3 (black) or H11 (orange). All values were normalized to the wild-type receptor expressing cells treated with IFN-λ3 (n=9). **d**, Relative quantification of pSTAT1 staining in cells expressing either the wild-type or **e**, mutant IFN-λR1with

**Figure 13, Continued**

3 alanine insertion by flow cytometry. Cells were treated with serial dilutions of IFN-ω (red), IFN-λ3 (black) or H11 (orange) for 15 min. Curves were fit to a first-order logistic model. Error bars represent ± SEM (n=3). *p < 0.05; **p < 0.01; ***p < 0.001; ****p < 0.0001.

### 3.09 *In vitro* antiviral activities of type III IFNs match those of type I IFNs in mutant IFN-λR1 cell lines

Following the initial discovery for their antiviral properties, type I IFNs, and later type III IFNs, have since garnered much therapeutic interest in use against viral infections. In particular, several forms of type I IFNs – IFN-α and IFN-β subtypes – have found successful mainstream applications in the treatment of chronic hepatitis B and C viruses (HBV, HCV) either as a monotherapy or in combination with other classes of antiviral medications[138-141]. Although IFN-λs have yet to be approved for clinical use, extensive testing so far has established a favorable safety profile of type III IFNs for further use[142-144]. A number of clinical trials are currently underway with early promising results. A recently completed phase 2 trial by the National Institutes of Health Clinical Center (NCT02765802) utilized the pegylated version of IFN-λ1 as a monotherapy against chronic hepatitis D infection (HDV)[145]. Another phase 3 trial (NCT01866930) with a combined regimen of pegylated IFN-λ1/ribavirin (RBV)/daclatasvir (DCV) for HCV and HIV co-infected patients reported high sustained virologic response rates that were comparable to those by IFN-α implemented treatments with added advantages of much improved tolerability and toxicity profiles[146].

Most recently, the SARS-COV-2 global outbreak has precipitated a tremendous research effort into utilizing IFNs to reduce disease severity and risk of transmission. Thus far, a landmark study of IFN-β1a alone or in tandem with remdesivir (NCT04492475) conducted by National Institute of Allergy and Infectious Diseases (NIAID) associated worse clinical

outcomes due to severe adverse events with IFN-β1a treatment[147]. Although adverse effects are notably lower with pegylated IFN-λ1, phase 2 clinical trial data have so far been mixed. One study indicated a significant reduction in viral load and improved viral clearance whereas another reported no clinical benefits to treatment with IFN-λ1 over placebo[148,149]. It is evident that the use of IFN-λs as broad antivirals, and strategies to enhance their potency, may have important clinical and public health implications in current and emerging epidemics.

Therefore, we next sought out to determine if the antiviral potency of type III IFNs can be improved by signaling through geometry-optimized IFN-λR1 receptor complex. The wild-type and mutant IFN-λR1 expressing cell lines were infected with a recombinant vesicular stomatitis virus linked to a green fluorescent protein construct (VSV-GFP) (Figure 14b). Consistent with the previous pSTAT1 signaling assay, type III IFNs showed complete loss of antiviral activity in 2 alanine inserted IFN-λR1 cells whereas IFN-ω induced similar antiviral responses across all cell lines (Figure 14c and f). The wild-type IFN-λ3 and its high-affinity variant, H11, which were 111 and 13-fold lower in activity ($EC_{50}$) than IFN-ω respectively in wild-type IFN-λR1 expressing cells, effectively matched their antiviral activities to IFN-ω in 3 alanines inserted IFN-λR1 receptor expressing cells (Figure 14a).

A previous study conducted in HCV-infected Huh7.5 cells reported that the antiviral activities of type III IFNs can be improved 12-fold by a 150-fold improvement in the stability of the extracellular heterodimeric receptor complex through the engineered high-affinity ligand, H11. However, despite the significant gain in antiviral activity, H11 was 10-fold less potent than IFN-ω[100]. Here, we show that the antiviral activity of type III IFNs is highly responsive to the increased pSTAT1 signaling potency modulated by the change in the intracellular IFN-λR1 register. Notably, our results indicate that optimization of the intracellular receptor-JAK

geometry can potentiate the antiviral activities of type III IFNs, regardless of their receptor affinities, to similar extents achieved with type I IFNs.

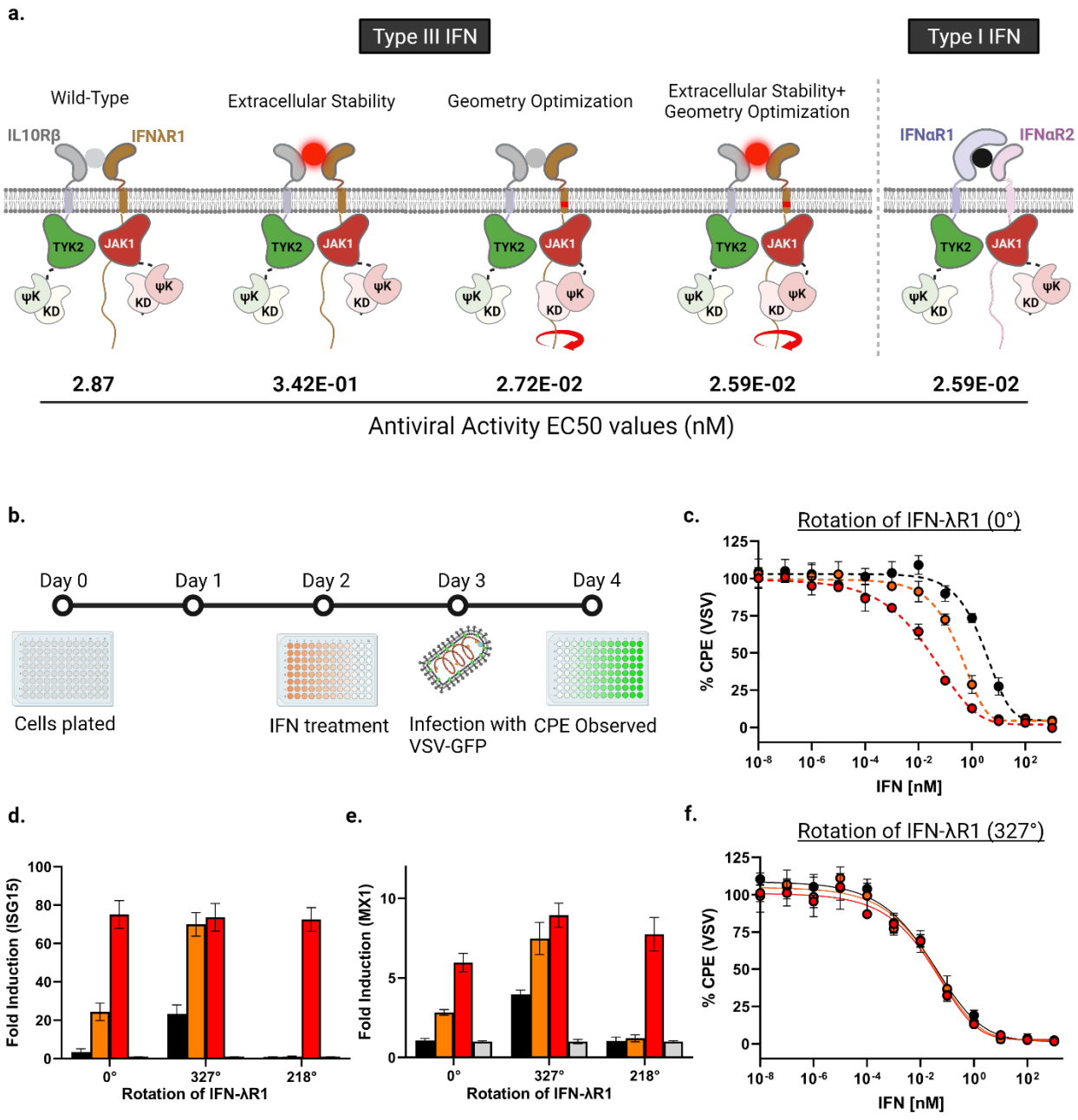


**Figure 14: Register optimization improves antiviral responses against VSV infection. a**, Schematic diagram summarizing the optimization strategies and their respectively associated $EC_{50}$ values (nM) of the antiviral assay and calculated fold-changes relative to IFN-ω treated wild-type IFN-λR1 expressing cells (assigned value 1). **b**, Schematic diagram depicting the antiviral assay set up. **c**, Antiviral activity of IFNs in cells expressing either the wild-type or **f**, mutant IFN-λR1 with 3 alanine insertion. Cells were incubated with serial dilutions of IFN-λ3

**Figure 14, Continued**

(black), H11 (orange) or IFN-ω (red) for 24h prior to VSV-GFP viral infection at 80,000 PFU/well. Fluorescence levels were recorded 18h post-infection. Curves were fit to a first-order logistic model. Error bars represent ± SEM (n=3). **d,** PCR quantification of fold changes in induction of ISG15, **e**, MX1 at 6h post treatment with 100nM each of IFN-λ3 (black), H11 (orange), or IFN-ω (red) in wild-type or mutant cell lines. Mean changes ± SEM in gene expression were determined relative to untreated cells (grey, assigned value of 1) and normalized to 18S (n=4).

### 3.10 Optimization of receptor orientation improves *in vitro* anti-proliferative responses to IFN-λs

In addition to their most prominent role as antivirals, type I IFNs are also known for their antitumor properties[36]. Type I IFNs engage both the innate and adaptive arms of immune system to prevent and suppress aberrant tumor growth. It has been shown that IFNs can upregulate MHC class I expression to promote antigen presentation to immune cells, activate cytotoxic T-cells, natural killer (NK) and dendritic cells (DC), and promote apoptosis[150,151]. Both the recombinant and pegylated forms of certain type I IFNs, IFN-α subtypes in particular, have been in clinics for some cancers such as melanoma, hairy-cell leukemia and Kaposi's sarcoma[55]. However, due to the near ubiquitous expression of type I IFN receptors in tissues, the systemic administration of type I IFNs inevitably leads to off-target side effects. Given the overlapping gene expression profile between type I and III IFNs, type III IFNs with their limited receptor distribution and tissue abundance are increasingly regarded as more specific and less toxic alternatives to type I IFNs in cancer therapy[152]. Despite the muted response in *in vitro* anti-proliferative assays, IFN-λs have been shown to effectively promote tumor suppressive activities *in vivo*. Studies in mouse models of aggressive B16 melanoma, murine fibrosarcoma and CT26 colon cancers have so far indicated that type III IFNs elicit these antitumor effects via recruiting cytotoxic NK/NKT cells, increasing lymphocytic infiltrates in tumor microenvironment, and inducing cell-cycle arrest[152-154].

Studies have indicated that the minimal anti-proliferative activity observed *in vitro* for IFN-λs may be attributed to the limited expression of IFN-λR1 on the cell lines assayed[152]. In cells transduced to express IFN-λR1, however, anti-proliferative responses can be strongly induced by IFN-λs[100,155]. Here, we found that the anti-proliferative activities were most efficiently induced by IFN-ω across all cell lines (Figure 15a). The activity of IFN-ω is approximately ~8,500-fold over that of wild-type IFN-λ3 signaling through wild-type IFN-λR1. Analogous to pSTAT1 signaling, 2 alanine inserted IFN-λR1 receptor expressing cells displayed negligible anti-proliferative activity when treated with IFN-λs. Remarkably, the near 4-log difference in activities between the type I and III IFN was reduced to just ~30-fold in the geometry-optimized IFN-λR1 expressing cells stimulated with high-affinity H11 ligand, which represents a >280-fold improvement in activity (Figure 15c and f).

It has previously been shown that the anti-proliferative activity of type III IFNs can be modulated via cell surface receptor density and the stability of the extracellular complex[100,155]. Here, our results indicate that the geometry of the intracellular signaling components also contributes to the anti-proliferative response. Notably, an analysis of the fold-changes in activity induced in different cell lines by two IFN-λ ligands suggests a possible synergy between the affinity of ligand and the register of receptor-JAK complex in modulating anti-proliferative activities. When evaluated on the basis of receptor usage, the fold-increase in activity in response to the change in ligand affinity was significantly lower in the wild-type cells than in 3 alanine inserted IFN-λR1 cells. Similarly, when evaluated on the basis of ligand usage, the fold-increase in response to the change in receptor geometry was significantly lower for IFN-λ3 than its high-affinity counterpart, H11. Maximum anti-proliferative effects were achieved only when the

stimulation with high-affinity ligand was accompanied by cell signaling through geometry-optimized mutant IFN-λR1 receptor.

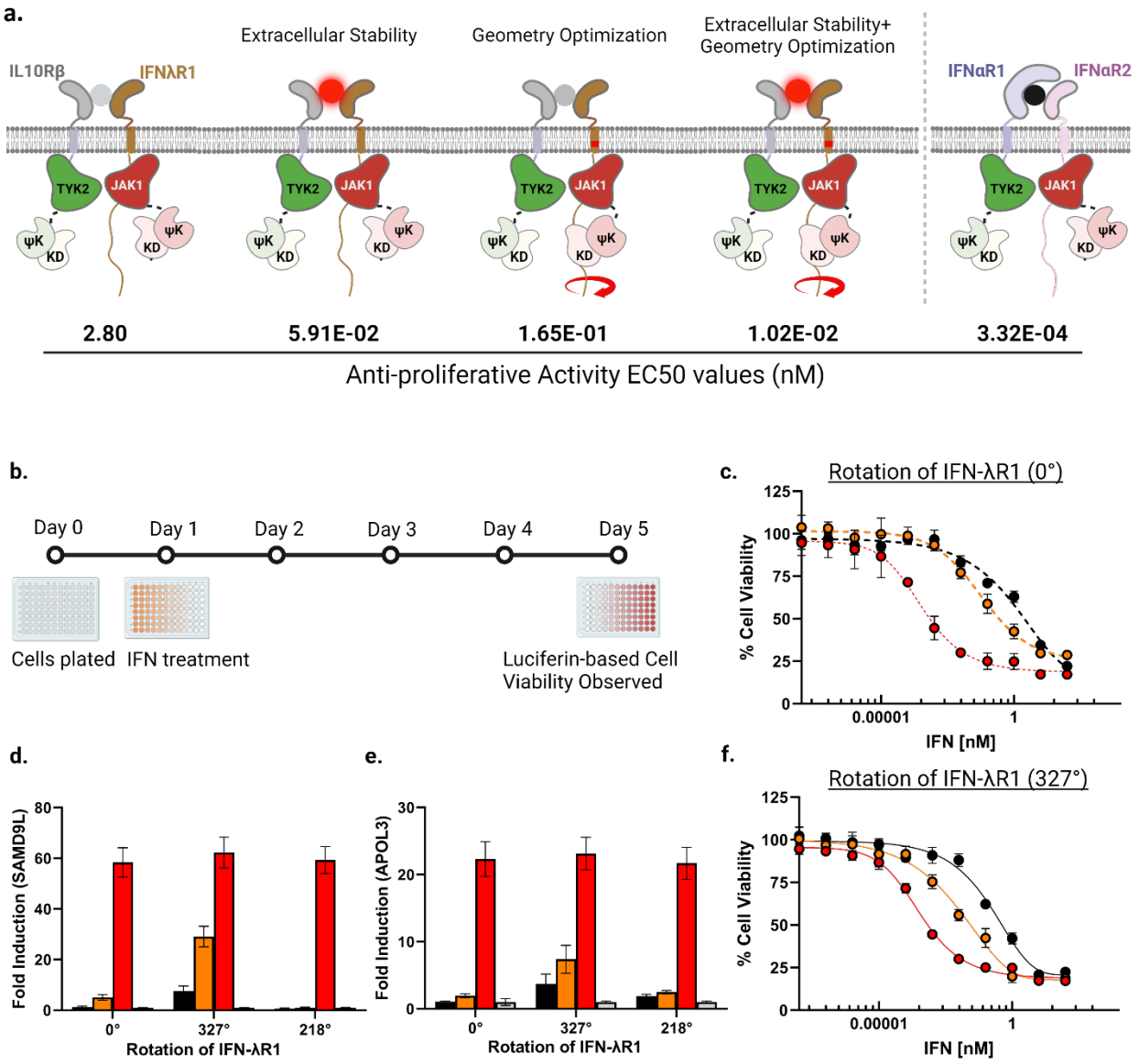


**Figure 15: Mutant IFN-λR1 receptors with 3 alanine insertion upregulate anti-proliferative activities of type III IFNs. a,** Schematic diagram summarizing the optimization strategies and their respectively associated $EC_{50}$ values (nM) of the anti-proliferative assay and calculated fold-changes relative to IFN-ω treated wild-type IFN-λR1 expressing cells (assigned value 1). **b**, schematic diagram showing the experimental set-up of the assay. **c**, Anti-proliferative activity of IFNs in cells expressing either the wild-type or **f,** mutant IFN-λR1 with 3 alanine insertion. Cells were incubated with serial dilutions of IFN-λ3 (black), H11 (orange) or IFN-ω (red) for 4 days. Curves were fit to a first-order logistic model. Error bars represent ± SEM (n=3). **d**, PCR quantification of fold changes in induction of SAMD9L, **e**, APOL3 at 6h post treatment with 100nM each of IFN-λ3 (black), H11 (orange), or IFN-ω (red) in wild-type or mutant cell lines.

**Figure 15, Continued**

Mean changes ± SEM in gene expression were determined relative to untreated cells (grey, assigned value of 1) and normalized to 18S (n=4).

### 3.11 ISG induction levels are elevated for IFN-λs signaling through engineered IFN-λR1 receptors

We next quantified the transcriptional levels of a representative antiviral and anti-proliferative gene set. For antiviral genes (MX1 and ISG15), stimulation with type III IFNs significantly increased the induction levels (3 to 8-fold) in 3 alanine inserted IFN-λR1 receptor expressing cells compared to the wild type (Figure 14d and e). Most notably, the gene induction levels by the high-affinity H11 effectively matched those of type I IFN, IFN-ω, in 3 alanine inserted IFN-λR1 expressing cells. Similarly, for anti-proliferative genes (APOL3 and SAMD9L), we observed large fold-increases (4 to 6-fold) in gene induction levels by type III IFNs in the mutant IFN-λR1 cells compared to the wild-type (Figure 15d and e). However, unlike the antiviral genes, the increased gene induction levels by type III IFNs were only a fraction of those exhibited by IFN-ω. On the contrary, at 24-hr post IFN treatment, type III IFNs, regardless of their receptor affinity, induced all genes except APOL3 to near equivalent levels of type I IFN (Figure 16a to d).

The gene induction study again highlights the importance of receptor geometry in downstream signaling outputs by IFNs. It should be noted that the two antiviral genes screened in this assay were more sensitive to the optimized register of the receptor than the anti-proliferative genes. This is consistent with our prior functional assays evaluating the antiviral and anti-proliferative activities of IFNs *in vitro*. Previously, we determined that the antiviral efficacy of type III IFNs was equivalent to that of type I IFN in cells signaling through the mutant 3

alanine inserted IFN-λR1 receptors whereas the anti-proliferative activities of type III IFNs, though significantly improved, remain weaker than those induced by type I IFN.

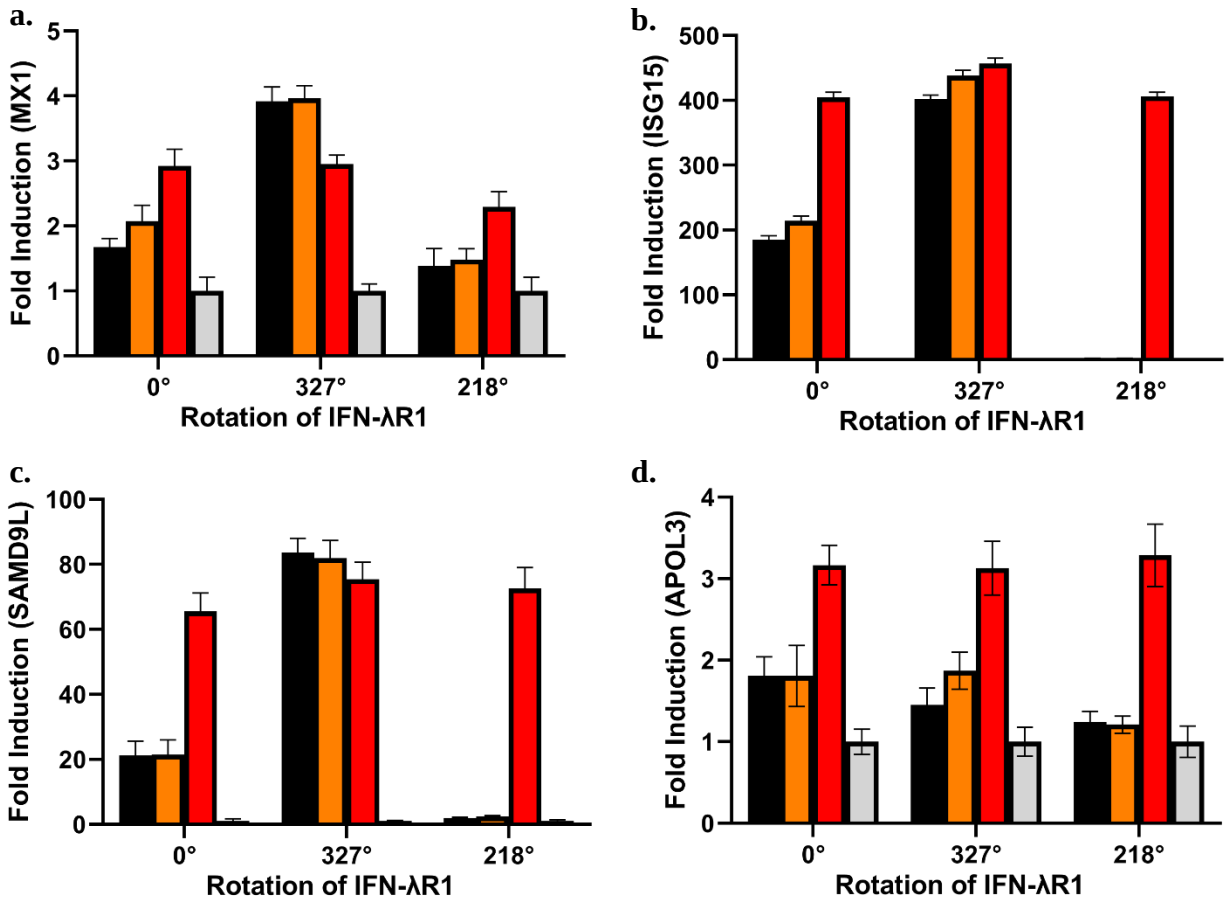


**Figure 16: Induction of antiviral and anti-proliferative genes is upregulated in 3 alanine inserted IFN-λR1 receptor expressing cells. a,** PCR quantification of fold changes in induction of MX1, **b**, ISG15, **c**, SAMD9L, **d**, APOL3 at 24h post treatment with 100nM each of IFN-λ3 (black), H11 (orange), or IFN-ω (red) in wild-type or mutant cell lines. Mean changes ± SEM in gene expression were determined relative to untreated cells (grey, assigned value of 1) and normalized to 18S (n=4).

### 3.12 Genome-wide transcriptional profiling reveals significant enhancements in ISG induction

We next carried out next generation RNA sequencing to further evaluate the differences in the transcriptional responses to type I and III IFNs in wild-type vs mutant 3 alanine-inserted IFN-λR1 expressing cells. Whole-genome transcriptional profiling of IFN treated cells after 24h

displayed strong correlation with the expression patterns of target antiviral and anti-proliferative gene sets obtained by qPCR. Principal component analysis (PCA) revealed four clusters – 1) untreated wild-type and mutant IFN-λR1 cells, 2) IFN-λ3 and H11 treated wild-type IFN-λR1 cells, 3) IFN-λ3 treated mutant IFN-λR1 cells, and 4) IFN-ω treated wild-type and mutant IFN-λR1 cells and H11 treated mutant IFN-λR1 cells (Figure 17a and b). Compared to wild-type cells, 3 alanine inserted IFN-λR1 cells displayed a significant increase in the abundance of overlapping differentially expressed genes (DEG) between type I and III IFNs treatments (Figure 17c). Overall, there was a significant increase in the number of upregulated genes in response to type III IFNs in engineered IFN-λR1 receptor expressing cells than in wild-type cells (Figure 17d). Specifically, the number and fold-change of core antiviral ISGs were markedly improved for both IFN-λ3 and H11 simulation in cells expressing mutant IFN-λR1 receptors than the wild-type counterparts (Figure 17e-j).

K-means clustering analysis of 2,400 most variable genes indicated six distinct enriched pathways (Figure 18a). In both cell lines, type I IFN treatment led to the activation of genes involved in pathogen sensing and antigen processing/presentation (cluster I, black), innate and adaptive immune responses to viral infections (cluster II, green), and tissue repair and barrier functions (cluster III and IV, brown and yellow respectively) (Figure 18b to e). On the contrary, there were significant differences in the transcriptional profiles between wild-type and mutant IFN-λR1 expressing cells for type III IFNs. As anticipated, type III IFNs induced much weaker transcriptional programs of antiviral and barrier function-associated genes than type I IFN in wild-type cells. In 3 alanine inserted IFN-λR1 expressing cells however, stimulation with H11 led to similar activation levels of gene subsets as type I IFN across all four clusters whereas stimulation with wild-type IFN-λ3 showed a marked elevation in transcription levels compared

to wild-type cells, although comparatively weaker than H11 or IFN-ω. Similarly, the activation states of core antiviral and anti-proliferative genes displayed clear enrichment patterns for IFNω and type III IFNs signaling through rotated IFNλR1 receptors (Figure 19a). Analysis of log2-transformed fold changes in individual select ISGs further indicated largely equivalent gene expression profiles among different IFN treatments in mutant IFN-λR1 expressing cell lines (Figure 19b to g). Through Ingenuity pathway analysis (IPA), we further quantified the activation state of individual pathways involved in maintaining a state of immunity against pathogenic stimuli (Figure 19h). Consistent with our previous analyses, we observed an overlap in the enrichment of genes central to IFN-mediated antiviral responses between type I IFN treated cells and H11 treated mutant IFN-λR1 cells.

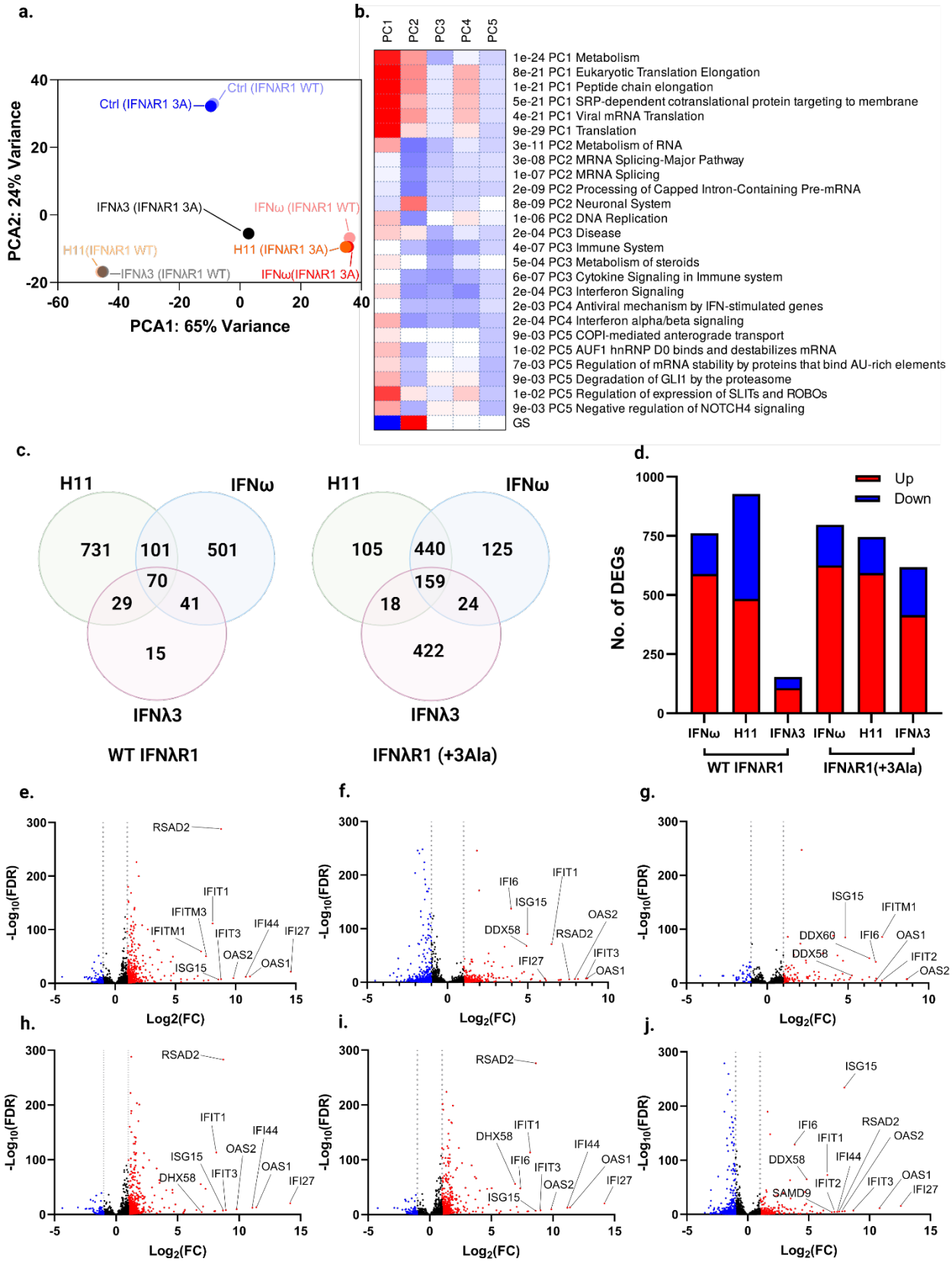


**Figure 17: Human transcriptome analysis over 20,000 genes shows that differential gene**

**Figure 17, continued**

**expression (DEG) profile of mutant IFN-λR1 cells treated with high-affinity IFN-λ3 H11 ligand is near identical to the profiles of cells treated with IFN-ω. a**, PCA plot showing the distribution of WT and mutant IFN-λR1 cell clusters treated with IFNω, IFNλ3 and H11 ligands for 24h. **b**, A heatmap showing the pathways involved in PCA analysis. **c**, Venn diagrams comparing the number of upregulated genes in cells expressing either WT (left) or 3 alanine inserted mutant (right) IFN-λR1 treated with indicated IFNs. **d**, A bar plot showing the quantification of DEGs in IFN-treated cells compared to untreated controls. **e-g,** Volcano plots showing decreased (blue) and increased (red) gene expression levels in cells expressing either WT or **h-j**, 3 alanine inserted mutant IFN-λR1 treated with IFNω, H11 or IFNλ3 (left to right) compared to untreated controls. DE cutoffs were set at a log2 fold change of |1| and adjusted p-value < 0.01.

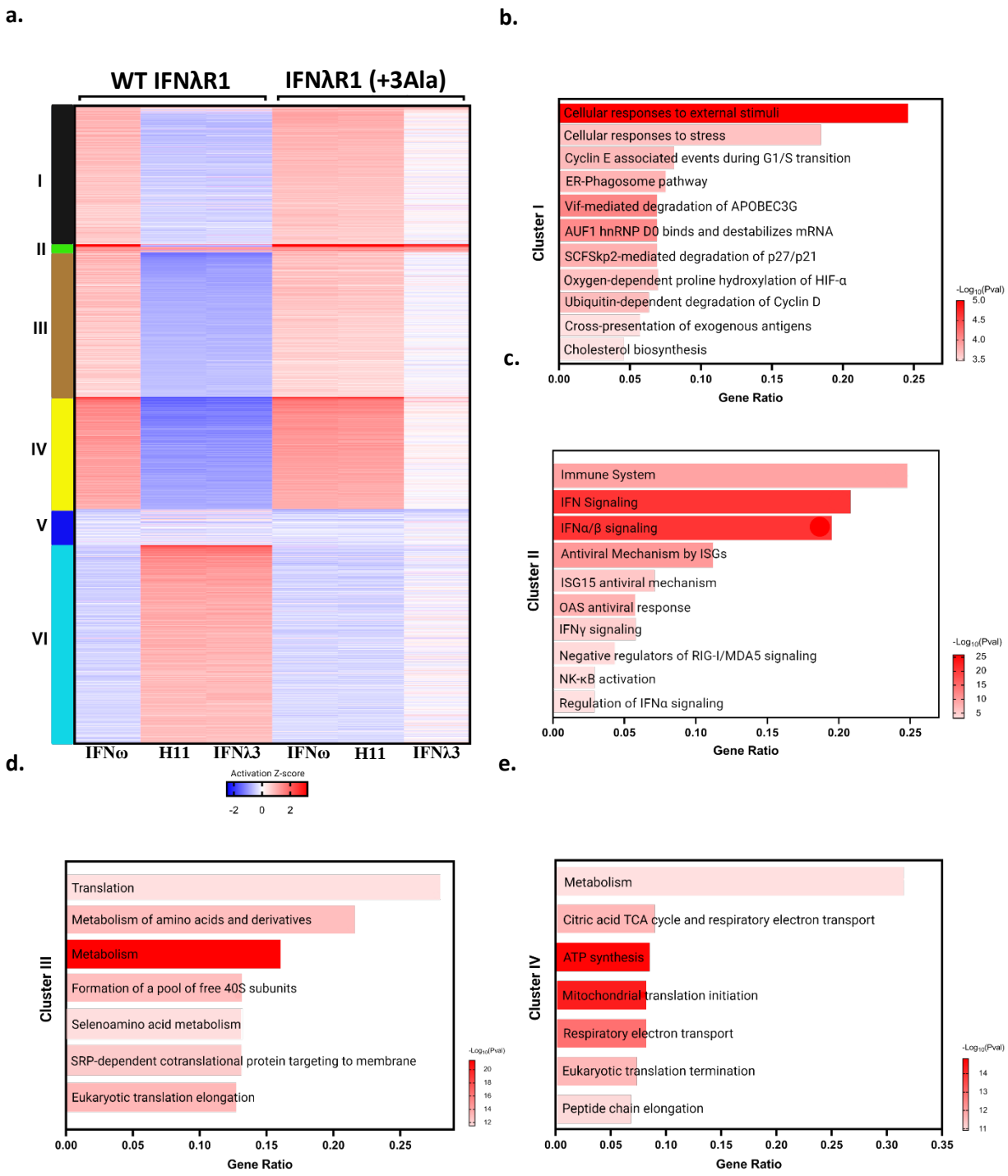


**Figure 18: K-means analysis indicates six distinct enriched clusters. a,** Heatmap showing the mean expression levels of 2,400 most variable genes across six sample sets (N=2). b-e, Bar plots detailing the enrichment pathways in the curated clusters. Bar size represents gene ratios within each enriched pathway, and color represents the -Log10 p-value of enrichment. Increases in −log10 p-value are indicative of increased statistical significance.

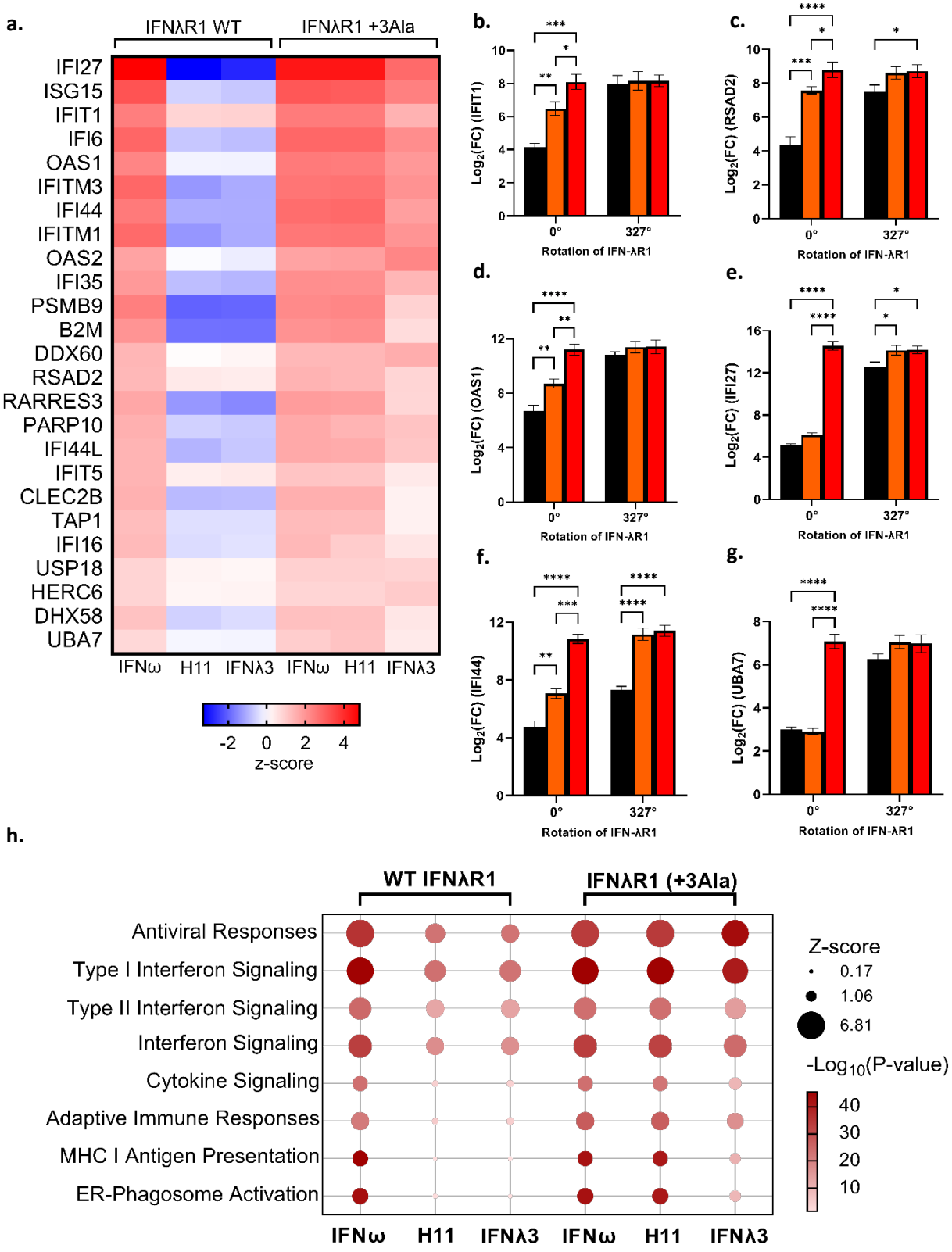


**Figure 19: IPA pathway analysis reveals that high-affinity H11 ligand induces similar**

**Figure 19, continued**

**subsets and fold-changes of potent antiviral ISGs as IFNω in 3 alanine inserted IFN-λR1 expressing cells. a,** Heatmap representation of activation levels of individual ISGs in cells expressing WT or 3 alanine inserted IFN-λR1 treated with indicated IFNs. **b**, Log2-transformed relative expression of select antiviral ISGs including IFIT1, **c**, RSAD2, **d**, OAS1 and anti-proliferative ISGS including **e**, IFI27, **f**, IFI44, and **g**, UBA7 in wild-type or mutant cell lines treated with IFN-λ3 (black), H11 (orange), or IFN-ω (red). Statistical significance was determined by two-way ANOVA test. **h**, Bubble plot representation of significantly enriched antiviral mechanisms using IPA. Bubble color represents activation Z scores, and bubble size represents the -Log10 p-value of enrichment. Statistical significance was determined by an activation Z score > |1| and a −log10 p > 1.32, which corresponds to a p-value of 0.05. Increases in −log10 p-value are indicative of increased statistical significance.

## Chapter 4: Discussion

### 4.01 Overview: Intracellular receptor-JAK axis provides another mode of modulating type III IFN signaling

Type I and III IFNs are two distinct families of IFNs that are crucial in arming the host system with an efficient and controlled state of immunity in response to noxious stimuli. Despite having low sequence homologies and signaling through different extracellular heterodimeric complexes, members of both IFN families share many important biological functions[55]. Type I and III IFNs, in a concerted effort, are expressed to modulate both the innate and adaptive arms of the immune system by activating gene expression programs involved in antiviral, anti-proliferative, antitumoral and other immunomodulatory pathways[30,31]. For both families, the cytokine production is similarly induced by cellular sensing of PAMPs from viral or non-viral pathogens via PRRs[43]. The upregulation of type I and III IFNs expression then initiates a chain of signaling cascades that lead to a robust transcriptional induction of related ISGs. Although there is a significant overlap in the pool of ISGs induced between type I and III IFNs, multiple studies have shown that the two pathways are non-redundant, but rather have complementary functions that serve to maintain an optimal state of immune protection.

There are features distinct to either type I or III IFNs that set them apart from each other. Among others, type I and III IFN responses display spatial segregation of labor[55]. This is in large part due to the restricted expression of type III IFN receptors in epithelial and barrier cells[56-58]. From a clinical application point of view, the spatial restriction in type III IFN-mediated responses is desirable in that the subsequent inflammation is inherently localized to specific tissues. In other words, type III IFNs have the potential of recapitulating the therapeutic

properties of type I IFNs without the accompanying systemic toxicity and adverse side effects. Secondly, type I and III IFN responses have been shown to follow different activation schedules. Type I IFN-induced responses to an immunological stimulus tend to be fast and short-lived whereas type III IFNs are slower to react, building up to a peak after a delayed period of 24-48 h post-infectious challenge[63]. Collectively, such spatiotemporal division of labor between type I and III IFNs can be regarded as an essential component of any well primed immune system. Inflammatory responses mounted against infections must offer adequate protection to the host without causing rampant inflammation and collateral tissue damage. Thus, from an evolutionary standpoint, it is likely that type I and III IFNs have co-evolved to endow the host with a balanced state of immunity.

Perhaps, it is also down to evolutionary processes that type III IFNs exhibit significantly weaker biological responses compared to type I IFNs. Previous studies have shown that type III IFNs induce a weaker transcriptional profile of a smaller set of ISGs compared to type I IFNs[65,66,68]. Consequently, type III IFNs are less efficacious as antiviral or antitumoral agents compared to type I IFNs. Such a significant gap in potency currently presents an insurmountable hindrance in translating type III IFNs for clinical uses. This is reflected by the fact that no type III IFNs has been approved for use whereas many type I IFNs are already clinically utilized for cancers and viral infections. However, the therapeutic gains of type I IFNs are unfortunately offset by the adverse side effects in patients. Given the much more favorable toxicity profile of type III IFNs due to their inherent targeted responses, there is much vested research interest in understanding the key factors contributing to the lower potency of type III IFNs and developing strategies to overcome these limitations.

Previous efforts to account for the signaling differences between type I and III IFNs have taken a cellular 'outside-in' approach. In this case, the differences in the stability of the extracellular heterodimeric complexes formed by type I and III IFNs are first to be taken into consideration. It is well-established that type I IFNs bind with higher affinities to their receptors than type III IFNs[98-100]. To address this discrepancy, a high-affinity IFN-λ ligand that can improve the complex stability by a collective 150-fold over wild-type was engineered[100]. The study shows that the engineered ligand can significantly improve the signaling potency of type III IFNs but is nonetheless less potent than type I IFNs, indicating that the complex stability is simply one of several existent contributing factors. Additionally, receptor abundance has been pointed out as a limiting factor for type III IFN signaling. When IFN-λR1 receptors are overexpressed *in vitro*, certain biological activities have shown increased sensitivity to type III IFN treatment[100]. Although potentiation through increased receptor expression is an interesting proof-of-concept study, exogenous induction of receptors in cells of interest currently falls outside the realms of clinical viability. Summarily, despite the progress made, the potency of type III IFNs still lags significantly behind that of type I IFNs with no known actionable targets for closing the gap.

Notably, the differential signaling potency between type I and III IFNs is made more perplexing by the fact that both families share a near identical intracellular JAK/STAT signaling pathway (Figure 2). Unlike tyrosine kinase receptors, cytokine receptors lack an intrinsic kinase domain[71]. All IFNs thus utilize the JAK/STAT pathway to transmit signals through the intracellular domains to initiate signaling. More than 40 cytokine receptors signal through only four JAK proteins. Notwithstanding the extensive research and understanding, a lack of structural and biophysical information regarding full-length JAK proteins and/or JAKs in

complexes with full-length cytokine receptors has occluded some finer aspects of the JAK/STAT pathway from current understanding. As of this writing, there are only two reported structures of N-terminal FERM SH2 domains of JAKs in complex with partial ICDs of cytokine receptors, only one of the C-terminal pseudokinase and kinase domains of TYK2 in an asymmetric unit and a few of kinase domains[74,95,156-158]. However, without full-length JAK structures, it remains an open question how the C-terminal domain of a JAK is oriented relative to its receptor-bound N-terminal domain in its natural configuration. Additionally, it has yet to be addressed if and how JAK kinase domains reorient during and after ligand stimulation. For instance, when two JAKs are brought within a defined distance for transphosphorylation to occur, it is unclear how the kinase domains of complex sharing JAKs are oriented relative to each other, and whether the relative orientation is conserved or differs amongst distinct cytokine receptors. We hypothesize that efforts to address these fundamental questions concerning the intracellular geometry of JAKs can be of much significance in providing a molecular basis for the observed differences between type I and III IFN signaling and functions.

Here in this work, we continued the cellular 'outside-in' approach and interrogated the cytosolic receptor-JAK interactions in our attempt to fully account for the signaling differences between type I and III IFNs. Using protein engineering approaches, we introduced precise modifications to the receptor-JAK interface and evaluated the changes in downstream IFN signaling outputs. Previous studies have implicated a few key parameters of the receptor-JAK interactions that are crucial for maintaining proper IFN signaling[128-130]. Firstly, the complex-sharing JAKs must be within a defined proximity for transphosphorylation to occur[131]. Secondly, the vertical distance of the receptor-binding domains of JAKs (the box motifs) from the membrane has been implicated as a potential contributor to downstream signaling. Thirdly,

changes in the intracellular register of the receptor have been shown to modulate JAK activation, indicating that the orientation of JAKs is another key factor[135].

**4.02: Affinity of receptor-JAK interactions and effects can be explained by a model of competition for JAK**

Our work can be divided into two sections –the former focusing on the affinity of the receptor-JAK interaction and the latter, on the geometry of the proximal JAKs within a signaling complex. To evaluate the effect of the affinity of the interaction, we grouped type I and III IFN receptors into two based on their associated JAKs – 1) JAK1 binding receptors: IFN-λR1 and IFN-αR2, and 2) TYK2 binding receptors: IL-10Rβ and IFN-αR1. Within each group of receptors, we first determined if there were significant differences in their native binding affinities to the respective JAKs. Based on 'on-yeast' binding data, we concluded that IFN-λR1 and IFN-αR2 both bind with equivalently high affinity to JAK1 ($K_d$ <μM). Consequently, engineering of the JAK1 binding halves of the complexes to further improve the affinity was deemed unlikely to yield significant improvements. More importantly, the near equivalent affinities to JAK1 exhibited by the two IFN receptors indicate that these receptor-JAK interactions are unlikely to contribute to the differences observed in signaling potency between type I and III IFNs.

Interestingly, we found that IFN-αR1 and IL-10Rβ bind weakly to TYK2, consistent with previous reports stating that the short-chained receptors bind with weaker affinities to their associated JAKs than their long-chained counterparts[25]. Here, we quantitatively report the significant differences in the native binding affinities between IFN-αR1 and IL-10Rβ to TYK2. Although both receptors exhibit weak binding, IL-10Rβ binding to TYK2 was significantly weaker ($K_d$ >100μM) than that of IFN-αR1 ($K_d$ >1μM). This leads us to question if the

difference in affinity between the two receptors and TYK2 can potentially explain the difference in the magnitude of their respective IFN downstream signaling. To address this explicitly, we sought to equalize the binding affinities by engineering higher-affinity receptors of both chains via an affinity maturation approach using yeast display. The engineered receptors display significantly tighter binding to TYK2 compared to the wild-types; the mutant IL-10Rβ and IFN-αR1 receptors have comparable $K_d$ values of 65.9 ±5.4nM and 175.8 ±12.5nM respectively. The pSTAT1 analysis indicates that both cell lines expressing either the wild-type or mutant IFN-αR1 respond similarly to IFN stimulation both in terms of signaling potency and sensitivity. On the contrary, upon stimulation with type III IFNs, cells expressing mutant IL-10Rβ induced a more potent pSTAT1 response compared to the wild-type with an over 25% increase in $E_{max}$ values. Notably, we observed that the boost in signaling potency to IFN-λs in mutant IL-10Rβ cells is accompanied by a significant decrease in $E_{max}$ (~10%) to IFN-ω, a type I IFN.

A previous study has shown that cytokine signaling can be disrupted by exogenously expressed receptors competing for the same JAKs associated with the native receptors[103]. Assuming a limited pool of available JAKs within a cell, it is possible that certain receptors, by using higher affinity and/or abundance, can outcompete and titer the kinases away from other receptors sharing the same JAKs. We hypothesize that a similar competition for available TYK2 may exist between IL-10Rβ and IFN-αR1 in cell lines that are responsive to both type I and III IFNs. If the constitutive association with a kinase is prerequisite for an 'active' cytokine receptor, then it is likely that at any given time point, there are fewer active IL-10Rβ receptors ready for signaling than there are IFN-αR1 receptors due to the large discrepancy in their binding affinities toward TYK2. It then follows that by increasing the binding affinity of IL-10Rβ to TYK2, we have managed to increase the availability of 'active' IL-10Rβ receptors within a cell,

which leads to an increase in type III IFN-mediated responses. Our hypothesis is further supported by the fact that the pSTAT1 response to IFN-ω was significantly muted in cells expressing high-affinity IL-10Rβ receptors. On the other hand, we observed no appreciable changes in pSTAT1 signaling in cells expressing high-affinity IFN-αR1 receptors. We postulate that native IFN-αR1 receptors already bind with a higher affinity to TYK2 than other TYK2 sharing receptors present in the cells. Consequently, the number of 'active' IFN-αR1 receptors is not significantly altered by our engineering approach, leading to no functional gains.

Alternatively, the evident resistance to further improvements in type I IFN signaling may indicate a functional cap to IFN responses. If type III IFN signaling has evolved to elicit weaker biological responses than type I IFNs to prevent unabated inflammation, it is equally likely that specific negative regulatory feedback mechanisms exist that prevent type I IFN-mediated responses from breaching a certain threshold. Since there is a sizable gap between the potencies of type I and III IFNs, we reason that type III IFN signaling is likely to be more responsive to further attempts at improving the efficiency and potency of the pathway than type I IFN signaling.

**4.03: Type III IFN signaling activities can be drastically improved by fine-tuning the geometry of intracellular receptor-JAK complexes**

For the latter half of our work, we turned our focus to answering how the role of JAK-JAK orientation influences cytokine signaling and function. However, addressing this question is challenging due to the absence of high-resolution structures of full-length cytokine receptors or receptors in natural complexes with the JAKs. In the absence of structures, to directly interrogate the role of geometry in cytokine signaling, we sought to determine instead if modulations in the register of intracellular IFN-λR1-JAK1 axis can affect downstream JAK activation and

subsequent signaling outputs. We hypothesized that the lower potency of type III IFNs in comparison to type I IFNs may be due to slight misalignments in the proximal JAKs within the heterodimeric signaling complex. Using an alanine insertion mutagenesis approach, we engineered mutant IFN-λR1 receptors with precise twists in their intracellular registers. In transduced cells expressing 2 alanine inserted IFN-λR1 receptors, the near 180-degree flip induced by the addition of 2 alanine residues results in a nearly dead signaling and functional response to type III IFN treatment in cells. We reason that the kinase domain of JAK1 in this rearrangement is oriented front-to-back relative to that of TYK2 such that the two JAKs are unable to undergo phosphorylation and become activated.

More interestingly, with the exception of the 2 alanine residue-insertion, all other mutant cell lines of IFN-λR1 displayed significantly improved pSTAT1 signaling strength. Notably, the 33-degree counterclockwise (arbitrarily assigned) displacement of the receptor from its original position brought on by a 3 alanine residue insertion induced the greatest gains in signaling compared to the 76 or 109-degree clockwise turns resulting from the addition of 4 or 1 alanine residues respectively. Our results indicate that there is no loss of activity associated with register twists in either clockwise or counterclockwise direction. Since it has previously been established that the complex-sharing JAKs must be within a defined distance from each other, it may therefore seem counterintuitive that here the direction of rotation has no apparent impact on JAK activation. We propose that our findings are consistent with a model in which C-terminal bilobular pseudokinase and kinase domains of the proximal JAKs are located off-axis from their respective receptor-bound N-terminal FERM SH2 domains and tilted at an angle opposite from each other (Figure 20).

A previously reported 3D reconstruction of JAK1 informs us that the three major lobes constituting a highly asymmetrical JAK1 can adopt a wide range of conformations in 'free-floating' conditions[159]. A density mapping analysis with available crystal structures of JAK1 subdomains shows that a minor lobe belonging to the SH2 domain locates between the large N-terminal FERM lobe and the two other major lobes that correspond to pseudokinase and kinase domains. Based on the models, the N-terminal FERM domain is only loosely connected to the bi-lobed C-terminal kinase domains via a >20 amino acid-long inter-domain linker. The linker is speculated to provide the flexibility required for the FERM domain to adopt various orientations relative to the kinase domains. In an unbound state, the three major lobes of JAK1 can be aligned in a fully extended conformation along a common axis (open) or in a compact format in which the kinase domains are in closer proximity with the FERM domain (closed) or in any in-between configurations. It should be noted that the functional linkage between the configuration of JAKs and their activation status remains unknown[159]. Furthermore, it is unclear whether, or if, JAKs adapt their structural configuration in response to association with a receptor or a ligand-binding event.

Here we propose that in the context of type III IFN signaling complexes, the rotations afforded by the insertion of 1, 3 or 4 alanine residues in the transmembrane region of IFN-λR1 reorient the kinase domain of JAK1 relative to that of TYK2 bound to IL-10Rβ in such a way that the activation loops from both kinase domains are brought into closer proximity. If we assume an 'open' configuration of JAK1, we will expect to see a loss of activity when the register is rotated in the counterclockwise direction by the insertion of 1 or 4 alanine residues since the insertion of 3 alanine residues showed the greatest improvement in signaling. Since our findings indicate otherwise, we hypothesize that the active JAK1 in a type III IFN signaling

complex likely adopts a version of ‘closed’ configuration. In this proposed model, the back-to-back oriented lobes of C-terminal pseudokinase and kinase domains swing outward from the central axis of the complex with the kinase domains from two receptors facing opposite each other. Given the added flexibility afforded by the inter-domain linker of JAKs, we reason that the mutant IFN-λR1 receptors aid the autophosphorylation process via a combination of increased proximity and/or optimized orientation of JAKs.

We conducted a series of functional assays probing the pSTAT1 signaling, antiviral, anti-proliferative activities and ISG gene induction levels by stimulating wild-type and mutant IFN-λR1 receptor expressing cell lines with type I IFN (IFN-ω) and type III IFNs –wild-type IFN-λ3 and high-affinity H11 ligands. Our cytopathogenicity assay in cells infected with recombinant VSV-GFP virus shows that the antiviral efficacy of type I IFNs was effectively matched by type III IFNs signaling when JAK1-TYK2 geometry is optimized with the addition of 3 alanines inserted in the transmembrane region of IFN-λR1 receptors. This represents a 111-fold improvement in $EC_{50}$ values of type III IFNs in cells transduced to express wild-type IFN-λR1 receptors. Similarly, the anti-proliferative activities of type III IFNs show significant improvements in response to the change in the receptor register. In cells expressing geometry-optimized IFN-λR1 receptors, the $EC_{50}$ of high-affinity IFN-λ3 H11 was only 30-fold lower than that of IFN-ω, which is a drastic reduction of the near 4-log activity gap between IFN-ω and IFN-λ3 in cells transduced to express wild-type IFN-λR1 receptors.

Consistent with the increased pSTAT1 $E_{max}$ levels and improved functional activities, the IFN-inducible gene expression is also improved in the JAK geometry optimized IFN-λR1 expressing cells. At 6h post-stimulation with IFNs, the two antiviral genes (MX1 and ISG15) showed the most drastic differences between the wild-type and mutant receptor expressing cell

lines. Most notably, the high-affinity IFN-λ3 H11 ligand was able to match the antiviral gene induction levels exhibited by IFN-ω. Though significantly improved by receptor-JAK reorientation, the anti-proliferative gene expression levels (SAMD9L and APOL3) of IFN-λs, however, remained lower than those of type I IFNs. Interestingly, the transcriptional profiles obtained after 24h post-stimulation showed that both IFN-λs, regardless of their receptor affinities, induced expression of the antiviral (MX1 and ISG15) genes and SAMD9L, an anti-proliferative related gene, to equal extents as IFN-ω. For both type I and III IFNs, the expression levels of another anti-proliferative gene, APOL3, at 24h were significantly down (~60-80%) from their earlier values. Such sustained gene expression profile of type III IFNs again reinforces the notion that the immune responses of type I and III IFNs are temporally differentiated.

Whole-genome transcriptional analysis also showed that genes associated with mounting innate and adaptive immune responses against viral infections as well as maintaining tissue barrier functions were markedly upregulated in cells expressing mutant IFN-λR1 receptors when treated with type III IFNs. The extent of overall gene activation by the high-affinity ligand, H11, was near identical to that of IFNω whereas that by wild-type IFN-λ3 was weaker. However, when the analysis is limited to core antiviral ISG subsets, the wild-type IFN-λ3 was able to achieve similar expression levels as H11 when JAK1- TYK2 orientation is optimized, which is consistent with our antiviral assay in which both IFN-λ3 and H11 displayed similar $EC_{50}$ values toward VSV-GFP infection. The results indicate that while geometry optimization can significantly expand the number and fold-changes of ISGs activated by type III IFNs, the optimization must be accompanied by an improved extracellular complex stability through use of high-affinity ligands in order to match the transcriptional profile achieved by type I IFNs.

Ultimately, our results indicate that the receptor-JAK interface adds another layer of complexity in the functional differences between type I and III IFNs. By engineering intracellular protein-protein interactions, we have quantitatively determined the differences in the binding affinity between IFN receptors and their respectively associated JAKs, and how these differences translate to wide-ranging differentiations in downstream cellular activities. In addition, we have demonstrated that the suboptimal spatial alignment of transphosphorylating JAKs in a signaling complex is majorly responsible for the low potency of type III IFNs. We show that the functional activities of type III IFNs can be significantly enhanced by fine-tuning the intracellular geometry of their cognate receptor, IFN-λR1. Although our work is focused on type I and III IFNs, the engineering tools, workflow, and resultant insights into the intracellular signaling machinery can be applied to evaluate and/or further our understanding of broader cytokine systems. For instance, our findings here suggest that JAKs utilize subtle differences in binding biochemistry and geometry to elicit differential responses between type I and III IFNs. The same findings can be interpreted more generally to explain how a family of four JAKs manages to signal for over 40 different cytokine receptors with such high fidelity and cross-reactivity, two qualities that are seemingly at odds with each other. Our findings bring a new layer of understanding to cytokine signaling and provide novel opportunities to tune cytokine signaling and function.

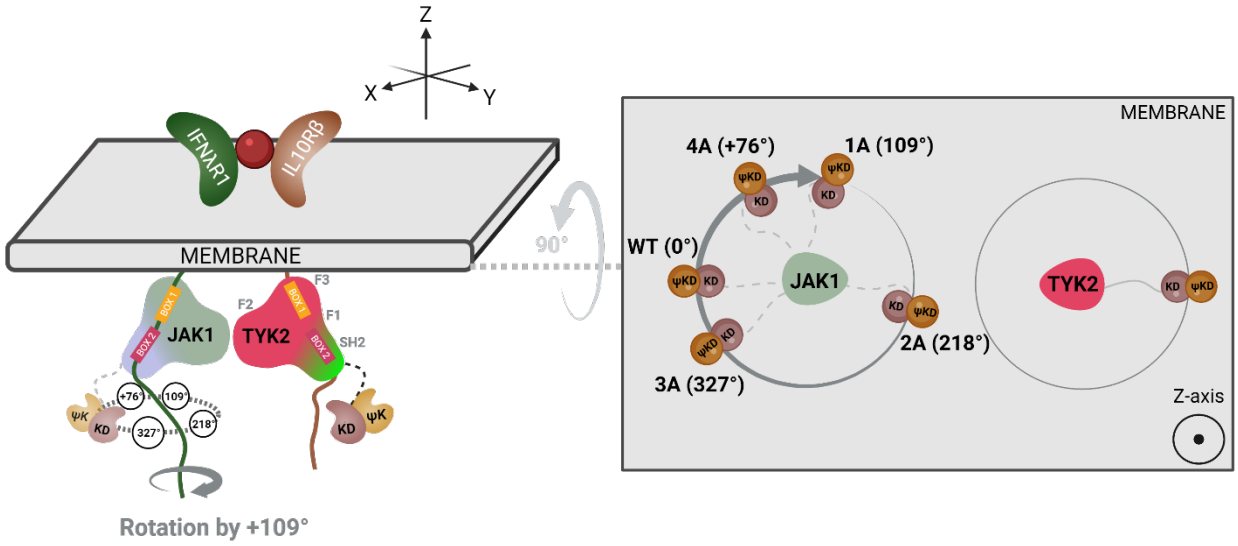


**Figure 20: A schematic diagram shows the proposed positioning of C-terminal kinase domain of JAK1 relative to its N-terminal FERM SH2 domain when viewed down the axis of rotation.** When 2 alanine residues are inserted in the transmembrane region of IFN-λR1 receptor, the near 180-degree rotation to the intracellularly associated JAK1 orients the kinase domains of JAK1 and TYK2 in a front-to-back manner, posing a physical barrier to transphosphorylation. On the contrary, the 327-degree rotation afforded by 3 alanine insertion decreases the distance between the kinase domains of JAK1 and TYK2 within the signaling complex, facilitating a more efficient transphosphorylation that leads to enhanced biological activities for type III IFNs.

### 4.04: Future Directions

Our work indicates that when manipulated individually, the affinity of the receptor-JAK axis and the spatial alignment of the transphosphorylating JAKs can each effectively modulate the signaling activities of type III IFNs. We have shown that manipulations directed at either aspect can lead to significant reductions in the potency gap between type I and III IFNs. What remains unknown is how these two modes of modifications, when introduced in tandem, affect the downstream IFN signaling. A question naturally arises as to whether such an approach can entirely eliminate the potency gap between type I and III IFNs. In order to address this experimentally, it would involve creating double mutant cell lines expressing both the register-

optimized IFN-λR1 receptor and affinity-matured IL-10Rβ receptor against TYK2. Functional assays conducted on these cell lines will likely provide a more informative picture of how the receptor-JAK interactions affect the downstream signaling of IFNs.

Our findings also raise an important question as to whether the effects observed in our *in vitro* experiments can be replicated *in vivo*. Two general frameworks may be of use in interrogating the *in vivo* anti-viral and anti-cancer activities. First approach involves the use of human xenograft or humanized chimeric mouse models. For instance, anti-cancer activities can be observed via a mouse xenograft model established by inoculating immunodeficient mice with a non IFN-λ responsive human tumor cell line transduced to express wild-type or mutant IFN-λR1. Since human orthologs are directly used to stimulate activities in human cell lines, this framework may provide a translationally relevant platform for evaluating the efficacy and toxicity of type III IFNs as potential therapeutics. Alternatively, a similar protein engineering approach outlined in this work can be applied to murine cytokines and receptors. Unlike the former, this framework allows the use of syngeneic tumor models to investigate the anti-cancer activities of type III IFNs both as a stand-alone therapy and in potential combination with immunotherapy. Another added advantage here is that we can determine if the murine ortholog of type III IFNs is at all sensitive to modifications in the receptor-JAK axis and if so, the extent and manner of such dependence. For instance, it is not unlikely that the intracellular geometry of IFN-λ signaling complex in mice differs significantly from that in human given that the sequence homology between human and mice type III IFNs and their receptors is only moderate (60-69%)[160]. Consequently, the optimal rotation of the murine IFN-λR1 receptor required for maximal signaling output may as well differ from that we previously determined for its human counterpart.

On a related note, we introduced the graduated rotations in the register of the intracellular domain by inserting additional alanine residues within the α-helical stretch of the juxtamembrane region. Although this particular method of engineering mutant IFN-λR1 receptors was apropos in establishing the role of receptor geometry in IFN signaling, it can be argued that this method is largely impractical from a therapeutic standpoint. We counter that the conclusions drawn from these experiments can be used to guide computational designs of mimetic IFN-λ3 ligands. Previous studies have shown that extracellular reorientation of a receptor complex can be effectively transmitted to its intracellular domains[129]. In an analogous fashion, these engineered ligands can induce register-rotating effects in the cytosolic domains of IFN-λR1 receptor by extracellularly binding the receptor in such a way that it reorients the receptor by the same degree as 3 alanine residue-insertion in the transmembrane region. Pending further characterizations, we propose that this strategy of generating geometry-guided ligands can potentially expand the preexisting efforts to translate type III IFNs for clinical applications.

**4.05: Conclusion**

Universal and crucial to signaling cascades initiated by a wide range of membrane receptors including over 40 cytokine receptors, the JAK/STAT pathway is one of the oldest and most intensely researched cellular machineries. However, significant gaps in knowledge remain in our current understanding of the cytokine receptor-JAK interactions and their role in determining the downstream signaling events. Our aim was to systematically mutate each of the two key parameters involved in the receptor-JAK axis – the affinity of the interaction and the geometry of proximal JAKs and observe how variations in each parameter translate to downstream biological activities of IFNs. Here, our results indicate that both parameters play important roles in determining the potency and efficiency of type III IFN signaling, though the

optimizations made to the intracellular geometry of the receptor eliciting greater responses than those made to the affinity of the interaction. We demonstrate that by fine-tuning the receptor-JAK interactions, we can significantly narrow, if not entirely eliminate in certain aspects, the expansive gap in potency between type I and III IFNs. Ultimately, our findings have opened up future venues for continued research that will have significant impact not only on expanding our canonical understanding of the JAK/STAT pathway in the context of IFN signaling but also on devising novel strategies for clinical translations of type III IFNs.

## References


1 Kany, S., Vollrath, J. T. & Relja, B. Cytokines in Inflammatory Disease. *International journal of molecular sciences* **20**, 6008, doi:10.3390/ijms20236008 (2019).

2 Zhang, J.-M. & An, J. Cytokines, inflammation, and pain. *International anesthesiology clinics* **45**, 27-37, doi:10.1097/AIA.0b013e318034194e (2007).

3 Oppenheim, J. J. Cytokines: past, present, and future. *Int J Hematol* **74**, 3-8, doi:10.1007/bf02982543 (2001).

4 Turner, M. D., Nedjai, B., Hurst, T. & Pennington, D. J. Cytokines and chemokines: At the crossroads of cell signalling and inflammatory disease. *Biochimica et Biophysica Acta (BBA) - Molecular Cell Research* **1843**, 2563-2582, doi:https://doi.org/10.1016/j.bbamcr.2014.05.014 (2014).

5 Ait-Oufella, H., Taleb, S., Mallat, Z. & Tedgui, A. Recent Advances on the Role of Cytokines in Atherosclerosis. *Arteriosclerosis, Thrombosis, and Vascular Biology* **31**, 969-979, doi:10.1161/ATVBAHA.110.207415 (2011).

6 Dinarello, C. A. Immunological and inflammatory functions of the interleukin-1 family. *Annu Rev Immunol* **27**, 519-550, doi:10.1146/annurev.immunol.021908.132612 (2009).

7 Wang, X., Lupardus, P., Laporte, S. L. & Garcia, K. C. Structural biology of shared cytokine receptors. *Annual review of immunology* **27**, 29-60, doi:10.1146/annurev.immunol.24.021605.090616 (2009).

8 Foster, J. R. The functions of cytokines and their uses in toxicology. *International journal of experimental pathology* **82**, 171-192, doi:10.1046/j.1365-2613.2001.iep0082-0171-x (2001).

9 Dinarello, C. A. Historical insights into cytokines. *European journal of immunology* **37 Suppl 1**, S34-S45, doi:10.1002/eji.200737772 (2007).

10 Morris, R., Kershaw, N. J. & Babon, J. J. The molecular details of cytokine signaling via the JAK/STAT pathway. *Protein science : a publication of the Protein Society* **27**, 1984-2009, doi:10.1002/pro.3519 (2018).

11 Boulay, J. L., O'Shea, J. J. & Paul, W. E. Molecular phylogeny within type I cytokines and their cognate receptors. *Immunity* **19**, 159-163, doi:10.1016/s1074-7613(03)00211-5 (2003).

12 Cohen, O., Weissman, D., Fauci, A. & Paul, W. (Lippincott-Raven Philadelphia, PA, 1999).

13 Bazan, J. F. Haemopoietic receptors and helical cytokines. *Immunol Today* **11**, 350-354, doi:10.1016/0167-5699(90)90139-z (1990).

14 Cosman, D. The hematopoietin receptor superfamily. *Cytokine* **5**, 95-106, doi:10.1016/1043-4666(93)90047-9 (1993).

15 Bazan, J. F. Shared architecture of hormone binding domains in type I and II interferon receptors. *Cell* **61**, 753-754, doi:10.1016/0092-8674(90)90182-e (1990).

16 de Vos, A. M., Ultsch, M. & Kossiakoff, A. A. Human growth hormone and extracellular domain of its receptor: crystal structure of the complex. *Science* **255**, 306-312, doi:10.1126/science.1549776 (1992).

17 Yawata, H. *et al.* Structure-function analysis of human IL-6 receptor: dissociation of amino acid residues required for IL-6-binding and for IL-6 signal transduction through gp130. *EMBO J.* **12**, 1705-1712 (1993).

18 Taga, T. & Kishimoto, T. Gp130 and the interleukin-6 family of cytokines. *Annu Rev Immunol* **15**, 797-819, doi:10.1146/annurev.immunol.15.1.797 (1997).

19 Bravo, J. & Heath, J. K. Receptor recognition by gp130 cytokines. *EMBO J.* **19**, 2399-2411, doi:10.1093/emboj/19.11.2399 (2000).

20 Tavernier, J. *et al.* A human high affinity interleukin-5 receptor (IL5R) is composed of an IL5-specific alpha chain and a beta chain shared with the receptor for GM-CSF. *Cell* **66**, 1175-1184, doi:10.1016/0092-8674(91)90040-6 (1991).

21 Bagley, C. J., Woodcock, J. M., Hercus, T. R., Shannon, M. F. & Lopez, A. F. Interaction of GM-CSF and IL-3 with the common beta-chain of their receptors. *J Leukoc Biol* **57**, 739-746, doi:10.1002/jlb.57.5.739 (1995).

22 Nicola, N. A., Smith, A., Robb, L., Metcalf, D. & Begley, C. G. The structural basis of the biological actions of the GM-CSF receptor. *Ciba Found Symp* **204**, 19-27; discussion 27-32, doi:10.1002/9780470515280.ch3 (1997).

23 Ozaki, K. & Leonard, W. J. Cytokine and cytokine receptor pleiotropy and redundancy. *J. Biol. Chem.* **277**, 29355-29358, doi:10.1074/jbc.R200003200 (2002).

24 Walter, M. R. Crystal structures of alpha-helical cytokine-receptor complexes: we've only scratched the surface. *Biotechniques* **Suppl**, 46-48, 50-47 (2002).

25 Renauld, J.-C. Class II cytokine receptors and their ligands: Key antiviral and inflammatory modulators. *Nature Reviews Immunology* **3**, 667-676, doi:10.1038/nri1153 (2003).

26 Spangler, J. B., Moraga, I., Mendoza, J. L. & Garcia, K. C. Insights into cytokine-receptor interactions from cytokine engineering. *Annu Rev Immunol* **33**, 139-167, doi:10.1146/annurev-immunol-032713-120211 (2015).

27 Logsdon, N. J., Jones, B. C., Josephson, K., Cook, J. & Walter, M. R. Comparison of interleukin-22 and interleukin-10 soluble receptor complexes. *J. Interferon Cytokine Res.* **22**, 1099-1112, doi:10.1089/10799900260442520 (2002).

28 Jones, B. C., Logsdon, N. J. & Walter, M. R. Structure of IL-22 bound to its high-affinity IL-22R1 chain. *Structure* **16**, 1333-1344, doi:10.1016/j.str.2008.06.005 (2008).

29 Bach, E. A. *et al.* Ligand-induced assembly and activation of the gamma interferon receptor in intact cells. *Mol Cell Biol* **16**, 3214-3221, doi:10.1128/mcb.16.6.3214 (1996).

30 Isaacs, A. & Lindenmann, J. Virus interference. I. The interferon. *Proc R Soc Lond B Biol Sci* **147**, 258-267, doi:10.1098/rspb.1957.0048 (1957).

31 Vilček, J. & Feldmann, M. Historical review: Cytokines as therapeutics and targets of therapeutics. *Trends in Pharmacological Sciences* **25**, 201-209, doi:https://doi.org/10.1016/j.tips.2004.02.011 (2004).

32 de Weerd, N. A. & Nguyen, T. The interferons and their receptors--distribution and regulation. *Immunology and cell biology* **90**, 483-491, doi:10.1038/icb.2012.9 (2012).

33 Wack, A., Terczyńska-Dyla, E. & Hartmann, R. Guarding the frontiers: the biology of type III interferons. *Nature Immunology* **16**, 802-809, doi:10.1038/ni.3212 (2015).

34 Lee, A. J. & Ashkar, A. A. The Dual Nature of Type I and Type II Interferons. *Frontiers in Immunology* **9**, doi:10.3389/fimmu.2018.02061 (2018).

35 Mendoza, J. L. *et al.* Structure of the IFNγ receptor complex guides design of biased agonists. *Nature* **567**, 56-60, doi:10.1038/s41586-019-0988-7 (2019).

36 Pestka, S., Langer, J. A., Zoon, K. C. & Samuel, C. E. Interferons and their actions. *Annu. Rev. Biochem* **56**, 727-777, doi:10.1146/annurev.bi.56.070187.003455 (1987).

37 Pestka, S., Krause, C. D. & Walter, M. R. Interferons, interferon-like cytokines, and their receptors. *Immunol Rev* **202**, 8-32, doi:10.1111/j.0105-2896.2004.00204.x (2004).

38 Thomas, C. *et al.* Structural linkage between ligand discrimination and receptor activation by type I interferons. *Cell* **146**, 621-632, doi:10.1016/j.cell.2011.06.048 (2011).

39 Kotenko, S. V. *et al.* IFN-lambdas mediate antiviral protection through a distinct class II cytokine receptor complex. *Nat Immunol* **4**, 69-77, doi:10.1038/ni875 (2003).

40 Sheppard, P. *et al.* IL-28, IL-29 and their class II cytokine receptor IL-28R. *Nat Immunol* **4**, 63-68, doi:10.1038/ni873 (2003).

41 O'Brien, T. R., Prokunina-Olsson, L. & Donnelly, R. P. IFN-λ4: The Paradoxical New Member of the Interferon Lambda Family. *Journal of Interferon & Cytokine Research* **34**, 829-838, doi:10.1089/jir.2013.0136 (2014).

42 Donnelly, R. P., Sheikh, F., Kotenko, S. V. & Dickensheets, H. The expanded family of class II cytokines that share the IL-10 receptor-2 (IL-10R2) chain. *J Leukoc Biol* **76**, 314-321, doi:10.1189/jlb.0204117 (2004).

43 Levy, D. E., Marié, I. J. & Durbin, J. E. Induction and function of type I and III interferon in response to viral infection. *Current opinion in virology* **1**, 476-486, doi:10.1016/j.coviro.2011.11.001 (2011).

44 Ford, E. & Thanos, D. The transcriptional code of human IFN-beta gene expression. *Biochim. Biophys. Acta* **1799**, 328-336, doi:10.1016/j.bbagrm.2010.01.010 (2010).

45 O'Neill, L. A. & Bowie, A. G. Sensing and signaling in antiviral innate immunity. *Curr Biol* **20**, R328-333, doi:10.1016/j.cub.2010.01.044 (2010).

46 Zahid, A., Ismail, H., Li, B. & Jin, T. Molecular and Structural Basis of DNA Sensors in Antiviral Innate Immunity. *Frontiers in Immunology* **11**, doi:10.3389/fimmu.2020.613039 (2020).

47 Kagan, J. C. *et al.* TRAM couples endocytosis of Toll-like receptor 4 to the induction of interferon-beta. *Nat Immunol* **9**, 361-368, doi:10.1038/ni1569 (2008).

48 Odendall, C., Voak, A. A. & Kagan, J. C. Type III IFNs Are Commonly Induced by Bacteria-Sensing TLRs and Reinforce Epithelial Barriers during Infection. *J Immunol* **199**, 3270-3279, doi:10.4049/jimmunol.1700250 (2017).

49 Honda, K., Takaoka, A. & Taniguchi, T. Type I interferon [corrected] gene induction by the interferon regulatory factor family of transcription factors. *Immunity* **25**, 349-360, doi:10.1016/j.immuni.2006.08.009 (2006).

50 Taniguchi, T., Ogasawara, K., Takaoka, A. & Tanaka, N. IRF Family of Transcription Factors as Regulators of Host Defense. *Annual Review of Immunology* **19**, 623-655, doi:10.1146/annurev.immunol.19.1.623 (2001).

51 Lazear, H. M. *et al.* IRF-3, IRF-5, and IRF-7 coordinately regulate the type I IFN response in myeloid dendritic cells downstream of MAVS signaling. *PLoS Pathog* **9**, e1003118, doi:10.1371/journal.ppat.1003118 (2013).

52 Osterlund, P. I., Pietilä, T. E., Veckman, V., Kotenko, S. V. & Julkunen, I. IFN regulatory factor family members differentially regulate the expression of type III IFN (IFN-lambda) genes. *J Immunol* **179**, 3434-3442, doi:10.4049/jimmunol.179.6.3434 (2007).

53 Odendall, C. *et al.* Diverse intracellular pathogens activate type III interferon expression from peroxisomes. *Nat Immunol* **15**, 717-726, doi:10.1038/ni.2915 (2014).

54 Pulverer, J. E. *et al.* Temporal and spatial resolution of type I and III interferon responses in vivo. *J Virol* **84**, 8626-8638, doi:10.1128/jvi.00303-10 (2010).

55 Lazear, H. M., Schoggins, J. W. & Diamond, M. S. Shared and Distinct Functions of Type I and Type III Interferons. *Immunity* **50**, 907-923, doi:10.1016/j.immuni.2019.03.025 (2019).

56 Kotenko, S. V. & Durbin, J. E. Contribution of type III interferons to antiviral immunity: location, location, location. *J. Biol. Chem.* **292**, 7295-7303, doi:10.1074/jbc.R117.777102 (2017).

57 Lazear, H. M., Nice, T. J. & Diamond, M. S. Interferon-λ: Immune Functions at Barrier Surfaces and Beyond. *Immunity* **43**, 15-28, doi:10.1016/j.immuni.2015.07.001 (2015).

58 Wells, A. I. & Coyne, C. B. Type III Interferons in Antiviral Defenses at Barrier Surfaces. *Trends Immunol* **39**, 848-858, doi:10.1016/j.it.2018.08.008 (2018).

59 Piehler, J., Thomas, C., Garcia, K. C. & Schreiber, G. Structural and dynamic determinants of type I interferon receptor assembly and their functional interpretation. *Immunological reviews* **250**, 317-334, doi:10.1111/imr.12001 (2012).

60 Teijaro, J. R. Type I interferons in viral control and immune regulation. *Curr Opin Virol* **16**, 31-40, doi:10.1016/j.coviro.2016.01.001 (2016).

61 Ingle, H., Peterson, S. T. & Baldridge, M. T. Distinct Effects of Type I and III Interferons on Enteric Viruses. *Viruses* **10**, 46, doi:10.3390/v10010046 (2018).

62 Stanifer, M. L., Guo, C., Doldan, P. & Boulant, S. Importance of Type I and III Interferons at Respiratory and Intestinal Barrier Surfaces. *Frontiers in Immunology* **11**, doi:10.3389/fimmu.2020.608645 (2020).

63 Forero, A. *et al.* Differential Activation of the Transcription Factor IRF1 Underlies the Distinct Immune Responses Elicited by Type I and Type III Interferons. *Immunity* **51**, 451-464.e456, doi:https://doi.org/10.1016/j.immuni.2019.07.007 (2019).

64 Liu, J. *et al.* Ligand-independent pathway that controls stability of interferon alpha receptor. *Biochem. Biophys. Res. Commun.* **367**, 388-393, doi:https://doi.org/10.1016/j.bbrc.2007.12.137 (2008).

65 Shaw, A. E. *et al.* Fundamental properties of the mammalian innate immune system revealed by multispecies comparison of type I interferon responses. *PLoS Biol* **15**, e2004086, doi:10.1371/journal.pbio.2004086 (2017).

66 Crotta, S. *et al.* Type I and type III interferons drive redundant amplification loops to induce a transcriptional signature in influenza-infected airway epithelia. *PLoS Pathog* **9**, e1003773, doi:10.1371/journal.ppat.1003773 (2013).

67 Doyle, S. E. *et al.* Interleukin-29 uses a type 1 interferon-like program to promote antiviral responses in human hepatocytes. *Hepatology* **44**, 896-906, doi:10.1002/hep.21312 (2006).

68 Marcello, T. *et al.* Interferons alpha and lambda inhibit hepatitis C virus replication with distinct signal transduction and gene regulation kinetics. *Gastroenterology* **131**, 1887-1898, doi:10.1053/j.gastro.2006.09.052 (2006).

69 Zhou, Z. *et al.* Type III interferon (IFN) induces a type I IFN-like response in a restricted subset of cells through signaling pathways involving both the Jak-STAT pathway and the mitogen-activated protein kinases. *J Virol* **81**, 7749-7758, doi:10.1128/jvi.02438-06 (2007).

70 Caine, E. A. *et al.* Interferon lambda protects the female reproductive tract against Zika virus infection. *Nat Commun* **10**, 280, doi:10.1038/s41467-018-07993-2 (2019).

71 O'Shea, J. J., Holland, S. M. & Staudt, L. M. JAKs and STATs in immunity, immunodeficiency, and cancer. *N Engl J Med* **368**, 161-170, doi:10.1056/NEJMra1202117 (2013).

72 Gough, D. J., Levy, D. E., Johnstone, R. W. & Clarke, C. J. IFNgamma signaling-does it mean JAK-STAT? *Cytokine Growth Factor Rev* **19**, 383-394, doi:10.1016/j.cytogfr.2008.08.004 (2008).

73 Murray, P. J. The JAK-STAT Signaling Pathway: Input and Output Integration. *The Journal of Immunology* **178**, 2623, doi:10.4049/jimmunol.178.5.2623 (2007).

74 Ferrao, R. *et al.* The Structural Basis for Class II Cytokine Receptor Recognition by JAK1. *Structure* **24**, 897-905, doi:10.1016/j.str.2016.03.023 (2016).

75 Zhang, D., Wlodawer, A. & Lubkowski, J. Crystal Structure of a Complex of the Intracellular Domain of Interferon λ Receptor 1 (IFNLR1) and the FERM/SH2 Domains of Human JAK1. *J. Mol. Biol.* **428**, 4651-4668, doi:10.1016/j.jmb.2016.10.005 (2016).

76 Wallweber, H. J., Tam, C., Franke, Y., Starovasnik, M. A. & Lupardus, P. J. Structural basis of recognition of interferon-α receptor by tyrosine kinase 2. *Nat Struct Mol Biol* **21**, 443-448, doi:10.1038/nsmb.2807 (2014).

77 Behrmann, I. *et al.* Janus kinase (Jak) subcellular localization revisited: the exclusive membrane localization of endogenous Janus kinase 1 by cytokine receptor interaction uncovers the Jak·

receptor complex to be equivalent to a receptor tyrosine kinase. *J. Biol. Chem.* **279**, 35486-35493 (2004).

78 Bousoik, E. & Montazeri Aliabadi, H. "Do We Know Jack" About JAK? A Closer Look at JAK/STAT Signaling Pathway. *Frontiers in Oncology* **8**, doi:10.3389/fonc.2018.00287 (2018).

79 Argetsinger, L. S. *et al.* Identification of JAK2 as a growth hormone receptor-associated tyrosine kinase. *Cell* **74**, 237-244, doi:10.1016/0092-8674(93)90415-m (1993).

80 Turkson, J. & Jove, R. STAT proteins: novel molecular targets for cancer drug discovery. *Oncogene* **19**, 6613-6626, doi:10.1038/sj.onc.1204086 (2000).

81 Schindler, C., Shuai, K., Prezioso, V. R. & Darnell, J. E., Jr. Interferon-dependent tyrosine phosphorylation of a latent cytoplasmic transcription factor. *Science* **257**, 809-813, doi:10.1126/science.1496401 (1992).

82 Shuai, K., Schindler, C., Prezioso, V. R. & Darnell, J. E., Jr. Activation of transcription by IFN-gamma: tyrosine phosphorylation of a 91-kD DNA binding protein. *Science* **258**, 1808-1812, doi:10.1126/science.1281555 (1992).

83 Schindler, C. & Darnell, J. E., Jr. Transcriptional responses to polypeptide ligands: the JAK-STAT pathway. *Annu. Rev. Biochem* **64**, 621-651, doi:10.1146/annurev.bi.64.070195.003201 (1995).

84 Yoshimura, A., Ito, M., Chikuma, S., Akanuma, T. & Nakatsukasa, H. Negative Regulation of Cytokine Signaling in Immunity. *Cold Spring Harb Perspect Biol* **10**, doi:10.1101/cshperspect.a028571 (2018).

85 Yoshimura, A. *et al.* A novel cytokine-inducible gene CIS encodes an SH2-containing protein that binds to tyrosine-phosphorylated interleukin 3 and erythropoietin receptors. *EMBO J.* **14**, 2816-2826 (1995).

86 Endo, T. A. *et al.* A new protein containing an SH2 domain that inhibits JAK kinases. *Nature* **387**, 921-924, doi:10.1038/43213 (1997).

87 Hunter, T. Protein kinases and phosphatases: the yin and yang of protein phosphorylation and signaling. *Cell* **80**, 225-236, doi:10.1016/0092-8674(95)90405-0 (1995).

88 Tonks, N. K. & Neel, B. G. Combinatorial control of the specificity of protein tyrosine phosphatases. *Curr Opin Cell Biol* **13**, 182-195, doi:10.1016/s0955-0674(00)00196-4 (2001).

89 Rawlings, J. S., Rosler, K. M. & Harrison, D. A. The JAK/STAT signaling pathway. *J. Cell Sci.* **117**, 1281-1283, doi:10.1242/jcs.00963 (2004).

90 O'Shea, J. J., Gadina, M. & Schreiber, R. D. Cytokine signaling in 2002: new surprises in the Jak/Stat pathway. *Cell* **109 Suppl**, S121-131, doi:10.1016/s0092-8674(02)00701-8 (2002).

91 Ghoreschi, K., Laurence, A. & O'Shea, J. J. Janus kinases in immune cell signaling. *Immunological reviews* **228**, 273-287, doi:10.1111/j.1600-065X.2008.00754.x (2009).

92 Wesoly, J., Szweykowska-Kulinska, Z. & Bluyssen, H. A. STAT activation and differential complex formation dictate selectivity of interferon responses. *Acta Biochim. Pol.* **54**, 27-38 (2007).

93 McComb, S. *et al.* Type-I interferon signaling through ISGF3 complex is required for sustained Rip3 activation and necroptosis in macrophages. *Proceedings of the National Academy of Sciences* **111**, E3206-E3213, doi:10.1073/pnas.1407068111 (2014).

94 Pelletier, S., Gingras, S., Funakoshi-Tago, M., Howell, S. & Ihle, J. N. Two domains of the erythropoietin receptor are sufficient for Jak2 binding/activation and function. *Mol Cell Biol* **26**, 8527-8538, doi:10.1128/mcb.01035-06 (2006).

95 Wallweber, H. J. A., Tam, C., Franke, Y., Starovasnik, M. A. & Lupardus, P. J. Structural basis of recognition of interferon-α receptor by tyrosine kinase 2. *Nature structural & molecular biology* **21**, 443-448, doi:10.1038/nsmb.2807 (2014).

96 Murray, P. J. Understanding and exploiting the endogenous interleukin-10/STAT3-mediated anti-inflammatory response. *Curr. Opin. Pharmacol.* **6**, 379-386, doi:10.1016/j.coph.2006.01.010 (2006).

97 El Kasmi, K. C. *et al.* General Nature of the STAT3-Activated Anti-Inflammatory Response. *The Journal of Immunology* **177**, 7880-7888, doi:10.4049/jimmunol.177.11.7880 (2006).

98 Jaks, E., Gavutis, M., Uzé, G., Martal, J. & Piehler, J. Differential receptor subunit affinities of type I interferons govern differential signal activation. *J. Mol. Biol.* **366**, 525-539, doi:10.1016/j.jmb.2006.11.053 (2007).

99 Lavoie, T. B. *et al.* Binding and activity of all human alpha interferon subtypes. *Cytokine* **56**, 282-289, doi:10.1016/j.cyto.2011.07.019 (2011).

100 Mendoza, J. L. *et al.* The IFN-λ-IFN-λR1-IL-10Rβ Complex Reveals Structural Features Underlying Type III IFN Functional Plasticity. *Immunity* **46**, 379-392, doi:10.1016/j.immuni.2017.02.017 (2017).

101 Dellgren, C., Gad, H. H., Hamming, O. J., Melchjorsen, J. & Hartmann, R. Human interferon-lambda3 is a potent member of the type III interferon family. *Genes Immun* **10**, 125-131, doi:10.1038/gene.2008.87 (2009).

102 Tan, J. C., Indelicato, S. R., Narula, S. K., Zavodny, P. J. & Chou, C. C. Characterization of interleukin-10 receptors on human and mouse cells. *J. Biol. Chem.* **268**, 21053-21059 (1993).

103 Dondi, E. *et al.* Down-modulation of Type 1 Interferon Responses by Receptor Cross-competition for a Shared Jak Kinase*. *J. Biol. Chem.* **276**, 47004-47012, doi:https://doi.org/10.1074/jbc.M104316200 (2001).

104 Levin, A. M. *et al.* Exploiting a natural conformational switch to engineer an interleukin-2 'superkine'. *Nature* **484**, 529-533, doi:10.1038/nature10975 (2012).

105 Labun, K. *et al.* CHOPCHOP v3: expanding the CRISPR web toolbox beyond genome editing. *Nucleic Acids Res.* **47**, W171-W174, doi:10.1093/nar/gkz365 (2019).

106 Ran, F. A. *et al.* Genome engineering using the CRISPR-Cas9 system. *Nature Protocols* **8**, 2281-2308, doi:10.1038/nprot.2013.143 (2013).

107 Chen, W. *et al.* Establishing a safe, rapid, convenient and low-cost antiviral assay of interferon bioactivity based on recombinant VSV expressing GFP. *Journal of Virological Methods* **252**, 1-7, doi:https://doi.org/10.1016/j.jviromet.2017.08.007 (2018).

108 Murakami, M. *et al.* Critical cytoplasmic region of the interleukin 6 signal transducer gp130 is conserved in the cytokine receptor family. *Proc Natl Acad Sci U S A* **88**, 11349-11353, doi:10.1073/pnas.88.24.11349 (1991).

109 Radtke, S. *et al.* The Jak1 SH2 domain does not fulfill a classical SH2 function in Jak/STAT signaling but plays a structural role for receptor interaction and up-regulation of receptor surface expression. *J. Biol. Chem.* **280**, 25760-25768, doi:10.1074/jbc.M500822200 (2005).

110 Tanner, J. W., Chen, W., Young, R. L., Longmore, G. D. & Shaw, A. S. The conserved box 1 motif of cytokine receptors is required for association with JAK kinases. *J. Biol. Chem.* **270**, 6523-6530, doi:10.1074/jbc.270.12.6523 (1995).

111 Usacheva, A. *et al.* Contribution of the Box 1 and Box 2 motifs of cytokine receptors to Jak1 association and activation. *J. Biol. Chem.* **277**, 48220-48226, doi:10.1074/jbc.M205757200 (2002).

112 Haan, C., Heinrich, P. C. & Behrmann, I. Structural requirements of the interleukin-6 signal transducer gp130 for its interaction with Janus kinase 1: the receptor is crucial for kinase activation. *Biochem. J* **361**, 105-111, doi:10.1042/0264-6021:3610105 (2002).

113 Richter, M. F., Duménil, G., Uzé, G., Fellous, M. & Pellegrini, S. Specific contribution of Tyk2 JH regions to the binding and the expression of the interferon alpha/beta receptor component IFNAR1. *J. Biol. Chem.* **273**, 24723-24729, doi:10.1074/jbc.273.38.24723 (1998).

114 Yan, H., Krishnan, K., Lim, J. T., Contillo, L. G. & Krolewski, J. J. Molecular characterization of an alpha interferon receptor 1 subunit (IFNaR1) domain required for TYK2 binding and signal transduction. *Mol Cell Biol* **16**, 2074-2082, doi:10.1128/mcb.16.5.2074 (1996).

115 Zhao, Y., Wagner, F., Frank, S. J. & Kraft, A. S. The amino-terminal portion of the JAK2 protein kinase is necessary for binding and phosphorylation of the granulocyte-macrophage colony-stimulating factor receptor beta c chain. *J. Biol. Chem.* **270**, 13814-13818, doi:10.1074/jbc.270.23.13814 (1995).

116 Greiser, J. S., Stross, C., Heinrich, P. C., Behrmann, I. & Hermanns, H. M. Orientational constraints of the gp130 intracellular juxtamembrane domain for signaling. *J. Biol. Chem.* **277**, 26959-26965, doi:10.1074/jbc.M204113200 (2002).

117 Velazquez, L., Fellous, M., Stark, G. R. & Pellegrini, S. A protein tyrosine kinase in the interferon alpha/beta signaling pathway. *Cell* **70**, 313-322, doi:10.1016/0092-8674(92)90105-l (1992).

118 Colamonici, O. R., Uyttendaele, H., Domanski, P., Yan, H. & Krolewski, J. J. p135tyk2, an interferon-alpha-activated tyrosine kinase, is physically associated with an interferon-alpha receptor. *J. Biol. Chem.* **269**, 3518-3522 (1994).

119 Colamonici, O. *et al.* Direct binding to and tyrosine phosphorylation of the alpha subunit of the type I interferon receptor by p135tyk2 tyrosine kinase. *Mol Cell Biol* **14**, 8133-8142, doi:10.1128/mcb.14.12.8133-8142.1994 (1994).

120 Domanski, P. *et al.* A Region of the β Subunit of the Interferon α Receptor Different from Box 1 Interacts with Jak1 and Is Sufficient to Activate the Jak-Stat Pathway and Induce an Antiviral State*. *J. Biol. Chem.* **272**, 26388-26393, doi:https://doi.org/10.1074/jbc.272.42.26388 (1997).

121 Ho, A. S., Wei, S. H., Mui, A. L., Miyajima, A. & Moore, K. W. Functional regions of the mouse interleukin-10 receptor cytoplasmic domain. *Molecular and cellular biology* **15**, 5043-5053, doi:10.1128/MCB.15.9.5043 (1995).

122 Finbloom, D. S. & Winestock, K. D. IL-10 induces the tyrosine phosphorylation of tyk2 and Jak1 and the differential assembly of STAT1 alpha and STAT3 complexes in human T cells and monocytes. *J Immunol* **155**, 1079-1090 (1995).

123 Walter, M. R. The molecular basis of IL-10 function: from receptor structure to the onset of signaling. *Current topics in microbiology and immunology* **380**, 191-212, doi:10.1007/978-3-662-43492-5_9 (2014).

124 Leonard, W. J. & O'Shea, J. J. Jaks and STATs: biological implications. *Annual review of immunology* **16**, 293-322 (1998).

125 Novick, D., Cohen, B. & Rubinstein, M. The human interferon αβ receptor: Characterization and molecular cloning. *Cell* **77**, 391-400, doi:https://doi.org/10.1016/0092-8674(94)90154-6 (1994).

126 Dickensheets, H., Sheikh, F., Park, O., Gao, B. & Donnelly, R. P. Interferon-lambda (IFN-λ) induces signal transduction and gene expression in human hepatocytes, but not in lymphocytes or monocytes. *J Leukoc Biol* **93**, 377-385, doi:10.1189/jlb.0812395 (2013).

127 Sheikh, F. *et al.* Cutting Edge: IL-26 Signals through a Novel Receptor Complex Composed of IL-20 Receptor 1 and IL-10 Receptor 2. *The Journal of Immunology* **172**, 2006, doi:10.4049/jimmunol.172.4.2006 (2004).

128 Livnah, O. *et al.* Functional mimicry of a protein hormone by a peptide agonist: the EPO receptor complex at 2.8 Å. *Science* **273**, 464-471 (1996).

129 Livnah, O. *et al.* An antagonist peptide–EPO receptor complex suggests that receptor dimerization is not sufficient for activation. *Nature structural biology* **5**, 993-1004 (1998).

130 Syed, R. S. *et al.* Efficiency of signalling through cytokine receptors depends critically on receptor orientation. *Nature* **395**, 511-516 (1998).

131 Muthukumaran, G., Kotenko, S., Donnelly, R., Ihle, J. N. & Pestka, S. Chimeric Erythropoietin-Interferon γ Receptors Reveal Differences in Functional Architecture of Intracellular Domains for Signal Transduction*. *J. Biol. Chem.* **272**, 4993-4999, doi:https://doi.org/10.1074/jbc.272.8.4993 (1997).

132 Watowich, S. S. The erythropoietin receptor: molecular structure and hematopoietic signaling pathways. *Journal of investigative medicine : the official publication of the American Federation for Clinical Research* **59**, 1067-1072, doi:10.2310/JIM.0b013e31820fb28c (2011).

133 Ealick, S. E. *et al.* Three-dimensional structure of recombinant human interferon-gamma. *Science* **252**, 698-702, doi:10.1126/science.1902591 (1991).

134 Fountoulakis, M., Zulauf, M., Lustig, A. & Garotta, G. Stoichiometry of interaction between interferon γ and its receptor. *Eur. J. Biochem.* **208**, 781-787, doi:https://doi.org/10.1111/j.1432-1033.1992.tb17248.x (1992).

135 Constantinescu, S. N., Huang, L. J.-s., Nam, H.-s. & Lodish, H. F. The Erythropoietin Receptor Cytosolic Juxtamembrane Domain Contains an Essential, Precisely Oriented, Hydrophobic Motif. *Molecular Cell* **7**, 377-385, doi:https://doi.org/10.1016/S1097-2765(01)00185-X (2001).

136 Meager, A., Visvalingam, K., Dilger, P., Bryan, D. & Wadhwa, M. Biological activity of interleukins-28 and -29: comparison with type I interferons. *Cytokine* **31**, 109-118, doi:10.1016/j.cyto.2005.04.003 (2005).

137 Hamming, O. J. *et al.* Interferon lambda 4 signals via the IFNλ receptor to regulate antiviral activity against HCV and coronaviruses. *The EMBO journal* **32**, 3055-3065, doi:10.1038/emboj.2013.232 (2013).

138 Janssen, H. L. *et al.* Pegylated interferon alfa-2b alone or in combination with lamivudine for HBeAg-positive chronic hepatitis B: a randomised trial. *Lancet* **365**, 123-129, doi:10.1016/s0140-6736(05)17701-0 (2005).

139 Yao, J. C. *et al.* Phase III prospective randomized comparison trial of depot octreotide plus interferon alfa-2b versus depot octreotide plus bevacizumab in patients with advanced carcinoid tumors: SWOG S0518. *Journal of Clinical Oncology* **35**, 1695 (2017).

140 Lau, G. K. *et al.* Peginterferon Alfa-2a, lamivudine, and the combination for HBeAg-positive chronic hepatitis B. *N Engl J Med* **352**, 2682-2695, doi:10.1056/NEJMoa043470 (2005).

141 Manns, M. P. *et al.* Peginterferon alfa-2b plus ribavirin compared with interferon alfa-2b plus ribavirin for initial treatment of chronic hepatitis C: a randomised trial. *Lancet* **358**, 958-965, doi:10.1016/s0140-6736(01)06102-5 (2001).

142 Phillips, S. *et al.* Peg-Interferon Lambda Treatment Induces Robust Innate and Adaptive Immunity in Chronic Hepatitis B Patients. *Front Immunol* **8**, 621, doi:10.3389/fimmu.2017.00621 (2017).

143 Muir, A. J. *et al.* A randomized phase 2b study of peginterferon lambda-1a for the treatment of chronic HCV infection. *Journal of Hepatology* **61**, 1238-1246, doi:https://doi.org/10.1016/j.jhep.2014.07.022 (2014).

144 Bristol-Myers, S. *Safety Study of Pegylated Interferon Lambda Plus Single or 2 Direct Antiviral Agents With Ribavirin*, <https://ClinicalTrials.gov/show/NCT01795911> (2014).

145 Eiger, B. *A Study to Evaluate Pegylated Interferon Lambda Monotherapy in Patients With Chronic Hepatitis Delta Virus Infection*, <https://ClinicalTrials.gov/show/NCT02765802> (2018).

146 Nelson, M. *et al.* Safety and Efficacy of Pegylated Interferon Lambda, Ribavirin, and Daclatasvir in HCV and HIV-Coinfected Patients. *J. Interferon Cytokine Res.* **37**, 103-111, doi:10.1089/jir.2016.0082 (2017).

147 Kalil, A. C. *et al.* Efficacy of interferon beta-1a plus remdesivir compared with remdesivir alone in hospitalised adults with COVID-19: a double-bind, randomised, placebo-controlled, phase 3 trial. *Lancet Respir Med* **9**, 1365-1376, doi:10.1016/s2213-2600(21)00384-2 (2021).

148 Feld, J. J. *et al.* Peginterferon lambda for the treatment of outpatients with COVID-19: a phase 2, placebo-controlled randomised trial. *Lancet Respir Med* **9**, 498-510, doi:10.1016/s2213-2600(20)30566-x (2021).

149 Jagannathan, P. *et al.* Peginterferon Lambda-1a for treatment of outpatients with uncomplicated COVID-19: a randomized placebo-controlled trial. *Nature Communications* **12**, 1967, doi:10.1038/s41467-021-22177-1 (2021).

150 Pfeffer, L. M. *et al.* Biological properties of recombinant α-interferons: 40th anniversary of the discovery of interferons. *Cancer research* **58**, 2489-2499 (1998).

151 Vilcek, J. Novel interferons. *Nature immunology* **4**, 8-9 (2003).

152 Lasfar, A. *et al.* Characterization of the Mouse IFN-λ Ligand-Receptor System: IFN-λs Exhibit Antitumor Activity against B16 Melanoma. *Cancer Research* **66**, 4468-4477, doi:10.1158/0008-5472.can-05-3653 (2006).

153 Sato, A., Ohtsuki, M., Hata, M., Kobayashi, E. & Murakami, T. Antitumor Activity of IFN-λ in Murine Tumor Models. *The Journal of Immunology* **176**, 7686-7694, doi:10.4049/jimmunol.176.12.7686 (2006).

154 Numasaki, M. *et al.* IL-28 Elicits Antitumor Responses against Murine Fibrosarcoma. *The Journal of Immunology* **178**, 5086, doi:10.4049/jimmunol.178.8.5086 (2007).

155 Moraga, I., Harari, D., Schreiber, G., Uzé, G. & Pellegrini, S. Receptor density is key to the alpha2/beta interferon differential activities. *Mol Cell Biol* **29**, 4778-4787, doi:10.1128/mcb.01808-08 (2009).

156 Lupardus, P. J. *et al.* Structure of the pseudokinase–kinase domains from protein kinase TYK2 reveals a mechanism for Janus kinase (JAK) autoinhibition. *Proceedings of the National Academy of Sciences* **111**, 8025, doi:10.1073/pnas.1401180111 (2014).

157 Zak, M. *et al.* Discovery and Optimization of C-2 Methyl Imidazopyrrolopyridines as Potent and Orally Bioavailable JAK1 Inhibitors with Selectivity over JAK2. *J. Med. Chem.* **55**, 6176-6193, doi:10.1021/jm300628c (2012).

158 Vasbinder, M. M. *et al.* Identification of azabenzimidazoles as potent JAK1 selective inhibitors. *Bioorg. Med. Chem. Lett.* **26**, 60-67, doi:https://doi.org/10.1016/j.bmcl.2015.11.031 (2016).

159 Lupardus, P. J. *et al.* Structural snapshots of full-length Jak1, a transmembrane gp130/IL-6/IL-6Rα cytokine receptor complex, and the receptor-Jak1 holocomplex. *Structure (London, England : 1993)* **19**, 45-55, doi:10.1016/j.str.2010.10.010 (2011).

160 Bartlett, N. W., Buttigieg, K., Kotenko, S. V. & Smith, G. L. Murine interferon lambdas (type III interferons) exhibit potent antiviral activity in vivo in a poxvirus infection model. *Journal of General Virology* **86**, 1589-1596, doi:https://doi.org/10.1099/vir.0.80904-0 (2005).

161 Rosebeck, S. & Leaman, D. W. Mitochondrial localization and pro-apoptotic effects of the interferon-inducible protein ISG12a. *Apoptosis* **13**, 562-572, doi:10.1007/s10495-008-0190-0 (2008).

162 Gytz, H. *et al.* Apoptotic properties of the type 1 interferon induced family of human mitochondrial membrane ISG12 proteins. *Biol Cell* **109**, 94-112, doi:10.1111/boc.201600034 (2017).

163 Chen, Y. *et al.* ISG12a inhibits HCV replication and potentiates the anti-HCV activity of IFN-α through activation of the Jak/STAT signaling pathway independent of autophagy and apoptosis. *Virus Res* **227**, 231-239, doi:10.1016/j.virusres.2016.10.013 (2017).

164 Liu, G. *et al.* ISG15-dependent activation of the sensor MDA5 is antagonized by the SARS-CoV-2 papain-like protease to evade host innate immunity. *Nat Microbiol* **6**, 467-478, doi:10.1038/s41564-021-00884-1 (2021).

165 Perng, Y.-C. & Lenschow, D. J. ISG15 in antiviral immunity and beyond. *Nature Reviews Microbiology* **16**, 423-439, doi:10.1038/s41579-018-0020-5 (2018).

166 Pichlmair, A. *et al.* IFIT1 is an antiviral protein that recognizes 5′-triphosphate RNA. *Nature Immunology* **12**, 624-630, doi:10.1038/ni.2048 (2011).

167 Diamond, M. S. IFIT1: A dual sensor and effector molecule that detects non-2'-O methylated viral RNA and inhibits its translation. *Cytokine & growth factor reviews* **25**, 543-550, doi:10.1016/j.cytogfr.2014.05.002 (2014).

168 Tahara, E., Jr. *et al.* G1P3, an interferon inducible gene 6-16, is expressed in gastric cancers and inhibits mitochondrial-mediated apoptosis in gastric cancer cell line TMK-1 cell. *Cancer Immunol Immunother* **54**, 729-740, doi:10.1007/s00262-004-0645-2 (2005).

169 Meyer, K. *et al.* Interferon-α inducible protein 6 impairs EGFR activation by CD81 and inhibits hepatitis C virus infection. *Sci Rep* **5**, 9012, doi:10.1038/srep09012 (2015).

170 Ghosh, A., Sarkar, S. N., Guo, W., Bandyopadhyay, S. & Sen, G. C. Enzymatic activity of 2'-5'-oligoadenylate synthetase is impaired by specific mutations that affect oligomerization of the protein. *J. Biol. Chem.* **272**, 33220-33226, doi:10.1074/jbc.272.52.33220 (1997).

171 Donovan, J., Dufner, M. & Korennykh, A. Structural basis for cytosolic double-stranded RNA surveillance by human oligoadenylate synthetase 1. *Proc Natl Acad Sci U S A* **110**, 1652-1657, doi:10.1073/pnas.1218528110 (2013).

172 Leisching, G., Cole, V., Ali, A. T. & Baker, B. OAS1, OAS2 and OAS3 restrict intracellular M. tb replication and enhance cytokine secretion. *International Journal of Infectious Diseases* **80**, S77-S84, doi:https://doi.org/10.1016/j.ijid.2019.02.029 (2019).

173 Yang, G., Xu, Y., Chen, X. & Hu, G. IFITM1 plays an essential role in the antiproliferative action of interferon-γ. *Oncogene* **26**, 594-603, doi:10.1038/sj.onc.1209807 (2007).

174 Spence, J. S. *et al.* IFITM3 directly engages and shuttles incoming virus particles to lysosomes. *Nature Chemical Biology* **15**, 259-268, doi:10.1038/s41589-018-0213-2 (2019).

175 Power, D. *et al.* IFI44 suppresses HIV-1 LTR promoter activity and facilitates its latency. *Virology* **481**, 142-150, doi:https://doi.org/10.1016/j.virol.2015.02.046 (2015).

176 Huang, W.-C., Tung, S.-L., Chen, Y.-L., Chen, P.-M. & Chu, P.-Y. IFI44L is a novel tumor suppressor in human hepatocellular carcinoma affecting cancer stemness, metastasis, and drug resistance via regulating met/Src signaling pathway. *BMC Cancer* **18**, 609, doi:10.1186/s12885-018-4529-9 (2018).

177 Xiahou, Z. *et al.* NMI and IFP35 serve as proinflammatory DAMPs during cellular infection and injury. *Nat Commun* **8**, 950, doi:10.1038/s41467-017-00930-9 (2017).

178 Das, A., Dinh, P. X. & Pattnaik, A. K. Trim21 regulates Nmi-IFI35 complex-mediated inhibition of innate antiviral response. *Virology* **485**, 383-392, doi:10.1016/j.virol.2015.08.013 (2015).

179 Kalaora, S. *et al.* Immunoproteasome expression is associated with better prognosis and response to checkpoint therapies in melanoma. *Nature Communications* **11**, 896, doi:10.1038/s41467-020-14639-9 (2020).

180 Pidugu, V. K., Pidugu, H. B., Wu, M.-M., Liu, C.-J. & Lee, T.-C. Emerging Functions of Human IFIT Proteins in Cancer. *Frontiers in Molecular Biosciences* **6**, doi:10.3389/fmolb.2019.00148 (2019).

181 Chikhalya, A. *et al.* Human IFIT3 Protein Induces Interferon Signaling and Inhibits Adenovirus Immediate Early Gene Expression. *mBio* **12**, e02829-02821, doi:10.1128/mBio.02829-21.

182 Zhang, B., Liu, X., Chen, W. & Chen, L. IFIT5 potentiates anti-viral response through enhancing innate immune signaling pathways. *Acta Biochim Biophys Sin (Shanghai)* **45**, 867-874, doi:10.1093/abbs/gmt088 (2013).

183 Panne, D., Maniatis, T. & Harrison, S. C. An atomic model of the interferon-beta enhanceosome. *Cell* **129**, 1111-1123, doi:10.1016/j.cell.2007.05.019 (2007).

184 Paul, A., Tang, T. H. & Ng, S. K. Interferon Regulatory Factor 9 Structure and Regulation. *Frontiers in Immunology* **9**, doi:10.3389/fimmu.2018.01831 (2018).

185 Chitra, P., Bakthavatsalam, B. & Palvannan, T. Beta-2 microglobulin as an immunological marker to assess the progression of human immunodeficiency virus infected patients on highly active antiretroviral therapy. *Clin. Chim. Acta* **412**, 1151-1154, doi:10.1016/j.cca.2011.01.037 (2011).

186 Chiou, S.-J. *et al.* A novel role for β2-microglobulin: a precursor of antibacterial chemokine in respiratory epithelial cells. *Scientific Reports* **6**, 31035, doi:10.1038/srep31035 (2016).

187 Abdelhaleem, M., Maltais, L. & Wain, H. The human DDX and DHX gene families of putative RNA helicases. *Genomics* **81**, 618-622, doi:https://doi.org/10.1016/S0888-7543(03)00049-1 (2003).

188 Loo, Y.-M. & Gale, M., Jr. Immune signaling by RIG-I-like receptors. *Immunity* **34**, 680-692, doi:10.1016/j.immuni.2011.05.003 (2011).

189 Gizzi, A. S. *et al.* A naturally occurring antiviral ribonucleotide encoded by the human genome. *Nature* **558**, 610-614, doi:10.1038/s41586-018-0238-4 (2018).

190 Pichlmair, A. *et al.* Activation of MDA5 Requires Higher-Order RNA Structures Generated during Virus Infection. *Journal of Virology* **83**, 10761-10769, doi:10.1128/JVI.00770-09 (2009).

191 Soliman, M., El-Diwany, R., Wheelan, S., Thomas, D. L. & Balagopal, A. Identification of CMPK2 as an Interferon Stimulated Gene that Restricts HIV Infection. *The Journal of Immunology* **198**, 158.112 (2017).

192 Anderson, A. M. *et al.* The metastasis suppressor RARRES3 as an endogenous inhibitor of the immunoproteasome expression in breast cancer cells. *Scientific Reports* **7**, 39873, doi:10.1038/srep39873 (2017).

193 Takeyama, K. *et al.* The BAL-binding protein BBAP and related Deltex family members exhibit ubiquitin-protein isopeptide ligase activity. *J. Biol. Chem.* **278**, 21930-21937, doi:10.1074/jbc.M301157200 (2003).

194 Zhang, Y. *et al.* PARP9-DTX3L ubiquitin ligase targets host histone H2BJ and viral 3C protease to enhance interferon signaling and control viral infection. *Nat Immunol* **16**, 1215-1227, doi:10.1038/ni.3279 (2015).

195 Dong, B. *et al.* Phospholipid scramblase 1 potentiates the antiviral activity of interferon. *J Virol* **78**, 8983-8993, doi:10.1128/jvi.78.17.8983-8993.2004 (2004).

196 Sung, P.-S. & Hsieh, S.-L. CLEC2 and CLEC5A: Pathogenic Host Factors in Acute Viral Infections. *Frontiers in Immunology* **10**, doi:10.3389/fimmu.2019.02867 (2019).

197 Liu, J., McFadden, G. & Imperiale, M. J. SAMD9 Is an Innate Antiviral Host Factor with Stress Response Properties That Can Be Antagonized by Poxviruses. *Journal of Virology* **89**, 1925-1931, doi:10.1128/JVI.02262-14.

198 Davidsson, J. *et al.* SAMD9 and SAMD9L in inherited predisposition to ataxia, pancytopenia, and myeloid malignancies. *Leukemia* **32**, 1106-1115, doi:10.1038/s41375-018-0074-4 (2018).

199 Van Kaer, L., Ashton-Rickardt, P. G., Ploegh, H. L. & Tonegawa, S. TAP1 mutant mice are deficient in antigen presentation, surface class I molecules, and CD4-8+ T cells. *Cell* **71**, 1205-1214, doi:10.1016/s0092-8674(05)80068-6 (1992).

200 Unterholzner, L. *et al.* IFI16 is an innate immune sensor for intracellular DNA. *Nature Immunology* **11**, 997-1004, doi:10.1038/ni.1932 (2010).

201 Malakhov, M. P., Malakhova, O. A., Kim, K. I., Ritchie, K. J. & Zhang, D. E. UBP43 (USP18) specifically removes ISG15 from conjugated proteins. *J. Biol. Chem.* **277**, 9976-9981, doi:10.1074/jbc.M109078200 (2002).

202 Arimoto, K. I. *et al.* STAT2 is an essential adaptor in USP18-mediated suppression of type I interferon signaling. *Nat Struct Mol Biol* **24**, 279-289, doi:10.1038/nsmb.3378 (2017).

203 Wong Joyce Jing, Y., Pung Yuh, F., Sze Newman, S.-K. & Chin, K.-C. HERC5 is an IFN-induced HECT-type E3 protein ligase that mediates type I IFN-induced ISGylation of protein targets.

*Proceedings of the National Academy of Sciences* **103**, 10735-10740, doi:10.1073/pnas.0600397103 (2006).

204 Paine, I. *et al.* Paralog Studies Augment Gene Discovery: DDX and DHX Genes. *Am J Hum Genet* **105**, 302-316, doi:10.1016/j.ajhg.2019.06.001 (2019).

205 Lian, Q. & Sun, B. Interferons command Trim22 to fight against viruses. *Cellular & Molecular Immunology* **14**, 794-796, doi:10.1038/cmi.2017.76 (2017).

206 Xue, B. *et al.* TRIM21 Promotes Innate Immune Response to RNA Viral Infection through Lys27-Linked Polyubiquitination of MAVS. *Journal of Virology* **92**, e00321-00318, doi:10.1128/JVI.00321-18.

207 Liu, S. *et al.* Insights into the evolution of the ISG15 and UBA7 system. *Genomics* **114**, 110302, doi:https://doi.org/10.1016/j.ygeno.2022.110302 (2022).

208 Wang, T. *et al.* Toll-Like Receptor 3-Initiated Antiviral Responses in Mouse Male Germ Cells In Vitro1. *Biology of Reproduction* **86**, 106, 101-110, doi:10.1095/biolreprod.111.096719 (2012).

209 Kutluay, S. B., Perez-Caballero, D. & Bieniasz, P. D. Fates of Retroviral Core Components during Unrestricted and TRIM5-Restricted Infection. *PLOS Pathogens* **9**, e1003214, doi:10.1371/journal.ppat.1003214 (2013).

**Table 1. List of primers used in the creation of SSM library for IFN-αR1 receptor ICD**

| Primer | Sequence |
|---|---|
| FF | GTAGCGGTGGGGGCGGT |
| FR | CTCGAGCAAGTCTTCTTCGGAGATAAGC |
| AR1-1F | AGGGTCCGAGCGGCGGATCCNNKTTCTTGAGATGCATCAATTA |
| AR1-2F | GTCCGAGCGGCGGATCCGTCNNKTTGAGATGCATCAATTATGT |
| AR1-3F | CGAGCGGCGGATCCGTCTTCNNKAGATGCATCAATTATGTCTT |
| AR1-4F | GCGGCGGATCCGTCTTCTTGNNKTGCATCAATTATGTCTTCTT |
| AR1-5F | GCGGATCCGTCTTCTTGAGANNKATCAATTATGTCTTCTTTCC |
| AR1-6F | GATCCGTCTTCTTGAGATGCNNKAATTATGTCTTCTTTCCATC |
| AR1-7F | CCGTCTTCTTGAGATGCATCNNKTATGTCTTCTTTCCATCACT |
| AR1-8F | TCTTCTTGAGATGCATCAATNNKGTCTTCTTTCCATCACTTAA |
| AR1-9F | TCTTGAGATGCATCAATTATNNKTTCTTTCCATCACTTAAACC |
| AR1-10F | TGAGATGCATCAATTATGTCNNKTTTCCATCACTTAAACCTTC |
| AR1-11F | GATGCATCAATTATGTCTTCNNKCCATCACTTAAACCTTCTTC |
| AR1-12F | GCATCAATTATGTCTTCTTTNNKTCACTTAAACCTTCTTCCAG |
| AR1-13F | TCAATTATGTCTTCTTTCCANNKCTTAAACCTTCTTCCAGTAT |
| AR1-14F | ATTATGTCTTCTTTCCATCANNKAAACCTTCTTCCAGTATAGA |
| AR1-15F | ATGTCTTCTTTCCATCACTTNNKCCTTCTTCCAGTATAGATGA |
| AR1-16F | TCTTCTTTCCATCACTTAAANNKTCTTCCAGTATAGATGAGTA |
| AR1-17F | TCTTTCCATCACTTAAACCTNNKTCCAGTATAGATGAGTATTT |
| AR1-18F | TTCCATCACTTAAACCTTCTNNKAGTATAGATGAGTATTTCTC |
| AR1-19F | CATCACTTAAACCTTCTTCCNNKATAGATGAGTATTTCTCTGA |
| AR1-20F | CACTTAAACCTTCTTCCAGTNNKGATGAGTATTTCTCTGAACA |
| AR1-21F | TTAAACCTTCTTCCAGTATANNKGAGTATTTCTCTGAACAGCC |
| AR1-22F | AACCTTCTTCCAGTATAGATNNKTATTTCTCTGAACAGCCATT |
| AR1-23F | CTTCTTCCAGTATAGATGAGNNKTTCTCTGAACAGCCATTGAA |
| AR1-24F | CTTCCAGTATAGATGAGTATNNKTCTGAACAGCCATTGAAGAA |
| AR1-25F | CCAGTATAGATGAGTATTTCNNKGAACAGCCATTGAAGAATCT |
| AR1-26F | GTATAGATGAGTATTTCTCTNNKCAGCCATTGAAGAATCTTCT |
| AR1-27F | TAGATGAGTATTTCTCTGAANNKCCATTGAAGAATCTTCTGCT |
| AR1-28F | ATGAGTATTTCTCTGAACAGNNKTTGAAGAATCTTCTGCTTTC |
| AR1-29F | AGTATTTCTCTGAACAGCCANNKAAGAATCTTCTGCTTTCAAC |
| AR1-30F | ATTTCTCTGAACAGCCATTGNNKAATCTTCTGCTTTCAACTTC |
| AR1-31F | TCTCTGAACAGCCATTGAAGNNKCTTCTGCTTTCAACTTCTGA |
| AR1-1R | GGATCCGCCGCTCGGAC |
| AR1-3R | GAAGACGGATCCGCCGCTC |
| AR1-4R | CAAGAAGACGGATCCGCCGC |
| AR1-5R | TCTCAAGAAGACGGATCCGCCG |
| AR1-6R | GCATCTCAAGAAGACGGATCCGC |
| AR1-7R | GATGCATCTCAAGAAGACGGATCCG |
| AR1-8R | ATTGATGCATCTCAAGAAGACGGATCCG |
| AR1-9R | ATAATTGATGCATCTCAAGAAGACGGATCCG |

**Table 1, Continued**

| | |
|---|---|
| AR1-10R | GACATAATTGATGCATCTCAAGAAGACGGATC |
| AR1-11R | GAAGACATAATTGATGCATCTCAAGAAGACGGA |
| AR1-12R | AAAGAAGACATAATTGATGCATCTCAAGAAGACG |
| AR1-13R | TGGAAAGAAGACATAATTGATGCATCTCAAGAAGA |
| AR1-14R | TGATGGAAAGAAGACATAATTGATGCATCTCAAGA |
| AR1-15R | AAGTGATGGAAAGAAGACATAATTGATGCATCTCAA |
| AR1-16R | TTTAAGTGATGGAAAGAAGACATAATTGATGCATCTCA |
| AR1-17R | AGGTTTAAGTGATGGAAAGAAGACATAATTGATGC |
| AR1-18R | AGAAGGTTTAAGTGATGGAAAGAAGACATAATTGATGC |
| AR1-19R | GGAAGAAGGTTTAAGTGATGGAAAGAAGACATAATTGA |
| AR1-20R | ACTGGAAGAAGGTTTAAGTGATGGAAAGAAGAC |
| AR1-21R | TATACTGGAAGAAGGTTTAAGTGATGGAAAGAAGACATA |
| AR1-22R | ATCTATACTGGAAGAAGGTTTAAGTGATGGAAAGAAGA |
| AR1-23R | CTCATCTATACTGGAAGAAGGTTTAAGTGATGGAAAG |
| AR1-24R | ATACTCATCTATACTGGAAGAAGGTTTAAGTGATGGAA |
| AR1-25R | GAAATACTCATCTATACTGGAAGAAGGTTTAAGTGATGG |
| AR1-26R | AGAGAAATACTCATCTATACTGGAAGAAGGTTTAAGTGATG |
| AR1-27R | TTCAGAGAAATACTCATCTATACTGGAAGAAGGTTTAAGT |
| AR1-28R | CTGTTCAGAGAAATACTCATCTATACTGGAAGAAGG |
| AR1-29R | TGGCTGTTCAGAGAAATACTCATCTATACTGGA |
| AR1-30R | CAATGGCTGTTCAGAGAAATACTCATCTATACTGG |
| AR1-31R | CTTCAATGGCTGTTCAGAGAAATACTCATCTATACTG |

**Table 2. List of primers used in the creation of 1st generation SSM library for IL-10Rβ receptor ICD**

| Primer | Sequence |
|---|---|
| FF | GTAGCGGTGGGGGCGGT |
| FR | CTCGAGCAAGTCTTCTTCGGAGATAAGC |
| 10RB-1F | ACAACACTTTGTTGTTCTTCNNKTTCCCATTGTCTGACGAAAA |
| 10RB-2F | ACACTTTGTTGTTCTTCTCTNNKCCATTGTCTGACGAAAACGA |
| 10RB-3F | CTTTGTTGTTCTTCTCTTTCNNKTTGTCTGACGAAAACGACGT |
| 10RB-4F | TGTTGTTCTTCTCTTTCCCANNKTCTGACGAAAACGACGTTTT |
| 10RB-5F | TGTTCTTCTCTTTCCCATTGNNKGACGAAAACGACGTTTTCGA |
| 10RB-6F | TCTTCTCTTTCCCATTGTCTNNKGAAAACGACGTTTTCGACAA |
| 10RB-7F | TCTCTTTCCCATTGTCTGACNNKAACGACGTTTTCGACAAGTT |
| 10RB-8F | CTTTCCCATTGTCTGACGAANNKGACGTTTTCGACAAGTTGTC |
| 10RB-9F | TCCCATTGTCTGACGAAAACNNKGTTTTCGACAAGTTGTCTGT |
| 10RB-10F | CATTGTCTGACGAAAACGACNNKTTCGACAAGTTGTCTGTTAT |
| 10RB-11F | TGTCTGACGAAAACGACGTTNNKGACAAGTTGTCTGTTATCGC |
| 10RB-12F | CTGACGAAAACGACGTTTTCNNKAAGTTGTCTGTTATCGCTGA |
| 10RB-13F | ACGAAAACGACGTTTTCGACNNKTTGTCTGTTATCGCTGAAGA |
| 10RB-14F | AAAACGACGTTTTCGACAAGNNKTCTGTTATCGCTGAAGACTC |
| 10RB-15F | ACGACGTTTTCGACAAGTTGNNKGTTATCGCTGAAGACTCTGA |
| 10RB-16F | ACGTTTTCGACAAGTTGTCTNNKATCGCTGAAGACTCTGAATC |
| 10RB-17F | TTTTCGACAAGTTGTCTGTTNNKGCTGAAGACTCTGAATCTGG |
| 10RB-18F | TCGACAAGTTGTCTGTTATCNNKGAAGACTCTGAATCTGGTAA |
| 10RB-19F | ACAAGTTGTCTGTTATCGCTNNKGACTCTGAATCTGGTAAGCA |
| 10RB-1R | GAAGAACAACAAAGTGTTGTGGTGTGGG |
| 10RB-2R | AGAGAAGAACAACAAAGTGTTGTGGTGTG |
| 10RB-3R | GAAAGAGAAGAACAACAAAGTGTTGTGGTGT |
| 10RB-4R | TGGGAAAGAGAAGAACAACAAAGTGTTGTG |
| 10RB-5R | CAATGGGAAAGAGAAGAACAACAAAGTGTTGT |
| 10RB-6R | AGACAATGGGAAAGAGAAGAACAACAAAGTGT |
| 10RB-7R | GTCAGACAATGGGAAAGAGAAGAACAACAAAG |
| 10RB-8R | TTCGTCAGACAATGGGAAAGAGAAGAACA |
| 10RB-9R | GTTTTCGTCAGACAATGGGAAAGAGAAGAAC |
| 10RB-10R | GTCGTTTTCGTCAGACAATGGGAAAGAG |
| 10RB-11R | AACGTCGTTTTCGTCAGACAATGGG |
| 10RB-12R | GAAAACGTCGTTTTCGTCAGACAATGG |
| 10RB-13R | GTCGAAAACGTCGTTTTCGTCAGACA |
| 10RB-14R | CTTGTCGAAAACGTCGTTTTCGTCAGA |
| 10RB-15R | CAACTTGTCGAAAACGTCGTTTTCGTC |

**Table 2, Continued**

| | |
|---|---|
| 10RB-16R | AGACAACTTGTCGAAAACGTCGTTTTCG |
| 10RB-17R | AACAGACAACTTGTCGAAAACGTCGTT |
| 10RB-18R | GATAACAGACAACTTGTCGAAAACGTCGT |
| 10RB-19R | AGCGATAACAGACAACTTGTCGAAAACG |

**Table 3. List of primers used in the creation of 2nd generation SSM library for IL-10Rβ receptor ICD**

| Primer | Sequence |
|---|---|
| FF | GTAGCGGTGGGGGCGGT |
| FR | CTCGAGCAAGTCTTCTTCGGAGATAAGC |
| 10RB-1F | AGGGTCCGAGCGGCGGATCCNNKTTGTTGTGGTGTGTTTACAA |
| 10RB-2F | GTCCGAGCGGCGGATCCGCTNNKTTGTGGTGTGTTTACAAGAA |
| 10RB-3F | CGAGCGGCGGATCCGCTTTGNNKTGGTGTGTTTACAAGAAGAC |
| 10RB-4F | GCGGCGGATCCGCTTTGTTGNNKTGTGTTTACAAGAAGACTAA |
| 10RB-5F | GCGGATCCGCTTTGTTGTGGNNKGTTTACAAGAAGACTAAGTA |
| 10Rb-6F | GATCCGCTTTGTTGTGGTGTNNKTACAAGAAGACTAAGTACGC |
| 10RB-7F | CCGCTTTGTTGTGGTGTGTTNNKAAGAAGACTAAGTACGCTTT |
| 10RB-8F | CTTTGTTGTGGTGTGTTTACNNKAAGACTAAGTACGCTTTCTC |
| 10RB-9F | TGTTGTGGTGTGTTTACAAGNNKACTAAGTACGCTTTCTCTCC |
| 10RB-10F | TGTGGTGTGTTTACAAGAAGNNKAAGTACGCTTTCTCTCCAAG |
| 10RB-11F | GGTGTGTTTACAAGAAGACTNNKTACGCTTTCTCTCCAAGAAA |
| 10RB-12F | GTGTTTACAAGAAGACTAAGNNKGCTTTCTCTCCAAGAAACTC |
| 10RB-13F | TTTACAAGAAGACTAAGTACNNKTTCTCTCCAAGAAACTCTTT |
| 10RB-14F | ACAAGAAGACTAAGTACGCTNNKTCTCCAAGAAACTCTTTGCC |
| 10RB-15F | AGAAGACTAAGTACGCTTTCNNKCCAAGAAACTCTTTGCCACA |
| 10RB-16F | AGACTAAGTACGCTTTCTCTNNKAGAAACTCTTTGCCACAACA |
| 10RB-17F | CTAAGTACGCTTTCTCTCCANNKAACTCTTTGCCACAACACTT |
| 10RB-18F | AGTACGCTTTCTCTCCAAGANNKTCTTTGCCACAACACTTGAA |
| 10RB-19F | ACGCTTTCTCTCCAAGAAACNNKTTGCCACAACACTTGAAGGA |
| 10RB-20F | CTTTCTCTCCAAGAAACTCTNNKCCACAACACTTGAAGGAATT |
| 10RB-21F | TCTCTCCAAGAAACTCTTTGNNKCAACACTTGAAGGAATTCTT |
| 10RB-22F | CTCCAAGAAACTCTTTGCCANNKCACTTGAAGGAATTCTTGGG |
| 10RB-23F | CAAGAAACTCTTTGCCACAANNKTTGAAGGAATTCTTGGGTCA |
| 10RB-24F | GAAACTCTTTGCCACAACACNNKAAGGAATTCTTGGGTCACCC |
| 10RB-25F | ACTCTTTGCCACAACACTTGNNKGAATTCTTGGGTCACCCACA |
| 10RB-26F | CTTTGCCACAACACTTGAAGNNKTTCTTGGGTCACCCACACCA |
| 10RB-27F | TGCCACAACACTTGAAGGAANNKTTGGGTCACCCACACCACAA |
| 10RB-28F | CACAACACTTGAAGGAATTCNNKGGTCACCCACACCACAACAC |
| 10RB-29F | AACACTTGAAGGAATTCTTGNNKCACCCACACCACAACACTTT |
| 10RB-30F | ACTTGAAGGAATTCTTGGGTNNKCCACACCACAACACTTTGTT |
| 10RB-31F | TGAAGGAATTCTTGGGTCACNNKCACCACAACACTTTGTTGTT |
| 10RB-32F | AGGAATTCTTGGGTCACCCANNKCACAACACTTTGTTGTTCTT |
| 10RB-33F | AATTCTTGGGTCACCCACACNNKAACACTTTGTTGTTCTTCTC |
| 10RB-34F | TCTTGGGTCACCCACACCACNNKACTTTGTTGTTCTTCTCTCA |

**Table 3, Continued**

| | |
|---|---|
| 10RB-35F | TGGGTCACCCACACCACAACNNKTTGTTGTTCTTCTCTCATCC |
| 10RB-36F | GTCACCCACACCACAACACTNNKTTGTTCTTCTCTCATCCATT |
| 10RB-37F | ACCCACACCACAACACTTTGNNKTTCTTCTCTCATCCATTGTC |
| 10RB-38F | CACACCACAACACTTTGTTGNNKTTCTCTCATCCATTGTCTGA |
| 10RB-39F | ACCACAACACTTTGTTGTTCNNKTCTCATCCATTGTCTGACGA |
| 10RB-1R | GGATCCGCCGCTCGGACC |
| 10RB-2R | AGCGGATCCGCCGCTCG |
| 10RB-3R | CAAAGCGGATCCGCCGCT |
| 10RB-4R | CAACAAAGCGGATCCGCCGC |
| 10RB-5R | CCACAACAAAGCGGATCCGCC |
| 10RB-6R | ACACCACAACAAAGCGGATCCG |
| 10Rb-7R | AACACACCACAACAAAGCGGATCC |
| 10Rb-8R | GTAAACACACCACAACAAAGCGGATCC |
| 10RB-9R | CTTGTAAACACACCACAACAAAGCGGAT |
| 10RB-10R | CTTCTTGTAAACACACCACAACAAAGCGG |
| 10RB-11R | AGTCTTCTTGTAAACACACCACAACAAAGC |
| 10RB-12R | CTTAGTCTTCTTGTAAACACACCACAACAAAGC |
| 10RB-13R | GTACTTAGTCTTCTTGTAAACACACCACAACAAAG |
| 10RB-14R | AGCGTACTTAGTCTTCTTGTAAACACACCA |
| 10RB-15R | GAAAGCGTACTTAGTCTTCTTGTAAACACACC |
| 10RB-16R | AGAGAAAGCGTACTTAGTCTTCTTGTAAACACAC |
| 10RB-17R | TGGAGAGAAAGCGTACTTAGTCTTCTTGTAAAC |
| 10RB-18R | TCTTGGAGAGAAAGCGTACTTAGTCTTCTTGTA |
| 10RB-19R | GTTTCTTGGAGAGAAAGCGTACTTAGTCTTCTT |
| 10RB-20R | AGAGTTTCTTGGAGAGAAAGCGTACTTAGTCT |
| 10RB-21R | CAAAGAGTTTCTTGGAGAGAAAGCGTACTTAGT |
| 10RB-22R | TGGCAAAGAGTTTCTTGGAGAGAAAGC |
| 10RB-23R | TTGTGGCAAAGAGTTTCTTGGAGAGAAAG |
| 10RB-24R | GTGTTGTGGCAAAGAGTTTCTTGGAGAG |
| 10RB-25R | CAAGTGTTGTGGCAAAGAGTTTCTTGGA |
| 10RB-26R | CTTCAAGTGTTGTGGCAAAGAGTTTCTTGG |
| 10RB-27R | TTCCTTCAAGTGTTGTGGCAAAGAGTTTC |
| 10RB-28R | GAATTCCTTCAAGTGTTGTGGCAAAGAGTT |
| 10RB-29R | CAAGAATTCCTTCAAGTGTTGTGGCAAAGA |
| 10RB-30R | ACCCAAGAATTCCTTCAAGTGTTGTGGC |
| 10RB-31R | GTGACCCAAGAATTCCTTCAAGTGTTGTG |
| 10RB-32R | TGGGTGACCCAAGAATTCCTTCAAGTG |
| 10RB-33R | GTGTGGGTGACCCAAGAATTCCTTCA |

**Table 3, Continued**

| | |
|---|---|
| 10RB-34R | GTGGTGTGGGTGACCCAAGAATTC |
| 10RB-35R | GTTGTGGTGTGGGTGACCCAAG |
| 10RB-36R | AGTGTTGTGGTGTGGGTGACCC |
| 10RB-37R | CAAAGTGTTGTGGTGTGGGTGACC |
| 10RB-38R | CAACAAAGTGTTGTGGTGTGGGTGA |
| 10RB-39R | GAACAACAAAGTGTTGTGGTGTGGGT |

**Table 4. List of primers used in the creation of CRISPR/Cas9 knock-out cell lines**

| Primer | Sequence |
|---|---|
| sgRNA_IL10RB_top | CACCgcagcgtccgtccatggcgtg |
| sgRNA_IL10RB_bottom | AAACcacgccatggacggacgctgc |
| sgRNA_IFNAR1_top | CACCgcgtacaagcatctgatggaa |
| sgRNA_IFNAR1_bottom | AAACttccatcagatgcttgtacgc |
| PCR_IL10RB_fwd_1 | GGATCCcagtcctgggttggtgttgt |
| PCR_IL10RB_fwd_2 | GGATCCtatttgacttgacggcgcct |
| PCR_IL10RB_rev_1 | CGCGGCCGCgcccagacggtctgtaatcc |
| PCR_IL10RB_rev_2 | CGCGGCCGCctgagtttagggcccagacg |
| PCR_IFNAR1_fwd_1 | GGATCCtgtgagtttcctgagtgtgga |
| PCR_IFNAR1_fwd_2 | GGATCCtgtttgtgagtttcctgagtgt |
| PCR_IFNAR1_rev_1 | CGCGGCCGCaggcgtgtttccagactgtt |
| PCR_IFNAR1_rev_2 | CGCGGCCGCatcacaggcgtgtttccaga |
| Sanger Seq_fwd | CGCAAATGGGCGGTAGGCGTG |

**Table 5. List of primers used in PCR quantification assay of ISG gene induction**

| Primer | Sequence |
|---|---|
| ISG15_fwd | CGCAGATCACCCAGAAGATCG |
| ISG15_rev | TTCGTCGCATTTGTCCACCA |
| MX1_fwd | GTTTCCGAAGTGGACATCGCA |
| MX1_rev | CTGCACAGGTTGTTCTCAGC |
| APOL3_fwd | GGGACGAGTCTGGCCCTTA |
| APOL3_rev | TCAATCGGTCAATGCTGGTTG |
| SAMD9L_fwd | GAAACAGGAGCACTCAATCTCA |
| SAMD9L_rev | CAGCCTTACTGGTGATTTTCACA |
| 18S_fwd | GTAACCCGTTGAACC CCATT |
| 18S_rev | CCATCCAATCGGTAGTAGCG |

**Table 6. List of select ISGs induced and their primary functions**

| Genes | Function | Mechanism of action | Refs |
|---|---|---|---|
| IFI27 | Apoptosis | Release of cytochrome C; proteasomal degradation of viral proteins | 161-163 |
| ISG15 | Antiviral, antimycobacterial | ISGylation | 164,165 166,167 |
| IFIT1 | Antiviral | Viral ssRNA binding | 168,169 |
| IFI6 | Apoptosis, antiviral | Inhibition of EGFR pathway to block viral entry | 170-172 |
| OAS1, OAS2, OAS3 | Antiviral, apoptosis, cell growth and differentiation | Inhibition of protein synthesis; disruption of cholesterol homeostasis to prevent viral fusion; virion trapping for lysosomal degradation | 173,174 175,176 177-179 |
| IFITM1, IFITM3 | Antiviral, anti-proliferative | Inhibition of ERK; p53 dependent cell cycle arrest | 180-182 183,184 |
| IFI44, IFI44L | Antiviral, antitumor | Promotion of immune cell infiltration | |
| IFI35 | Immunoregulatory, antiviral | Extracellular DAMPs | 185,186 187,188 |
| PSMB9 | Antigen processing | IFN-γ inducible proteolytic processing | 189 |
| IFIT3, IFIT2, IFIT5 | Antiviral, anti-proliferative | Activation of TBK1 and IRF3 to enhance IFN induction; upregulation of negative cell cycle regulators | 190 |
| IRF7, IRF9 | Antiviral | Transcriptional regulator of type I IFN; induction of PSMB9 | 191 192 |
| B2M | Antimicrobial, antibacterial | Class I MHC mediated antigen presentation | 193,194 195 |
| DDX58, DDX60, DDX60L | Antiviral | Viral dsRNA sensing; induction of type I IFNs and proinflammatory cytokines | 196 197,198 199 |
| RSAD2 | Antiviral | Chain termination of RNA-dependent RNA polymerases to inhibit viral replication; induction of type I IFNs | 200 |
| IFIH1/MDA5 | Antiviral, apoptosis | Induction of IFNs; enhanced NK cell function | 201,202 |
| CMPK2 | Antiviral, immunomodulatory | TLR9 inflammasome-based cytokine release | 203 |
| RARRES3 | Anti-proliferative | Enhanced lipid metabolism and degradation | 204 |
| DTX3L | Antiviral | ISG upregulation | 205,206 |
| PLSCR1 | Antiviral, apoptosis | DNA binding; phospholipid organization | 207 |
| CLEC2B | Antiviral | NET formation by neutrophils; proinflammatory cytokine production | 208 |

| **Table 6, Continued** | | | |
|---|---|---|---|
| SAMD9, SAMHD1 | Apoptosis, anti-proliferative | Downstream target of TNF-α signaling; inflammatory response to tissue injury | [209] |
| TAP1 | Immunomodulatory | ABC transporter associated with class I MHC antigen processing | |
| IFI16 | Antiviral, anti-proliferative | Induction of IFN-β; modulation of cell cycle regulatory factors | |
| USP18 | Negative regulator of type I IFNs | De-ISGylation; downregulation of ternary type I IFN complexes | |
| HERC6 | Antiviral | Enhanced ISGylation | |
| DHX58 | Antiviral | Enhanced recognition of RIG-I and MDA5 by unwinding or stripping nucleoproteins of viral RNA | |
| TRIM22, TRIM21 | Antiviral | Ubiquitinylation | |
| UBA7 | Apoptosis, antiviral | Activation of target protein ubiquitinylation; catalysis of ISGylation | |
| EIF2AK2 | Antiviral | Inhibition of viral protein synthesis via integrated stress response | |
| TRIM5 | Antiviral | Binding viral capsids | |